REAL-TIME ESTIMATION OF MATERIAL REMOVAL RATE (MRR) IN COPPER CHEMICAL MECHANICAL PLANARIZATION (CMP) USING WIRELESS TEMPERATURE SENSOR

By

EKANSH GUPTA

Bachelor of Engineering (Mechanical)

Institute of Engineering and Technology,

Devi Ahilya University, Indore, INDIA

2007

Submitted to the Faculty of the
Graduate College of
Oklahoma State University
in partial fulfillment of
the requirements for the Degree of
MASTER OF SCIENCE
August, 2010

REAL-TIME ESTIMATION OF

MATERIAL REMOVAL RATE (MRR) IN

COPPER CHEMICAL MECHANICAL PLANARIZATION (CMP)

USING WIRELESS TEMPERATURE SENSOR

Thesis Approved:

Dr. Ranga Komanduri

Thesis Advisor

Dr. Satish Bukkapatnam

Committee member

Dr. Sandip P. Harimkar

Committee member

Dr. Mark E. Payton

Dean of the Graduate College

ACKNOWLEGEMENTS

I would like to thank my venerated advisor Dr. Ranga Komanduri, Regents Professor and A.H. Nelson, Jr. Endowed Chair in Engineering, School of Mechanical and Aerospace Engineering. He helped me to build a new perspective towards research and process development by emphasizing on basic science and real world application as a building block for good research. He gave me independence to try new things and decide my objectives.

I express my earnest appreciation towards my co-advisor Dr. Satish Bukkapatnam. He helped me to set my goals and guided me with a practical solution whenever I was in a dilemma regarding my research work. Without his guidance this work could not have been accomplished. I'am thankful to Dr. James Kong for giving me helpful suggestions about my work.

I sincerely thank my seniors Dr. Rutuparna Narulkar and Dr. Milind Malshe for their consistent help and guidance.

I thank my colleagues Amit and Prahalad for their help and support in completing the tasks related to project like procuring materials, designing and fabricating the polishing setup, troubleshooting and solving problems in setup and sensors, and conducting experiments systematically. Their company made the hours in the lab enjoyable.

I thank my colleagues Omer and Puneet for helping me with data analysis and usage of the Buehler polishing machine respectively.

This project was funded by a grant (CMMI 0700680) from the National Science Foundation (NSF), Division of Design, Manufacturing, and Industrial Innovation. The authors thank Dr. George Hazelrigg for his interest and support of this work.

TABLE OF CONTENTS

LIST OF FIGURES

LIST OF TABLES

Chapter 1: Introduction

1.1: Need for Chemical Mechanical Planarization

In an integrated circuit, there are millions of micro-devices such as transistors, capacitors, diodes, and resistors on a single chip [1]. Each of the micro-device is formed by semiconductor, metal, and dielectric layers arranged in a particular pattern. Further, these micro-devices are interconnected through metal interconnects which are isolated using a dielectric material. Multiple layers of such patterns are repeatedly stacked over each other to accommodate millions of micro-devices in order to have high speed and high performance of the IC chip. Such an arrangement is called as multilevel metallization [2]. This scheme created enormous challenges for fabrication at the wafer level. The major source of challenge is the uneven topography buildup as the number of interconnect levels increase as shown in Fig. 1-1a. This surface unevenness has negative impact on pattern transfer which would subsequently lead to failure of multilevel interconnect network. Thus, the levels are required to be planarized to a very high degree of planarization enabling very even interconnect levels over each other as shown in Fig. 1-1b. The method most commonly used in the semiconductor industry for planarization is Chemical Mechanical Planarization (CMP) process.

In CMP, extremely small abrasive particles on the order of a few nanometers are used compared to micrometer sized abrasive particles in conventional polishing or lapping processes. Also, in CMP, the chemistry of the slurry plays an important role in softening and dissolving a thin layer of material on the surface which is further polished due to abrasive action. In contrast to this, in the conventional polishing

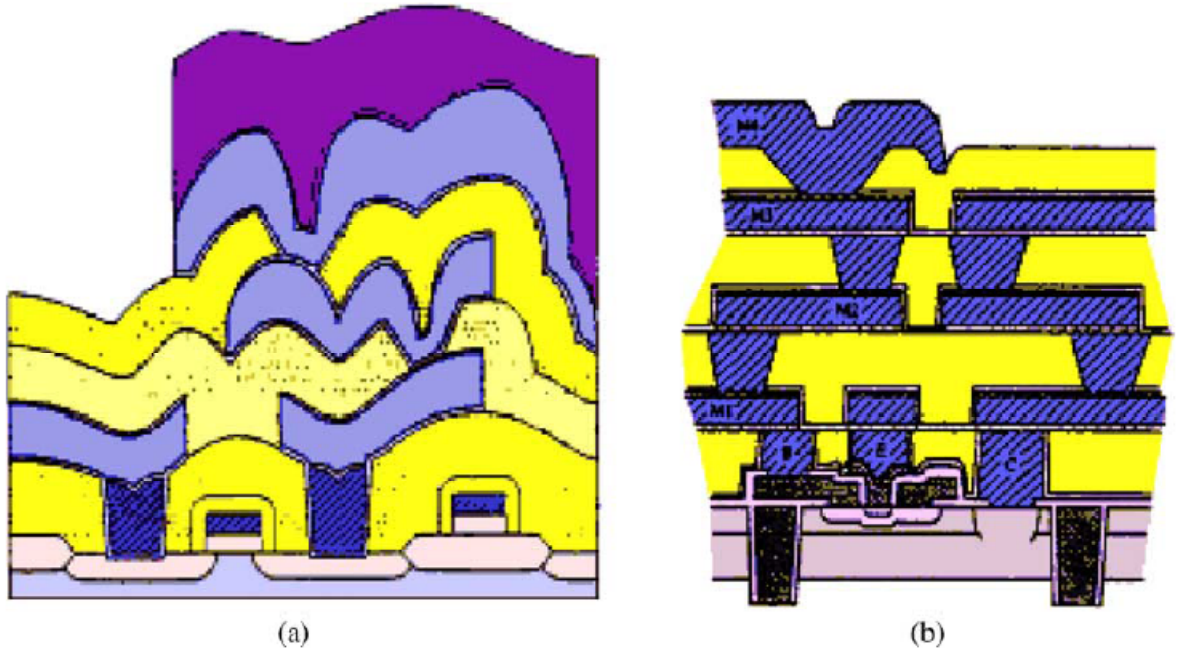

Fig. 1-1: Schematic of (a) non-planarized and (b) planarized multilevel metallization structure [2]

the material is removed only by abrasion from abrasive particles. Because of selective dissolution of material, MRR tends to be lower in CMP. This facilitates in giving precise removal, uniformity in polishing and fewer scratches and defects. The CMP process is therefore, preferred for planarization in ICs [3]. The advantages of CMP over other planarization methods are tabulated in Table 1-1.

Table 1-1: Advantages of CMP over other polishing methods [3]

Benefits	**Remarks**
Planarization	Achieves global planarization
Planarize different materials	A wide range of wafer surfaces can be planarized
Reduce severe topography	Reduces severe topography to allow fabrication with tighter design rules and additional interconnection levels

Alternative method of metal patterning	Provides an alternate means of patterning metal, eliminating the need to plasma etch, difficult to etch metals and alloys
Improved metal step coverage	Improves metal step coverage due to reduction in topography
Increased IC reliability	Contributes to increasing IC reliability, speed, yield (lower defect density) of sub 0.5 mm and circuits
Reduce defects	CMP is a subtractive process and can remove surface defects

1.2: Chemical mechanical polishing process

Chemical mechanical planarization is a polishing process for smoothening the topography of surfaces. It is used in devices to reduce their vertical heights, hence shrinking the size of the devices and maintaining the flatness of the devices to ensure pattern transfer with maximum precision. Depending on whether CMP is used to planarize metal or dielectric, the CMP process can be classified as metal or dielectric CMP.

A typical setup of CMP is shown in Fig. 1-2. A wafer carrier holds the wafer which is pressed and rotated against a polishing pad made up of a polymeric material. The direction of rotation of the pad can be in the same direction or opposite that of the wafer. Polishing process utilizes rotary motion and orbital or translational-type between the pad and the wafer. Slurry is circulated on the pad which acts as a coolant and also provides abrasive action. The slurry also consists of various other chemicals which react with the layer being polished and makes the layer softer by partial dissolution. The surface layer gets modified to more fragile state making material removal easy by abrasive action. Since the pad gets worn, eventually with the polishing process depleting its sharp asperities, the pad tends to remove material with non-uniform material removal rate. For this reason, the pad is simultaneously conditioned by a

conditioner which is a diamond grit disc pressed against the polishing pad maintaining the pad roughness as the polishing progresses. The relative motion between the wafer and the pad and the down force makes the abrasives in the slurry to get embedded in the pad which ploughs out the material from the wafer layer being polished [4].

Copper has replaced aluminum for metal interconnect in ICs because of its various advantages over aluminum such as lower resistivity, lower RC delay, higher heat dissipation, better thermo-mechanical properties and better stress migration resistance. Copper CMP is the process applied to remove and planarize copper layers on the substrates. Copper CMP is prone to some problems such as dishing and erosion. Dishing is the recessed height of copper line compared to the neighboring oxide line whereas erosion is the difference between the original oxide height and the height of oxide after polishing [5].

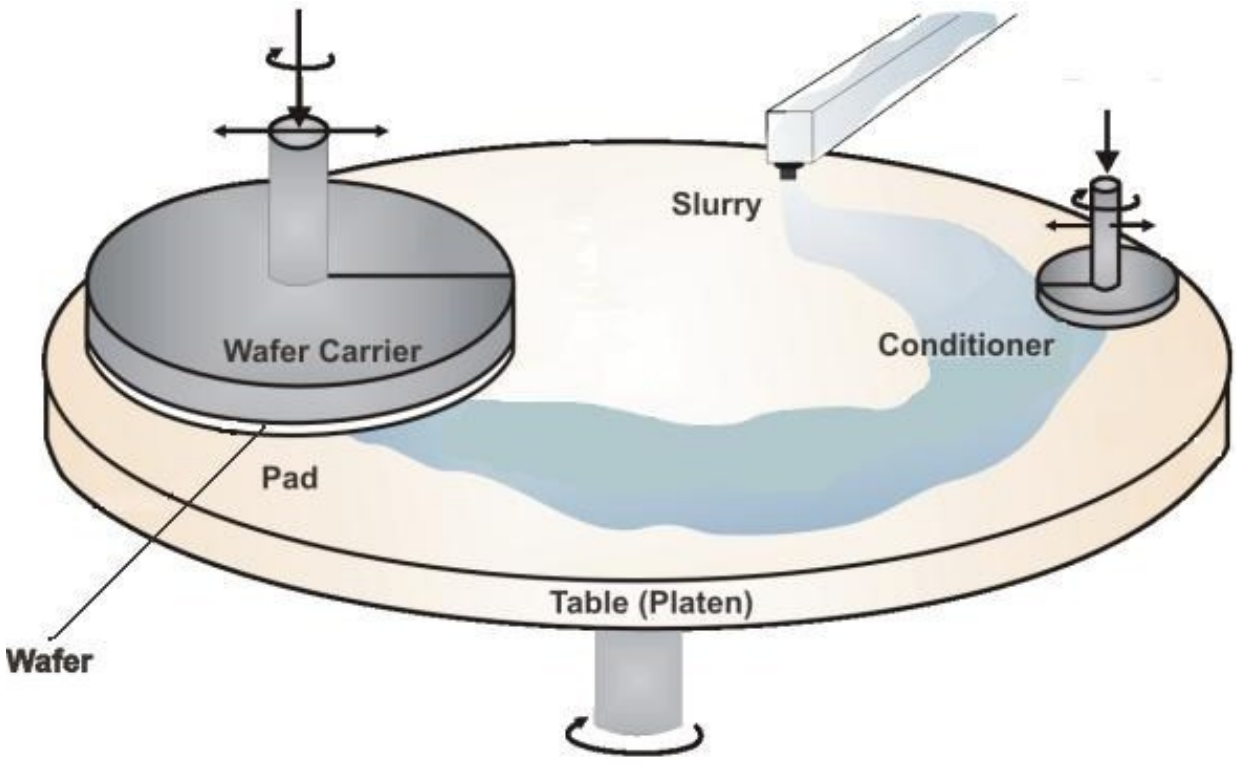

Fig. 1-2: Chemical Mechanical Planarization setup [3]

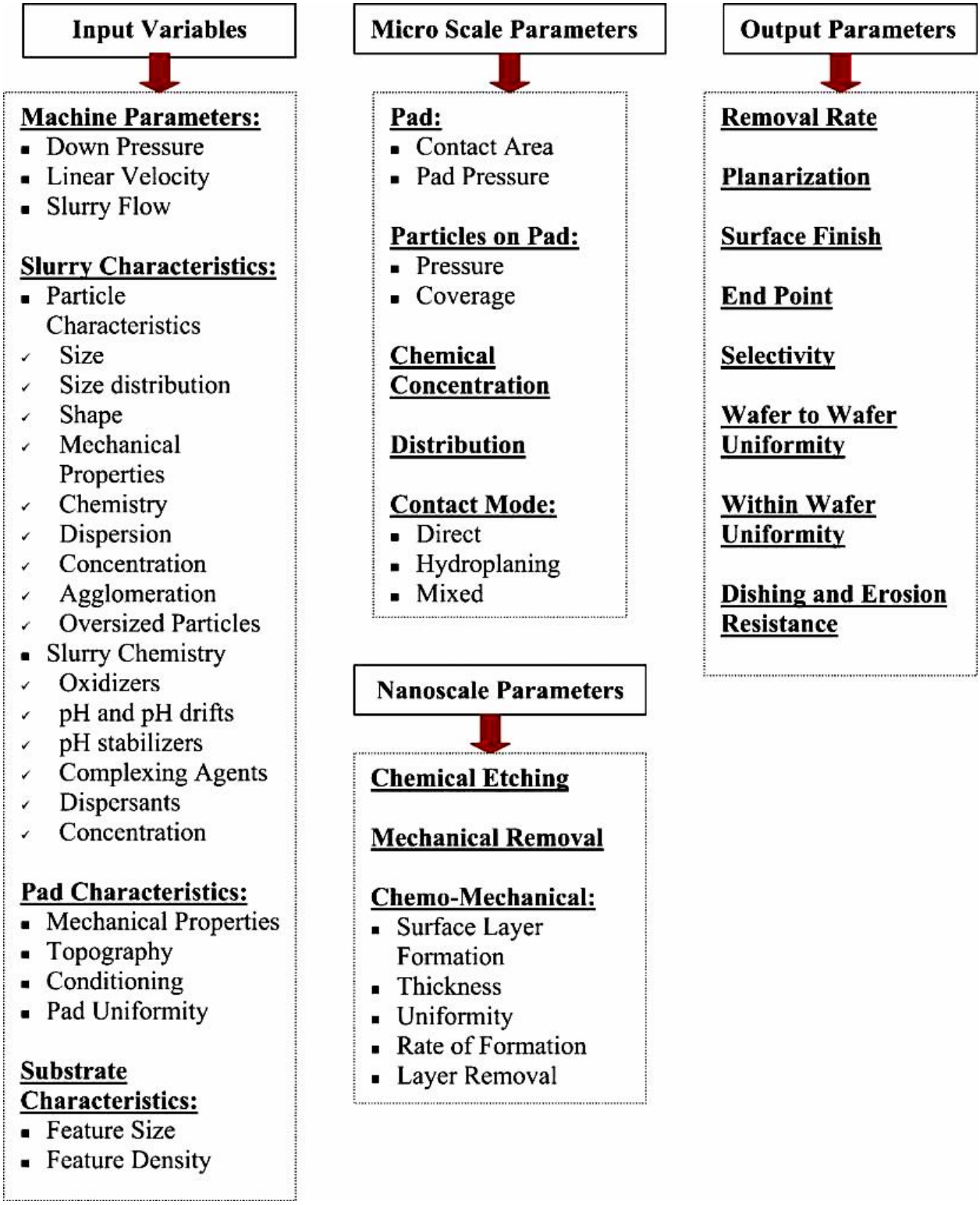

Fig. 1-3: Various parameters governing the CMP process [6]

1.3: Parameters governing CMP

The parameters and variables that govern CMP have been illustrated in Fig. 1-3.

Influence of machine parameters: The machine parameters in CMP mainly include the down force, sliding velocity, and the slurry flow. Higher down force and sliding velocity increases the MRR. It is discussed in detail in Section 2.5. With lower down force, the planarization improves but uniformity decreases. Slurry flow pattern is an important parameter which effects both material removal rate and within-wafer-non-uniformity (WIWNU). Because of the rotation of the platen the flow pattern would be different as the slurry is fed at different positions on the pad. Fig. 1-4a shows different positions of slurry feeding on the platen. The material removal would not be uniform if the slurry cannot reach the pad-wafer contact points. Fig. 1-4b shows the material removal rate obtained at various points on the pad. It can be observed that position around the center is a better location to feed slurry to attain high MRR [7].

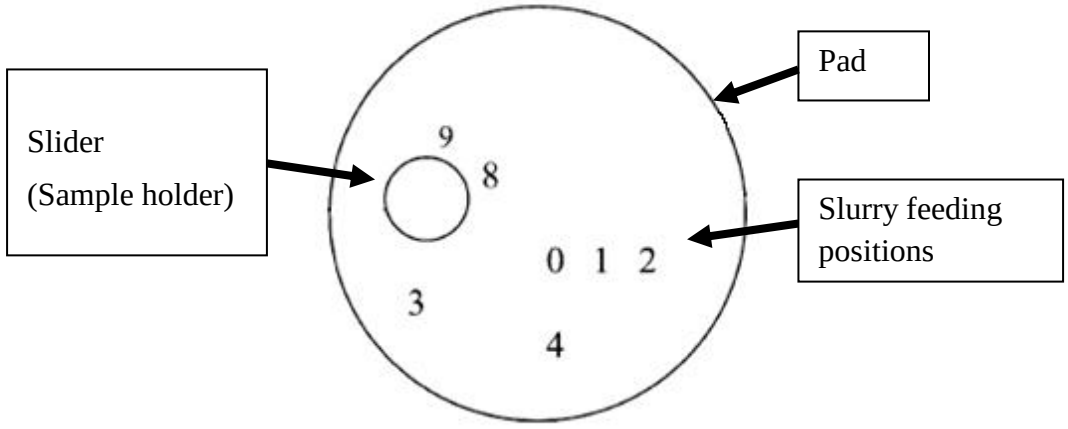

(a)

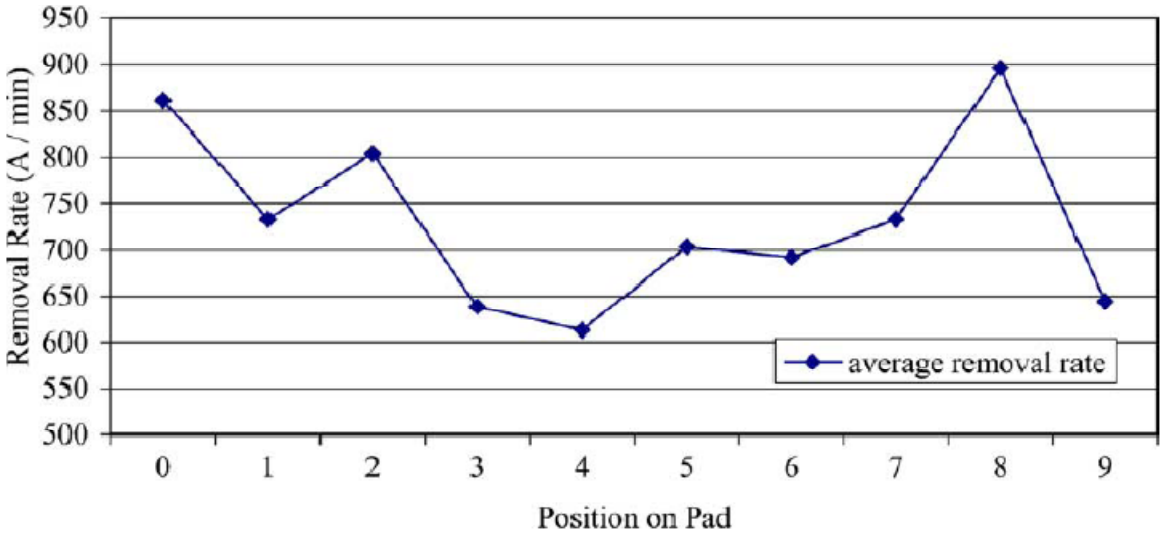

(b)

Fig. 1-4: (a) Slurry feeding positions in the experiment (b) Average MRR obtained corresponding to these positions [7]

1.4: CMP consumables

CMP Pads: Pad is an important consumable in CMP. Pad transports and delivers slurry on the wafer surface. Pad also transmits normal and shear forces from polisher to wafer. The polishing pad has significant influence on the removal rate, WIWNU, wafer-to-wafer-non-uniformity (WTWNU) and defects. CMP process is a combination of chemical and mechanical processes. The polishing pad is exposed to repeated mechanical stress and chemical attacks. The consistent down force, shear force, and frictional force applied on the pad makes it prone to severe compression and abrasion. Various chemicals like oxidizers and acids present in the slurry tend to corrode and weaken the pad. Thus the pad should have sufficient mechanical strength and chemical resistance to cope up with these conditions. Also pad has an important function of transporting slurry efficiently. Pad should be sufficiently hydrophilic in nature and should have either pores or grooves to enhance the transfer of slurry. Polishing pads are

usually made of polymeric materials, such as polycarbonates, nylons, polysulphones and polyurethane [8]. The main types of pads used in CMP are:

Type I: Felts and polymer impregnated felts

Type II: Porometrics (microporous synthetic leathers)

Type III: Filled polymer sheets (films)

Type IV: Unfilled textured polymer sheets (films)

Pads can have a wide range of microstructures, textures, and fillers and are fabricated using various manufacturing processes, such as casting, molding, extrusion, web coating, and sintering. Not only the mechanical and chemical properties of the pad are important, but also the microstructure of the pad plays major role in the polishing process. Whether the pad surface is flat or has pores or grooves, their properties have significant influence on the polishing performance. The polishing performance at a wafer level mainly includes MRR, polishing non uniformity, edge effects, micro scratches, and pad life. At a die level, it includes planarization and defectivity. At the feature level, it includes dishing, erosion, defects, and surface roughness [9]. How pad properties affect the polishing performance is discussed further.

Pad roughness: Pad roughness is the presence of pores and asperities which hold the abrasive particles and contribute to the material removal. As the polishing process progresses, the asperities wear-off and the surfaces gets flattened. If the pad is not conditioned to get back sharp asperities, the material removal rate decreases. But a rougher pad causes more defects, such as scratches and residual particles on the wafer surfaces. This is because, for the same load, rougher pad tends to indent the abrasives deeper into the wafer. In the case of patterned wafer polish, the rougher pad gives more dishing problem [10].

Pad porosity/density: Pad having more pores has lesser density and stiffness. Pad pores help in transporting the slurry over pad surface and thereby removing the material. Pads having lesser porosity have lower removal rates because of this reason. Since nonporous pads have higher stiffness and strength, they have lesser variations in their physical properties and thus give more consistent and uniform polish. Also, because of being harder and stronger, the nonporous pads have higher abrasion resistance or lower pad wear rate than porous pads for the same polishing conditions. Porous pads can trap polishing debris and residual particles and thus tend to give more scratches and defects [11].

Pad Young's modulus/flexibility: Pads having higher Young's modulus give good overall planarization because they do not bend and thereby planarize the high points first which tones down the topography differences on the surface. But as the pads with higher modulus do not comply with the wafer surface, they do not give a uniform polishing. In contrast to this, the flexible pads comply with the surface profile variations and remove material equally from all the regions. The flexible pads maintain the surface profile being polished and give a uniform polish but the overall planarization is poor. Dishing and erosion problems increase with more bending ability of the pad [12], [13]. Table 1-2 summarizes various pad properties and their effects on polishing at wafer, die, and feature scale.

Table 1-2: Relation between pad properties and polishing performance [8]

Pad Property	**Polishing scale**		
	Wafer	**Die**	**Feature**
Density (porosity)	Removal rate, non uniformity	Defectivity	Dishing, erosion
Hardness	Macroscratches	Defectivity	Defectivity, roughness, dishing, erosion
Tensile strength	Pad life		

Abrasion resistance	Pad life		
Modulus	Non uniformity	Planarization	
Thickness	Pad life		
Pad texture	Pad life, removal rate, non uniformity		
Pad roughness	Removal rate, non uniformity	Planarization	Dishing, erosion
Hydrophilicity	Removal rate		

CMP Slurry: Slurry is the carrier of abrasive particles and various chemicals which cause mechanical and chemical removal of material respectively. Thus slurry is the basic component of the CMP process. There can be numerous parameters in CMP slurry such as pH, solution chemistry, charge type, complexing agent, oxidizers, buffering agents, corrosion inhibitors, surfactants, etchants, chelating agents, abrasive related properties, such as size, shape, hardness, and concentration of the abrasives. These parameters are selected according to the polishing requirements [14]. Ideal CMP slurry should achieve high MRR, excellent global planarization, good surface finish, low defectivity, high selectivity and should prevent corrosion. There should be a synergy between the chemical etching and mechanical material removal. Mechanical material removal produces higher friction forces, thus can produce scratches and adversely affect surface topography. Also, the pressure variations at local points vary the removal rate and thus effect global planarization. In contrast to this, excess chemical etching adversely effects surface planarity and induce defects associated with corrosion. Thus the chemical and mechanical parameters of the slurry have to be optimized [3]. The prime design concerns for CMP slurry are shown in Fig. 1-5.

Global Planarization

Formation of a thin passivated surface layer

Minimization of chemical etching

Minimization of mechanical polishing

Removal (Polishing) Rate

Rapid formation of a thin surface layer

Control of the mechanical/interfacial properties of the surface layer

Indentation-based wear

Fracture/delamination-based removal

Surface Defectivity

Rapid formation of a thin surface layer

Minimization of mechanical polishing

Control of particle size distribution

Selectivity

Top-layer chemomechanical polishing

Bottom-layer mechanical polishing

Reduction of mechanical component in slurry

Slurry Handling

Formation of stable slurries

Control of interparticle and particle-surface interactions

Steric-force-based repulsion in ionic systems

Fig. 1-5: Main concerns during selection of a CMP slurry [6]

As shown in Fig. 1-6, a passivation layer is formed at the interface between the wafer and the pad which is softer than the substrate material and thus can be abraded with more ease. The passivation layer has to be thinner than the difference in the height of the high and low regions in wafer and pad to avoid within-wafer-non-uniformity (WIWNU) [6]. The formation of passivation layer is accelerated by oxidizers, such as hydrogen peroxide and corrosion damage to the surface is prevented by corrosion inhibitors, such as Benzotriazole (BTA) [15]. Maintaining a particular pH, which depends on the substrate, is important for the formation of passivation layer. The time required for the formation of a passivation layer should be minimized to avoid surface defects [16].

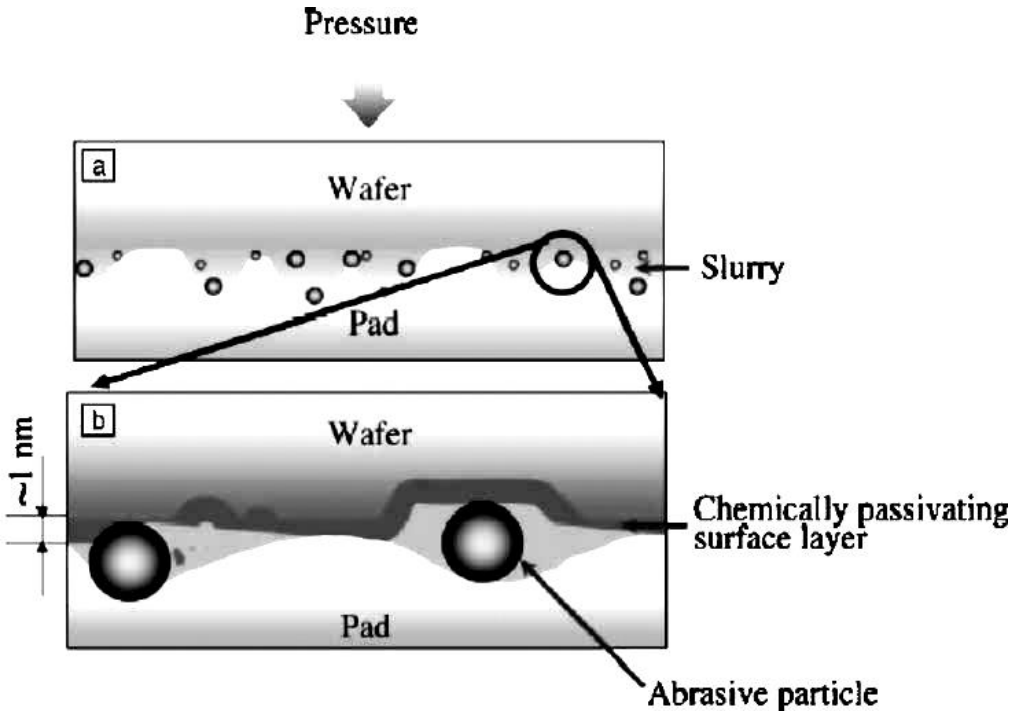

Fig. 1-6: Schematic diagram of passivation layer at (a) microscale and (b) nanoscale level [18]

Selectivity is an important feature of the slurry. It is the difference in the removal rates of different materials by the same slurry. Higher the selectivity of the slurry, the more effective is the end

point detection for polishing of a particular step. For example, to polish copper the slurry should act separately on copper and should spare the barrier layer of Ta and underlying layer of silica [17].

In addition to the chemical components, abrasives are present in the slurry to remove material by cutting action. The abrasive particles enhance the mechanical strength of the pad and transmit the downforce and shear force to the wafer thereby removing material by wear. Also the abrasives serve as adsorption sites to the reaction by-products and polishing debris and assist in their transportation and removal from the wafer surface. A wide variety of materials have been used as abrasive particles in the CMP process. They include alumina, silica, ceria, zirconia, titania and diamond. The selection of the abrasives are done on the basis of their properties, such as hardness, particle size, bulk particle density, particle crystallinity and shape as suitable to the polishing requirements. Nano particle size silica and alumina are the most commonly used abrasives in CMP. The physical appearance of these abrasives is white powder. These materials should be ultrapure and have nearly uniform size and shape to ensure consistent polishing [9].

Chapter 2: Literature Review

2.1: Friction and heat generation in CMP

In the CMP process heat is generated during polishing. The reason for this heat is the friction between the pad, wafer and abrasive particles in the slurry. The abrasives which are present in the polishing slurry are responsible for causing abrasion on the copper wafer. There can be two kinds of abrasion, namely two-body and three-body abrasion, in which the material is removed by the abrasives as shown in Fig. 2-1:

Two-Body abrasive wear: In this the abrasives get embedded in the pad and are rigid enough to act as a cutting tool to remove the material from the wafer.

Three-Body abrasive wear: In this the abrasive particles are free to move and thus roll and slide between the wafer and the pad. The material removal is about ten times slower in this kind of abrasion [19].

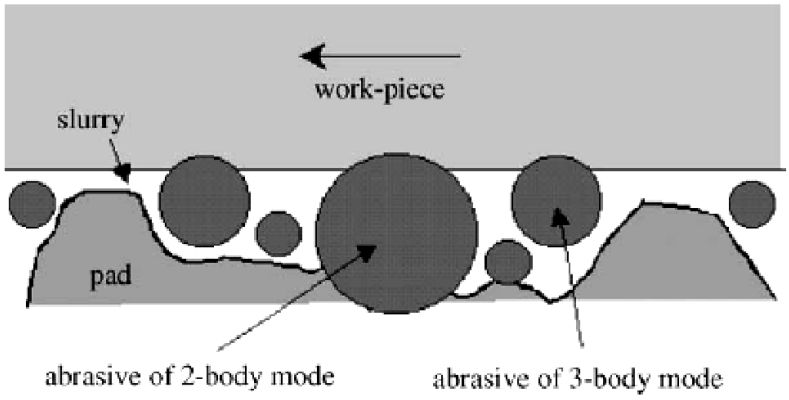

Fig. 2-1: Two types of mode of abrasion in CMP [19]

The abrasives not only remove the material from the wafer but also from the pad. However, the material removal from the pad is relatively less because pad is softer than the wafer. The asperities present in the pad are responsible for trapping the abrasive particles and to enhance two-body abrasion which is the main contributor to the material removal and the heat generation process. The asperities of the pad and the abrasive particles embedded in the pad are directly related to the overall friction between the wafer and the pad during polishing. The work done to generate relative motion between the wafer and the pad in the presence of this friction is the frictional work. Assuming that frictional force is proportional to the normal load but independent of the contact area, the mechanical work would be:

$W = F_f.V$, where F_f is the frictional force exerted by the contact area and V is the relative velocity between the wafer and the pad. This can also be written as:

$W = \mu FV$, where μ is the coefficient of friction and F is the normal force applied on the pad by the wafer.

This work is converted into heat completely which is conducted /convected into the wafer, pad and slurry. Thus, the factors which mainly contribute to the amount of heat generated are load or pressure (P), relative velocity between the wafer and the pad (V), pad properties and the abrasive properties. Increase in P or V increase the product of P and V, i.e. PV value which is the mechanical power input and thus the heat generated increases. Pad properties, such as pad asperity density, pad asperity hardness, ability of the pad to hold the abrasive particles in the pad influences the heat generated. Abrasive properties, such as hardness, shape, size, and concentration in the slurry influence the heat generated [19].

2.2: Heat flow in the CMP process

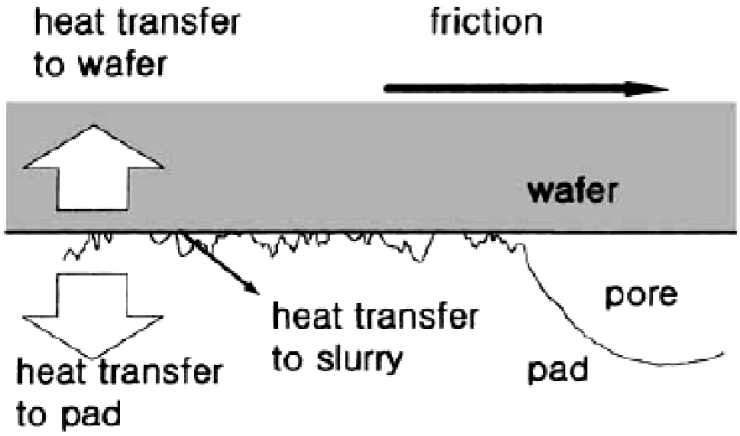

Fig. 2-2: Heat flow in the CMP process [20]

As shown in Fig. 2-2, the heat generated between the wafer and the pad is transferred to the pad, wafer and slurry. The heat is primarily partitioned or divided between pad and wafer [21]. Slurry acts as a medium which takes away part of heat from the wafer as well as from the pad. Some heat is convected away from the pad and the wafer by the surrounding air. Rest of the heat goes inside the wafer or pad and increase their temperatures. This heat is then transferred to the wafer carrier in case of wafer and platen in case of pad.

The heat partitioning depends upon various things, such as pad and wafer material properties, slurry properties and sliding velocity. Regarding the pad and wafer material properties, the more conducting material takes away more heat which is always the wafer. Heat partitioning also depends upon the size of the wafer. The smaller the wafer, more heat is partitioned in it. Heat partitioning also depends on the slurry properties, such as slurry flow rate and slurry heat capacity. More the slurry flow rate and heat capacity more heat would be taken off from the wafer as well as pad by the slurry. Given below is the heat partitioning factor between the wafer and the pad representing the fraction of heat going into the wafer [21].

$$\gamma_w = \frac{\kappa_w}{\kappa_w + 0.627\kappa\sqrt{\frac{Vr_w}{D}}}$$

where γ_w is the heat partitioning fraction, K_w is the thermal conductivity of the copper wafer, K is the thermal conductivity of the pad, V is the relative sliding velocity, r_w is the radius of the wafer and D is the thermal diffusivity of the pad.

It can be observed that the heat partitioning fraction is directly related to the conductivity of the wafer material, inversely related to the radius of wafer, and the sliding velocity. Fig. 2-3 shows the heat partitioning between wafer and pad. The equations in the figure are that of heat partitioning fraction and the heat conducted in the wafer and pad.

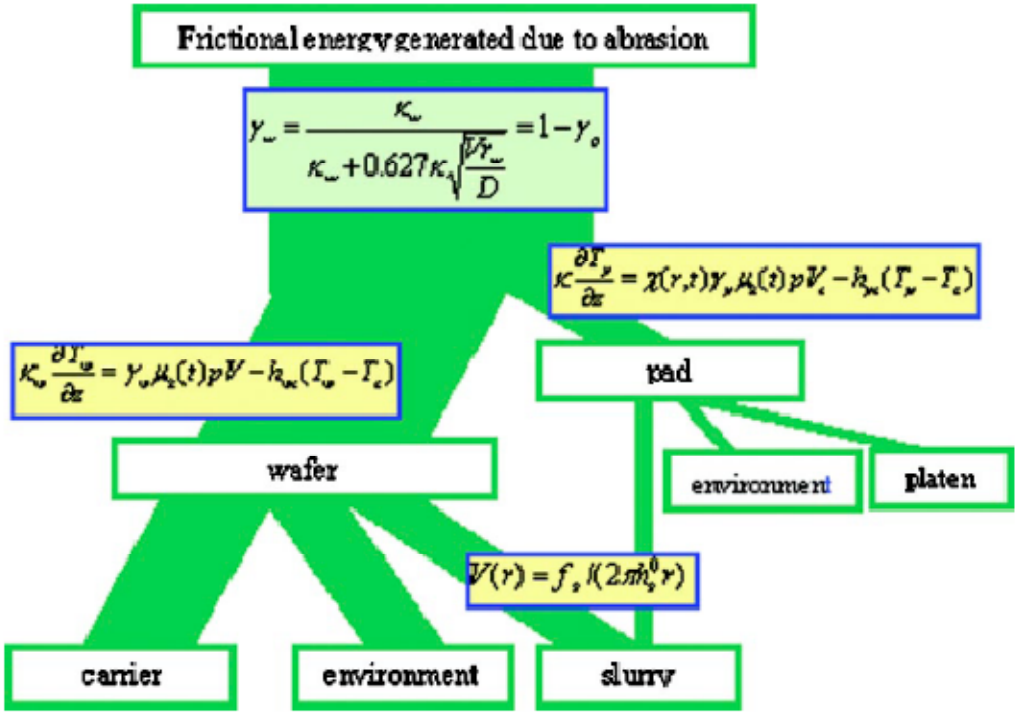

Fig. 2-3: Heat partitioning between pad and wafer [21]

2.3: Factors affecting the temperature rise in wafer

Sliding velocity: Temperature rise increase with velocity because an increase in V would increase the PV value and thus the amount of total heat generated. Fig. 2-4 shows the temperature increase from 24°C to 28°C with increase in the relative velocity from 10 m/min to 85 m/min at a constant pressure of 13.6 KPa. At higher pressure values of 30.9 KPa and 40.4 KPa the temperature rises to higher values at the same relative velocities. If the product of pressure and velocity is constant or the power input is fixed, temperature rise in the wafer is inversely related to the relative sliding velocity between the pad and the wafer. The reason is more convective cooling of the wafer at higher sliding velocities and comparatively more heat is dissipated away to give a lower temperature rise in the wafer than expected. The heat partition fraction is inversely proportional to the sliding velocity. Thus the fraction of heat going to the wafer decreases with increase in relative sliding velocity. Also, the heat transfer coefficient between the slurry and the wafer which represents the heat taken away by slurry is directly proportional to the square root of the velocity [20], which means at higher velocity more heat is dissipated from the wafer [21].

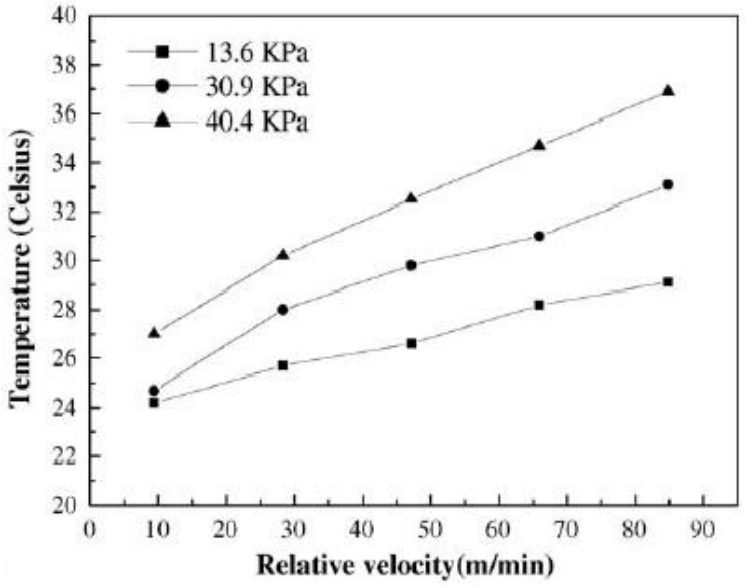

Fig. 2-4: Effect of increase in velocity on temperature rise [20]

Load: In general, increase of load or pressure increases the temperature because of increase in PV or power input. Fig. 2-5 shows that temperature increase from 24°C to 27°C when pressure increases from 12 to 42 KPa at a constant relative velocity of 9.4 m/min. The temperature rise values are higher at higher velocities for the same values of pressure. Also, for all the relative velocities the temperature values are higher than expected for higher load of 42 KPa compared to 12 and 31 KPa. Higher load increases the pad contact area with the wafer by pressing the pad asperities and voids to come in contact with the wafer which would have been otherwise not in contact at lesser load. The sliding contact of more asperities would generate more heat [19]. The difference between lower and higher load condition can be explained from Fig. 2-10. For lesser load, only the abrasive particles are in contact with the wafer, the pad contact with wafer is negligible and thus the heat generated is only due to abrasion or material removal. At higher load, the pad contact area with the wafer increases and there is considerably larger area of pad which is in contact with the wafer without the abrasive particles between them. The heat generated from this area is due to rubbing action and not due to abrasion from abrasives. Thus the heat generated in this case is more than expected to give higher temperature rise value in the wafer [23].

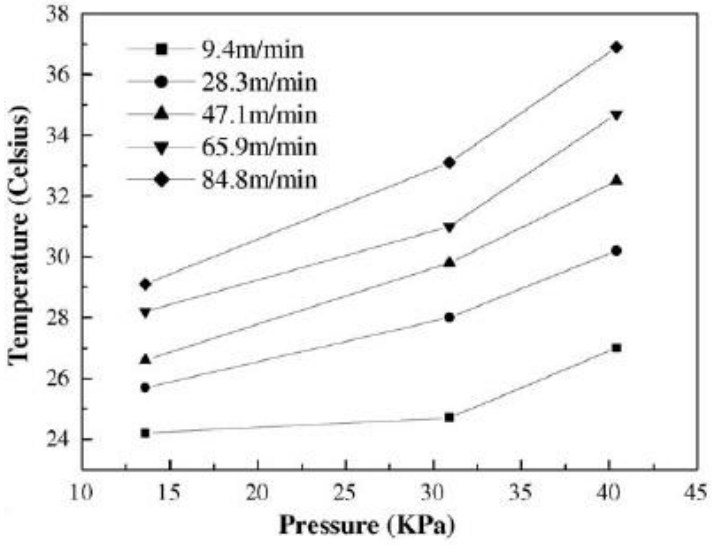

Fig. 2-5: Effect of pressure on temperature rise [19]

PV: The temperature rise in the wafer is directly proportional to the product of pressure or load and relative velocity. The reason being the input mechanical power i.e. PV is converted into heat. Thus increase in PV would imply increase in the heat generated and thus the temperature rise. Fig. 2-6 shows a linear relation between temperature and PV. Fig. 2-7 shows a three axis plot between temperature, pressure, and platen speed. The figure suggests that both pressure and velocity contribute to the temperature rise. Higher temperature values are observed when both pressure and speed values are high and the least temperature is observed for least values of pressure and speed. Also, more temperature rise is observed when the slurry is used for polishing compared to water at same PV values.

Coefficient of friction: The friction conditions between the pad and wafer change with the progress of polishing. It can be attributed to various factors such as roughness and hardness of the pad, abrasive particles, and wafer surface conditions. The extent of friction determines the total heat generated, heat partitioned to the wafer, and thus the temperature rise in it [20].

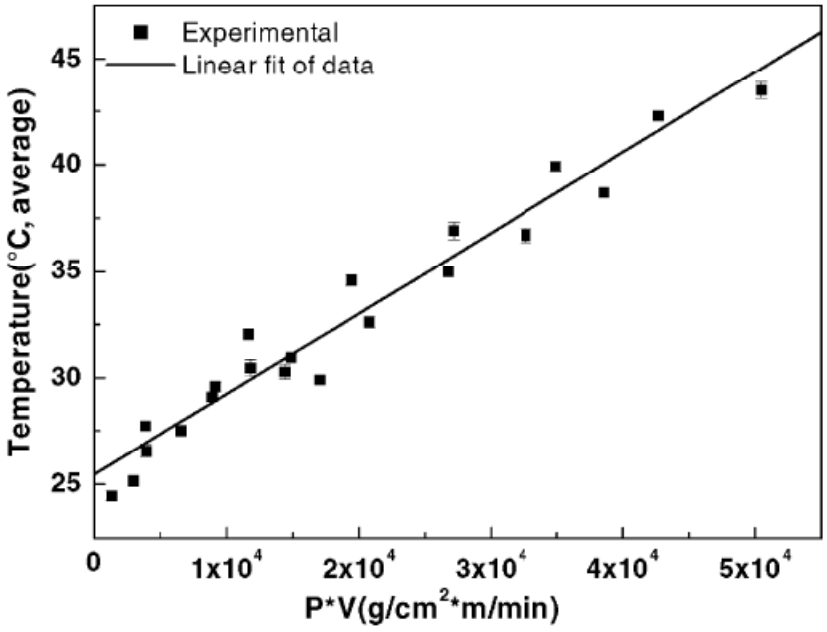

Fig. 2-6: Temperature variation with PV showing a linear variation [20]

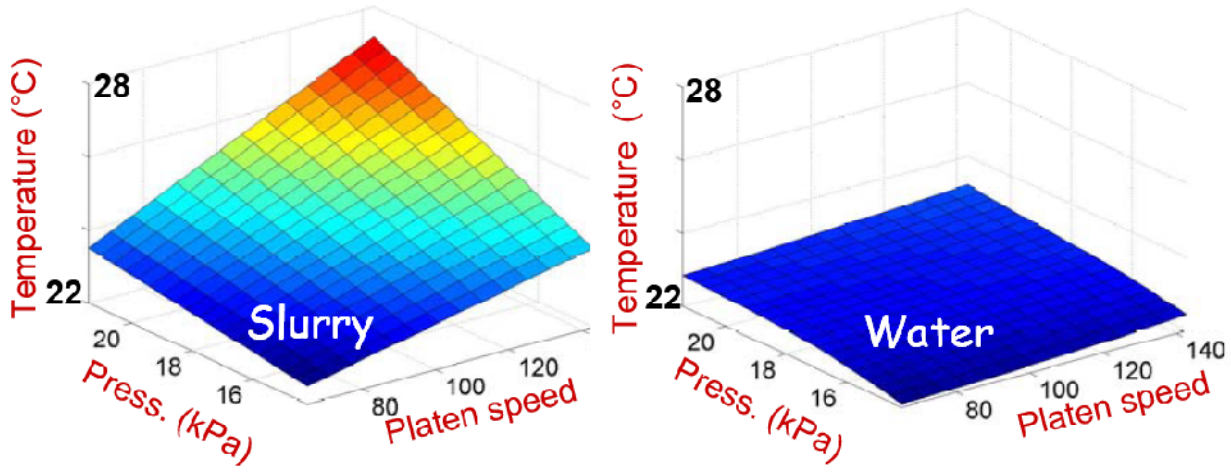

(a) (b)

Fig. 2-7: Three axis plot of Pressure, Speed and Temperature for (a) Slurry (b) Water [22]

Slurry Properties: Slurry heat capacity is the tendency of the slurry to dissipate heat away. More heat capacity of the slurry implies more heat taken away from the wafer per unit mass of the slurry and thus lesser temperature rise in the wafer. Slurry flow rate is the amount of slurry which is dispensed on the pad per unit time. The higher this amount more would be the heat taken away from the wafer.

Pad properties: Pad properties, such as asperity density and pad material property to embed the abrasives directly influence the total heat generated in the process. Many properties, such as mean asperity height and asperity hardness, elastic modulus of the pad which further influences the actual contact area of the pad with wafer change along with polishing. The thermal properties of the pad, such as thermal conductivity and thermal diffusivity of the pad are essential parameters to decide the amount of heat going into the wafer and consequent temperature rise for the wafer [19],[27].

Wafer properties: Apart from the surface roughness properties of the wafer which influence the coefficient of friction and the total heat generated, there are other properties of the wafer which can influence the temperature rise value. The conductivity of the wafer material is important parameter to

decide how much heat is partitioned into the wafer. The size and shape of the wafer is another parameter to determine the amount heat going into the wafer. For example, the heat partition for a copper disc and a copper wafer of the same size under the same polishing conditions would be different [21].

2.4: Material removal process in polishing

Material removal occurs when hard abrasive particles present in the slurry are pressed against a softer wafer and a relative motion is provided to shear off the material. Pad acts as a medium to rigidly hold the abrasives in their asperities and remove the material like a cutting tool. However, all the abrasive particles are not engaged in this process; some of them are inactive as they are located in the voids of the pads. Some abrasives may not be held rigid enough to perform a two-body abrasion, rather they roll between the surfaces of pad and wafer to give some material removal.

The basic difference between the material removal in CMP and conventional polishing or lapping is shown in Fig. 2-8. The real contact area of the pad and the wafer is quite small compared to the apparent contact area because of the waviness and roughness of the pad. In the conventional polishing, size of the abrasives is large enough and is in the microscale which is same as the order of pad asperities. Thus in this case when the pad comes in contact with the wafer, the abrasive particles which are embedded in the voids or lower portions of the pad are large enough to cause two-body abrasion. Most of the abrasive particles contribute to the material removal in this case. In CMP, the size of the abrasive particles is in the nanoscale which is much smaller than the microscale order of the pad asperities. Most of the abrasive particles tend to be in the majority region where the pad and wafer are not in contact. They are free to move in the slurry medium and are either inactive or cause three-body abrasion, which contributes negligibly to the material removal. Fewer abrasive particles which are embedded in the pad regions in direct contact with wafer are responsible for the two-body abrasion and thus the material removal [23].

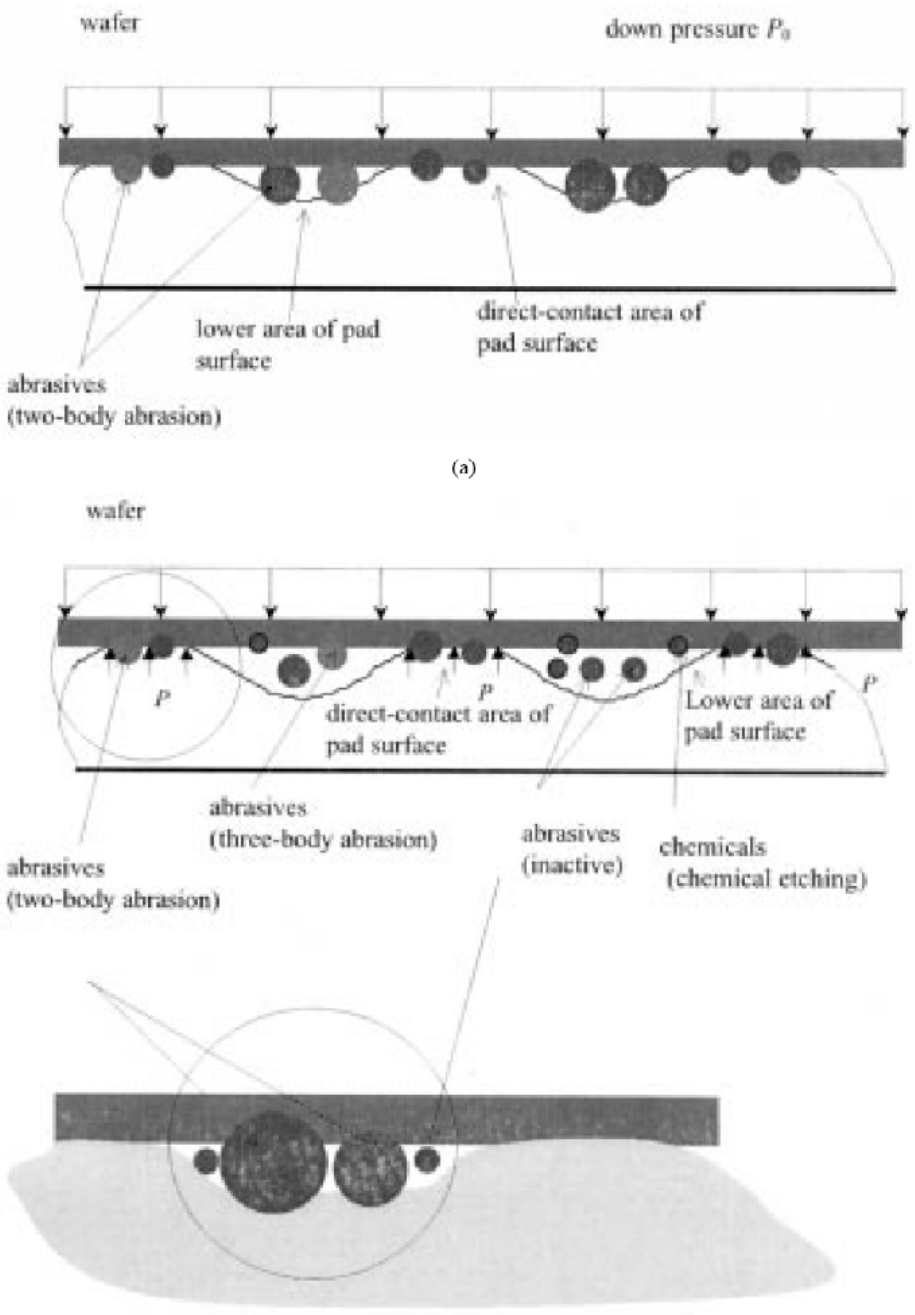

Fig. 2-8: Material removal mechanism in (a) conventional polishing and lapping and (b)in CMP [23]

2.5: Material removal mechanism in CMP

There are typically two contact modes in CMP between the pad, the slurry, and the wafer depending on the relative velocity and down pressure, namely, hydro-dynamic contact mode and solid-solid contact mode. Fig. 2-9 shows the two contact modes. In the hydro-dynamic contact mode, the down pressure applied on the wafer surface is quite less and the relative velocity of wafer and pad is quite high resulting in a thin fluid (slurry) film formation between the wafer and the pad. The thickness of the film is in microscale whereas the abrasive particles are in nanoscale. Most of the abrasives float in the slurry and become inactive, the material removal is accomplished by few of the abrasive particles by three-body abrasion. In the solid-solid contact mode, the relative velocity between the pad and the wafer is lower and the down pressure on the pad is higher resulting in contact of pad asperities with the wafer. The abrasive particles in those asperities which are in contact with the wafer get embedded in the pad and remove material by two-body abrasion [23].

Further details of solid-solid contact mode at the asperity level are given in Fig. 2-10. At a relatively less down pressure on the wafer, the pad asperity is not in direct contact with the wafer. Rather the pad asperity has the embedded abrasive particles in contact with the wafer. At a higher load, the pad tends to bend around the abrasive particles to get in contact with the wafer. This increases the actual area of contact between the pad and the wafer. There would be a change in the force applied on the abrasive particles in the two cases. In the first case, if it is assumed that there are N active abrasive particles, the force applied on the asperity is supported by these N particles. The mean force on each particle would be $F = PB/N$ where P is the pressure and B is the area of the asperity. In the second case, the force is distributed to a part of the asperities in contact with the wafer as well as the abrasives. The mean force on each particle would be $F = P (\pi/4) x^2$ where x is the diameter of the particles. The average area of the asperity per abrasive particle

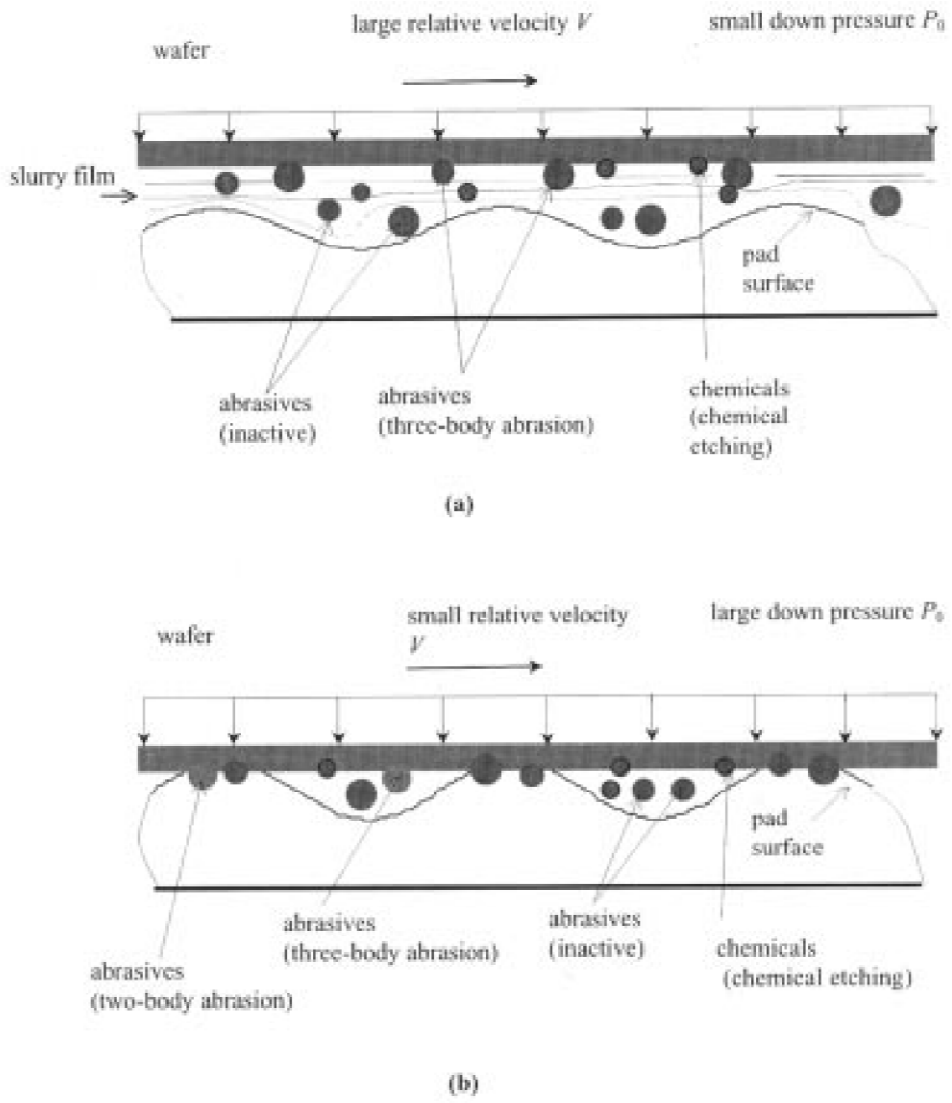

Fig. 2-9: Material removal mechanism in CMP (a) Hydrodynamic contact mode (b) Solid-Solid contact mode [23]

i.e. B/N is larger than the cross sectional area of abrasive i.e. $(\pi/4)\ x^2$. This implies that there is a reduction in the force on each particle with increase in pressure or increase in the area of contact. This results in a reduction of MRR compared to the expected values [23].

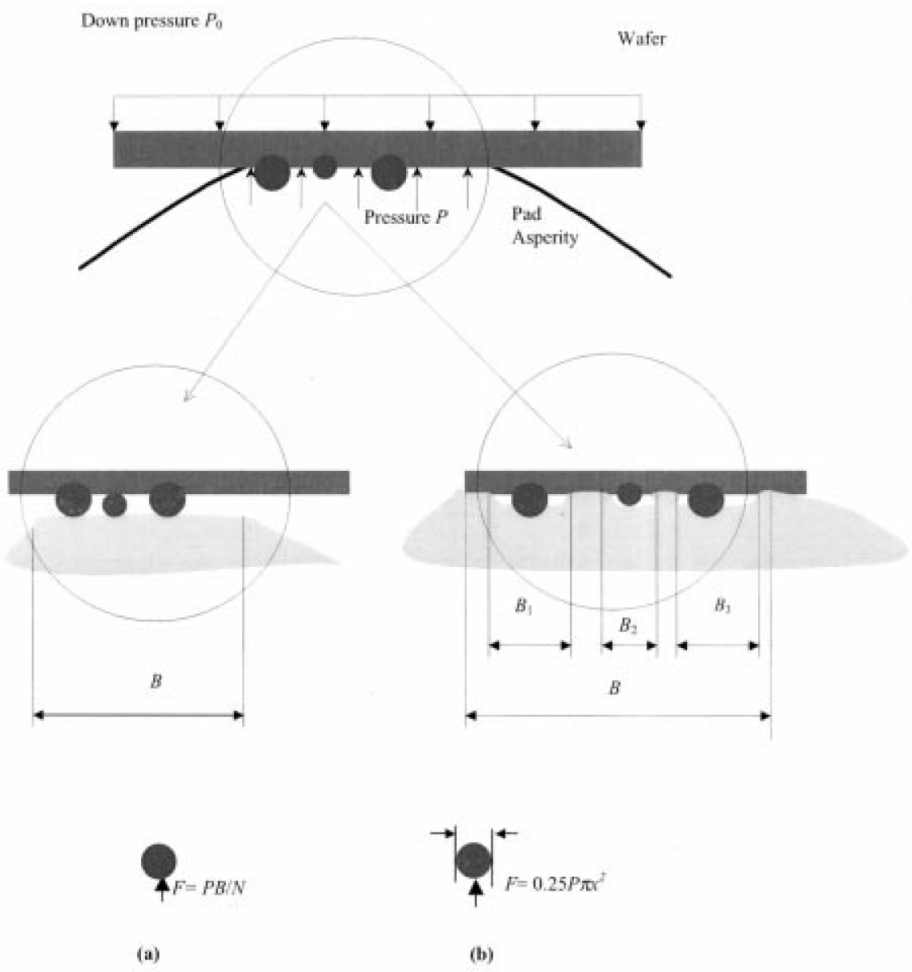

Fig. 2-10: Material removal in solid-solid contact mode in CMP (a) at relatively less down pressure (b) at higher down pressure [23]

The material removal is the product of average material removed by a single abrasive with the number of active abrasives per unit time. Similar equation was shown by Luo and Dornfeld [23] is:

MRR = $\rho N V_{ol,}$ where ρ is the density of the wafer, N is the number of active abrasives and V_{ol} is the volume of material removed by single abrasive.

Another way of representing MRR is to show it as a function of the input parameters such as pressure and velocity. Preston proposed an equation of the form:

MRR = K PV, where P is the pressure, V is the relative velocity and K is a constant, called, the Preston's constant.

MRR is proportional to the product of P and V which represents the mechanical power input and K represent the effect of other parameters. However, Preston's equation only shows the influence of process parameters including pressure and relative velocity. It neglects the effect of consumables, such as pad, abrasive particles, and wafer which have been shown experimentally to effect the MRR. Various things cannot be explained by Preston's equation, such as polishing differences between softer and harder pad or, in general, different materials of the pad, the effect of abrasive size and shape on MRR, abrasive and wafer hardness, abrasive-pad and pad-wafer interactions, decrease in the force applied on the abrasives with increase in the contact area which leads to lesser MRR and so on. It has been shown that the linear Preston's equation is ideally applicable for polishing with a pad whose hardness is similar to or more than that of abrasives and wafer being polished [24]. But in CMP, polishing pads are typically very soft compared to the abrasives and the wafer. The size of the nanoscale abrasives in CMP is much smaller than the size of the pad asperities exposing pad to contact the wafer, thus Young's modulus, hardness, roughness, shape, and asperity distribution of the pad play a significant role for MRR.

2.6: Factors effecting MRR

Load: An increase in the downforce or pressure applied on the wafer by the pad would increase the depth of penetration of the abrasive particles and thus giving more material removal. The increase of removal rate with pressure is linear and is shown in Fig. 2-11 for various RPM along with repeated tests. For polishing at a constant RPM of 50, the increase in pressure from 2 to 6 psi showed an increase in MRR from 400 to 700 A/min. For the same range of pressure, higher difference in the MRR is observed at higher RPM conditions. At higher load, due to an increase in the pad contact area the force on the abrasive particles is decreased which decreases the MRR compared to the expected values [23].

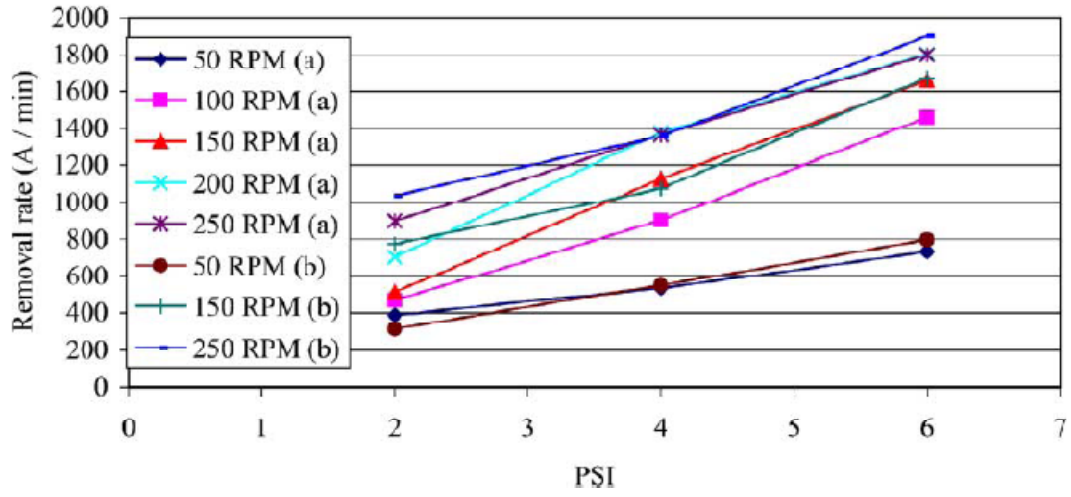

Fig. 2-11: Variation of material removal rate with pressure [24]

Velocity: Sliding velocity between the pad and the wafer determines the shear force applied on the abrasive particles. Higher velocity or RPM would imply higher shear force and thereby more material sheared off for the same depth of penetration of abrasive particles. For constant pressure, MRR increases with increase in the sliding velocity or RPM as shown in Fig. 2-12. Fig. 2-12 shows that MRR increases from 400 A/min to 900 A/min with increase in the RPM from 50 to 250 at a constant pressure of 2 psi. The increase in MRR is higher for the same increase in RPM at higher pressures of 4 and 6 PSI.

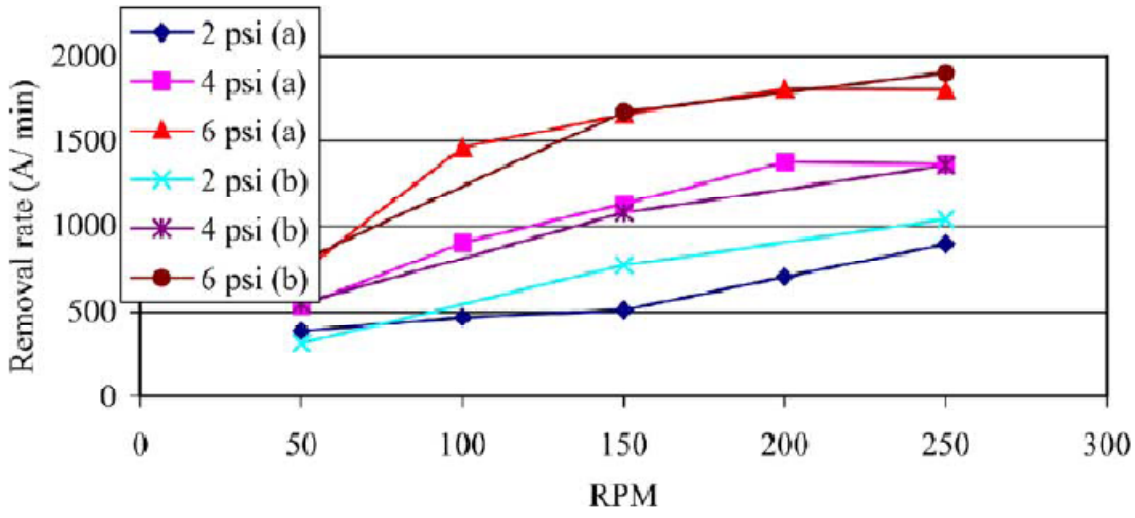

Fig. 2-12: Variation of material removal rate with RPM [24]

Abrasive concentration: Abrasive concentration increases the number of active abrasive particles. Material removal is directly related to the no of active abrasive particles as shown by Luo and Dornfeld [23].The Material removal rate increase linearly with abrasive concentration as shown in the Fig. 2-13. Figure shows that the MRR increases from nearly 0 to 1500 A/min with an increase of abrasive concentration from 0 to 30% in the slurry for abrasive sizes of 50 and 140nm. Abrasive size of 80nm was giving higher MRR compared to 50 and 140nm sized abrasive particles for the same abrasive concentration in the slurry.

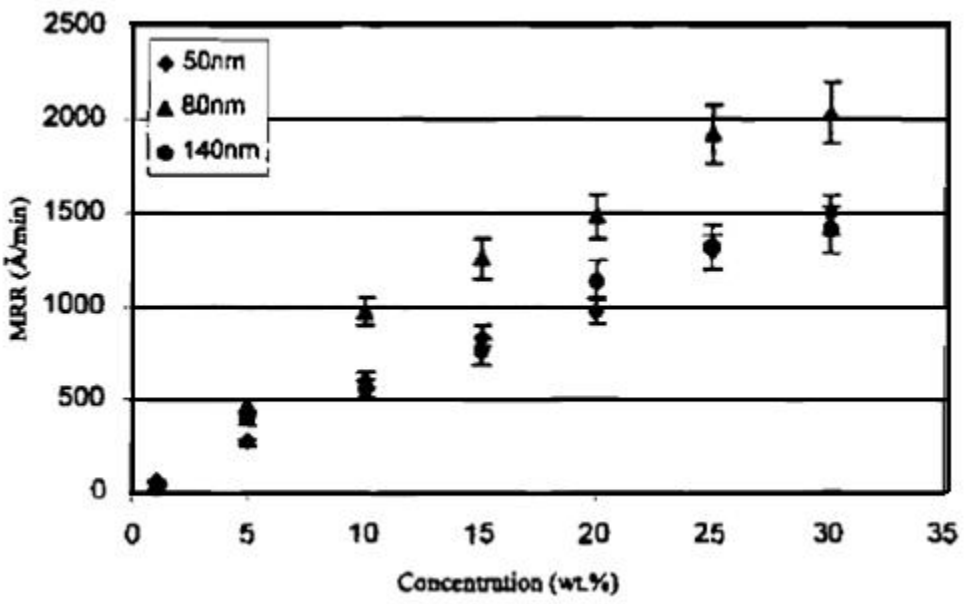

Fig. 2-13: Increase in MRR with abrasive concentration [28]

Abrasive size: The MRR increases with increase in the size of abrasive to a certain value of abrasive size and shows a decrease for further increase in the abrasive size. It is because when the particle size is larger than approximately twice of the nano film thickness, the MRR will decrease because it is harder for the large particles to be entrained into the interface between wafer and pad asperities. Smaller particle size show lower MRR because the abrasives tend to be trapped in the valleys among pad asperities and will not contact the wafer to remove material. Thus, there is an optimal size of abrasive particles for a

combination of pad and wafer which gives highest MRR. Fig. 2-14 shows the variation of MRR with abrasive size. For constant P and V values, the MRR increases with increase of abrasive size until a particular value of abrasive size, for higher abrasive size the MRR shows decrease in value. In the experiments conducted by Zhou *et al.* [28], the highest MRR was obtained by 80 nm size abrasives.

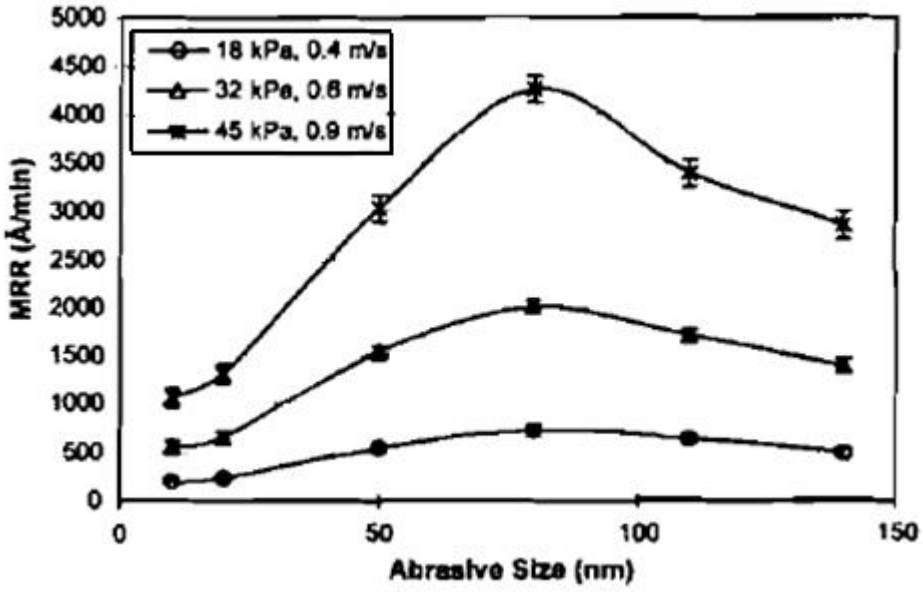

Fig. 2-14: Variation of MRR with abrasive size [28]

PV: The product of load or pressure and RPM or sliding velocity represents the power applied in the polishing process which is equivalent of the work done to move abrasives and thus shear material on the wafer in the presence of load applied by the pad. Thus the material removal would increase with the increase in applied load and sliding velocity. MRR shows a linear increase with product of pressure and RPM as shown in Fig. 2-15.

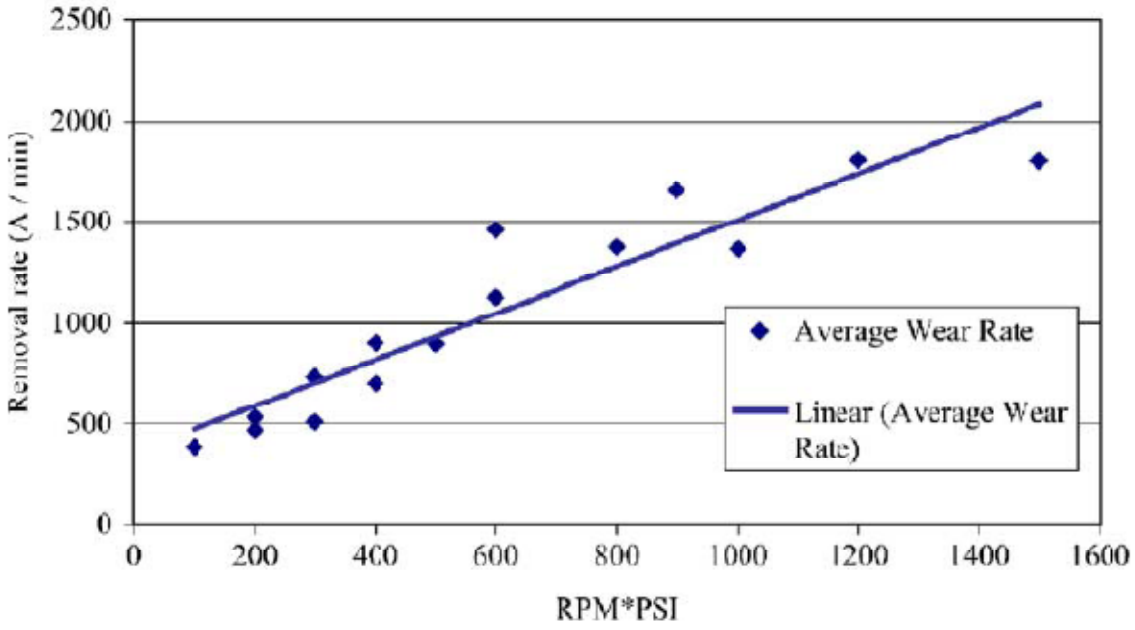

Fig. 2-15: MRR linear with product of RPM and pressure [29]

Pad properties: Material removal is strongly related to the properties of the pad. Roughness of the pad is an important parameter to determine MRR. If the pad is new, it is rough or has asperities hold the abrasives and remove material. But eventually with polishing the pad asperities get worn off or flattened which decreases its capability to hold abrasive particles and remove material. Thus the surface profile of the pad and the ability of the pad asperities to hold the abrasive particles influence the MRR. Another pad property is its hardness. A hard pad is less pliable whereas a soft pad has tendency to bend easily. Softer pad has tendency to bend around the abrasive particles and thus expose the pad directly to wafer whereas in hard pad only abrasive particles are in contact with wafer [25], [26], [27].

Wafer properties: An unpolished wafer yields more MRR for the same conditions compared to a polished wafer because of rougher topography and thus higher coefficient of friction to give higher MRR [20].

2.7: MRR decay

It has been observed that the MRR goes on decreasing in the polishing process with time if pad conditioning is not applied. Fig. 2-16(a) shows the decrease in normalized mean MRR from 0.36 to 0.26 for a polishing time of 50 minutes. Fig. 2-16(b) shows the decrease in the removal rate for various pads in a time span of 50 minutes.

The decrease in MRR can be attributed to the following reasons:

Decrease in coefficient of friction: The coefficient of friction (COF) between the pad and the wafer which comprises of many factors decrease with polishing time. Fig. 2-17 shows the decrease of COF from 0.35 to 0.13 in a polishing time of 500 seconds. The main reason for the decrease in the COF is the wear of pad asperities along with time. If the pad is not conditioned then the pad asperities tend to get leveled down along with the polishing time. The tendency to anchor the abrasive particles is decreased and thus the MRR decreases. If the slurry being circulated is not reconditioned, the abrasives get blunt

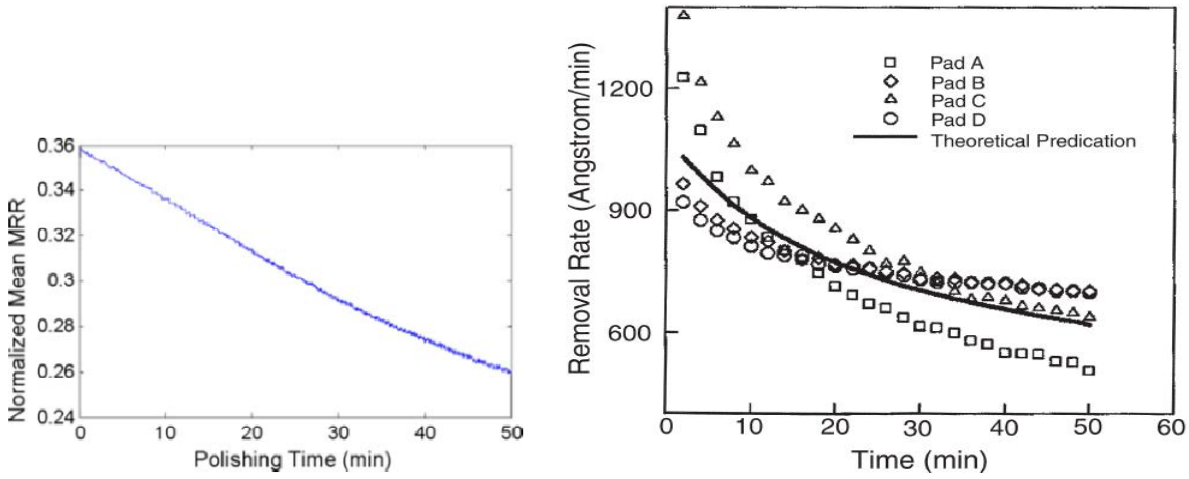

(a) (b)

Fig. 2-16 (a), (b): Decrease in MRR with time [25], [26]

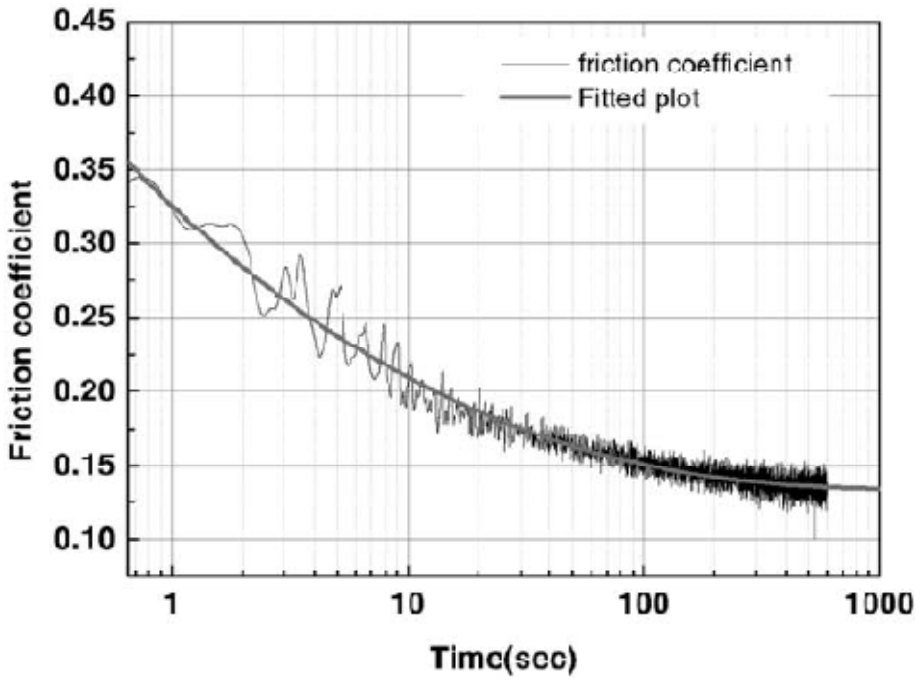

Fig. 2-17: Coefficient of friction decreasing with time during polishing [20]

along with polishing time and their abrasion ability gets lesser. Also, the wafer being polished gets smoother along with polishing. Thus there is an overall decrease in the COF along with polishing which decreases the MRR.

Increase in the pad contact area: The elastic modulus of the pad which is made of polymeric material is sensitive to heat and the modulus decreases with the rise in temperature in a continuous polishing process. The reduction in the modulus of elasticity of the pad implies the reduction in the hardness of the asperities. This means that at the same load, the pad is pressed more to increase the area of contact. Fig. 2-18 shows the increase in the area of contact with temperature. The normalized contact area increases from 1 to 2.2 with the increase in temperature from 20°C to 60°C. Also, the pad elastic modulus decreases from 29 to 11 MPa for the same increase in temperature. As already discussed, the increase in the pad contact area decreases the force on abrasive particles due to distribution of same load on more area and thus decreases the material removed by the abrasives.

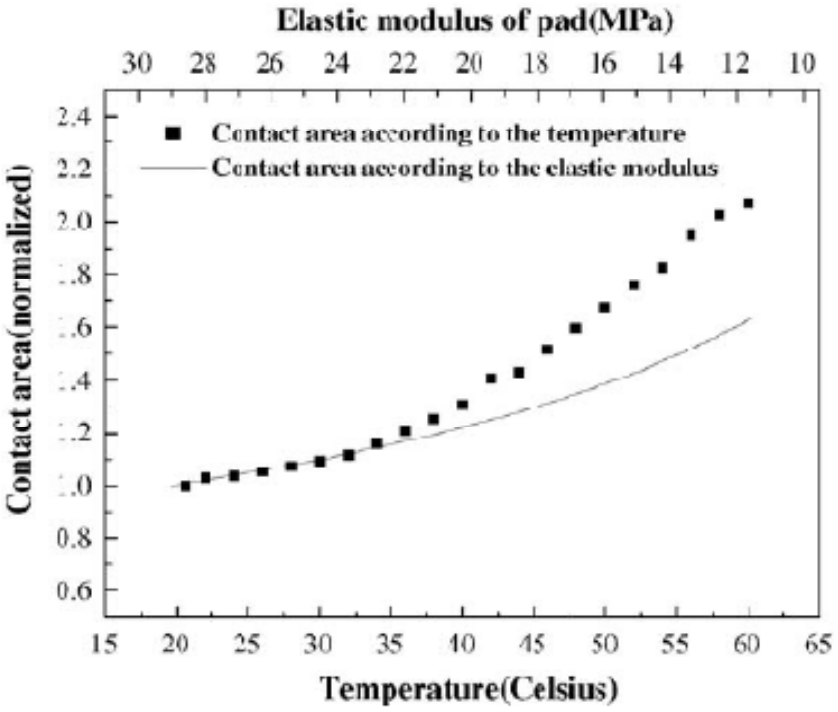

Fig. 2-18: Increase in the pad contact area and decrease in elastic modulus with Temperature [19]

2.8: Pad wear

The pad asperities tend to get flattened along with time during polishing process. The reason is wear of the pad asperities by the abrasive particles under the presence of load and shearing force. It implies that the pad becomes smoother or 'glazed' eventually with polishing. With the asperities of the pad getting blunt, their tendency to hold the abrasive particles decreases and thus the material removing ability of the pad decreases. Rpk which means 'reduced peak height' is an estimate of the peaks of pad asperities above the main plateau. It is related to the wear characteristics of the pad and it decreases with polishing time as the asperities get flattened. To avoid this situation pad conditioning is performed which involves pressing a rotating disc with a rough surface against the pad during the polishing process. The rough disc abrades the pad to convert the smooth and blunt asperities into rough, increasing Rpk and thereby MRR. Fig. 2-19 shows the reduction of Rpk and MRR with polish time, if pad conditioning is not

done, and both of them increase if pad is conditioned. Rpk decreases from 3.5 to 2.2 µm and removal rate decreases from 2500 to 1300 A/min in a polishing time of 30 min. Pad conditioning increases the Rpk value to 3.3 µm and removal rate to 2400 A/min.

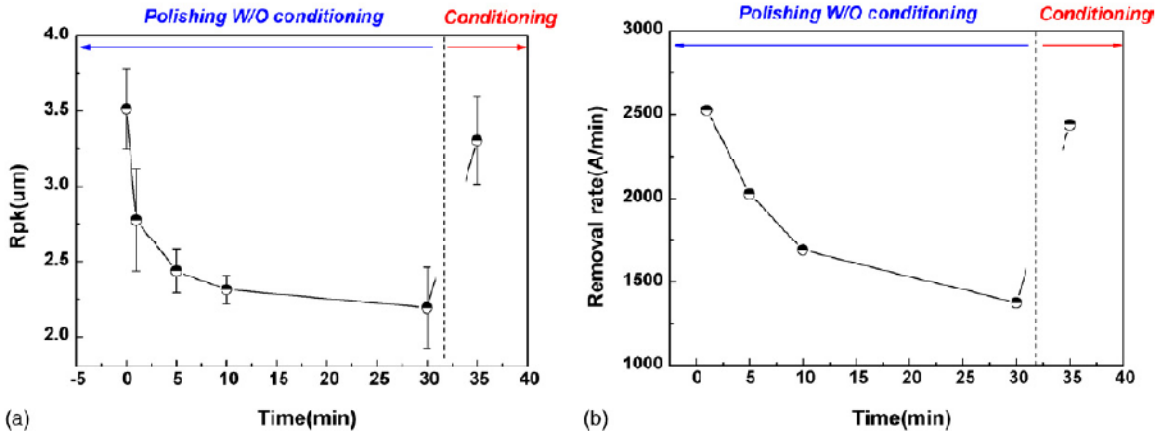

Fig. 2-19: Decrease of (a) Rpk and (b) MRR with polishing time and their increase with conditioning [27]

Chapter 3: Sensors in Chemical Mechanical Polishing

A sensor is an instrument which measures a physical quantity and converts that quantity into a signal which can be assessed by an observer or by an appliance.

3.1: Reasons for the use of sensors in Chemical Mechanical Planarization

End point detection: This is the most important reason for the use of sensors in CMP. Polishing end point may refer to polishing until the exposure of the barrier layer or removal of a required quantity of material. The variation in the sensor signal at polishing end point can be assessed by a controller and the polishing process can be stopped at that point to give precisely finished wafers. However, if the sensors are not used for this purpose, the method would be to stop polishing and check the wafer repeatedly. This would be slow and still an imprecise method. Almost all kinds of sensors: optical, temperature, pressure, acoustic, vibration, infra red and others can be used for end point detection because of the change in corresponding physical properties as soon as the barrier layer is exposed.

Uniform polishing of wafer: Uniform removal of material from the wafer surface is difficult to achieve in an uncontrolled process. As the relative velocities at the periphery of the wafer and at the center of the wafer are different, the material removed from these locations should be different. Sensors are attached behind the wafer to obtain a surface profile and controllers can change the parameters, such as pressure, temperature accordingly to make the contour uniform.

Defect detection: Defects in the form of scratches and metallurgical damage can arise in wafers due to excessive usage of abrasive, pressure, and unevenness in pressure. The unevenness in any parameter, such

as temperature, pressure, alignment, flow rate, can be detected by sensors and compared to the permissible values by controllers.

Detection of pad conditions: To ensure that pad profile and roughness are uniform throughout the surface, it is important to incorporate sensors in the CMP setup. The mechanical properties of the pad, such as elasticity and coefficient of friction are monitored by the sensors, e.g. pressure, vibration, etc. As the pad surface gradually gets smoother and blunt, it is important to decide the optimal amount of conditioning provided to the pad so that the wafer finish are within the tolerance limits.

To check the presence and proper positioning of the wafer: In the commercial CMP, it is important to detect the presence of wafer in all the wafer carriers. Also, during polishing, misalignment of the wafers, jumping of the wafer from the wafer carrier, and breakage of wafer can be detected by sensors, such as vibration, pressure, optical and so on.

To measure stresses in the wafer: Pressure and temperature sensors are used under the wafer to give pressure and temperature contours respectively for the wafer. These contours can be used to evaluate the stresses in the wafer during the polishing process.

General measurement purpose: Apart from positioning the sensors around wafer, pad, and slurry, sensors can be implemented in other parts of the CMP system. A temperature sensor can be used for temperature measurement in a temperature control unit, a pressure sensor can be used for measuring pressure in the fluid lines, a displacement sensor can be used for measuring the displacement of various moving components. The measurement from the sensors is assessed by a control unit which maintains the parameters to be optimal.

3.2: Different kind of sensors used in chemical mechanical polishing

Optical sensors: Optical sensors detect the presence of light or electromagnetic radiation. Laser interferometer, radiation sensors, light sensors also come in the same category. Their prime use is for end point detection in CMP. A light source emits light on the semiconductor wafer which reflects back to the optical sensor. As the end point of polishing is reached, a difference in the intensity of light is obtained because of different reflectivity of the under layer. Optical sensors can also be used for measuring the distance from a point.

Acoustic emission sensors: An acoustic emission sensor detects the acoustic emissions which are mechanical waves generated by the plastic deformation of two rubbing surfaces. As a wafer or a conditioner rubs against the pad, acoustic emissions are generated due to plastic deformation which can be detected by the sensor. By measuring the intensity of these waves the progress of the polishing process can be determined.

Infrared sensors: Infrared sensors detect the magnitude of the infrared rays. Infrared rays are generated during the polishing process because of the frictional heat generation between the wafer and the pad. Measurement of the infrared rays can indicate the temperature at the particular point. Infrared sensors can be used for detecting the polishing end point when more heat is generated during the polishing of the barrier layer.

Eddy current sensors: These sensors are used to measure the proximity and the thickness of the wafer. The sensors are placed at a fixed distance from the wafer. Sensor is made of a coil in which alternating current is passed which generates electromagnetic field around the wafer and thus generates eddy current in the wafer. The eddy current generated in the wafer vary the electromagnetic field in the sensor depending on the distance. This concept is used to measure the distance and thickness of the wafer.

Ultrasonic sensors: Ultrasonic sensors are quite similar to radiation or optical sensors in their functioning. They detect the sound waves of ultrasonic frequency. Ultrasonic waves emitted from a source and reflected back by a surface can be detected by an ultrasonic sensor. This can be used to measure the distance of the surface.

Displacement sensors: Displacement sensors are used to measure the distances in CMP. Distances can refer to the space between the wafer and the pad, thickness of the wafer, uniformity in wafer or pad and so on. Hall effect sensors, optical interrupter sensors, eddy current sensors are some of the displacement sensors which are also called proximity sensors.

pH sensors: These sensors are used in CMP for monitoring the pH of the slurry. A dynamic sensor is required as the pH of slurry keeps on changing due to mixing of the byproduct of the wafer polishing process. The pH can give various indications about polishing process.

3.3: Temperature sensors

Temperature measurement is an important task in many applications of technology. Temperature sensor estimates the value of temperature by using a specific physical property. The physical property might be variation of thermal coefficient of expansion, electrical resistance of conductor, voltage vs current characteristics of diode or so on with temperature. The term temperature sensor encompasses instruments from a thermometer to an advanced infrared sensor. For the context of CMP process, temperature sensors can be classified into two groups, non-contact and contact.

Non contact temperature sensors: Noncontact temperature sensors measure the thermal radiant power of the infrared or optical radiation that is received from a known or calculated area on a particular surface.

Contact temperature sensors: Contact temperature sensors are in physical contact with the body whose temperature has to be measured. The sensor actually measures its own temperature, and with an

assumption of thermal equilibrium with the body it is assumed that temperature at the contact surface of the sensor would be same as that of the body. Types of contact temperature sensors are:

1. Thermocouples
2. Resistance Temperature Detectors (RTDs)
3. Thermistors
4. Semiconductor/IC Temperature sensor

3.4: Purpose of using temperature sensors in CMP

3.4.1: End point detection

Change in the frictional heat: In the method proposed by Sandhu [30], either single or multiple sensors are mounted in the wafer carrier just above the wafer, just beneath the pad and besides the platen where slurry byproduct is falling as shown in Fig. 3-1. The purpose is to detect the end point. The substrate (wafer) has a cover layer which has to be planarized until the underlying layer is exposed. The underlying layer is made up of material having more coefficient of friction. The underlying layer thereby produces more heat on polishing. This increase in heat generation can be detected by temperature sensors and polishing can be stopped.

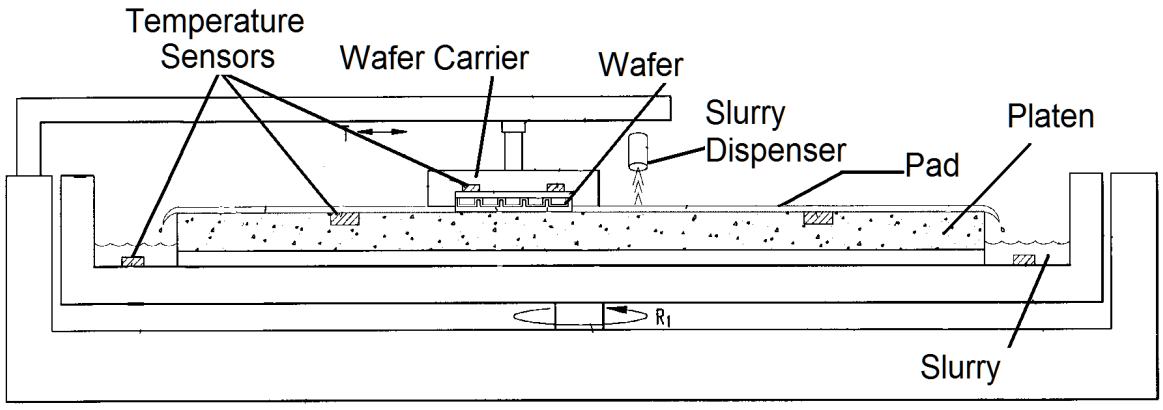

Fig. 3-1: CMP Setup proposed by Sandhu [30]

The arrangement for end point detection in CMP using temperature sensors as proposed by Koo *et al.* [31] is shown in Fig. 3-2. A temperature sensor is located in a cavity in the polishing pad. The sensor can be placed at the extreme top of the cavity to measure pad-wafer interface temperature or the sensor can be placed at the center of the cavity to measure temperature of the pad. Another sensor on the edge of the wafer carrier measures temperature of the slurry. There is a feedback controller and monitoring unit to compare the measured temperature values from the sensors with the predetermined and fixed values of temperature/ heat to determine the end point.

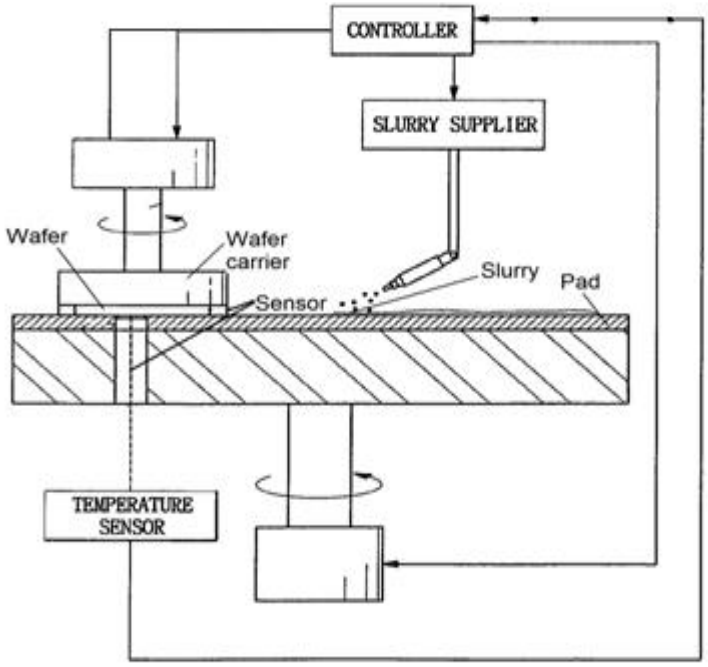

Fig. 3-2: CMP setup proposed by Koo et al. [31]

Endpoint on the basis of material thickness to be removed: In the method proposed by Ono *et al.* [32], the wafer carrier has a heating element just above the wafer as shown in Fig. 3-3. There is a temperature sensor in the pad which shows the pad-wafer interface temperature. A fixed amount of heat is given by the heating element which is transmitted through the wafer and is detected by the sensor. As the polishing progresses, the thickness of the wafer decreases and there is a variation in the heat detected by

the temperature sensor. A controller is used for comparing the temperature values from the sensor with predetermined values. Polishing is stopped when desired amount of material has been removed from the substrate.

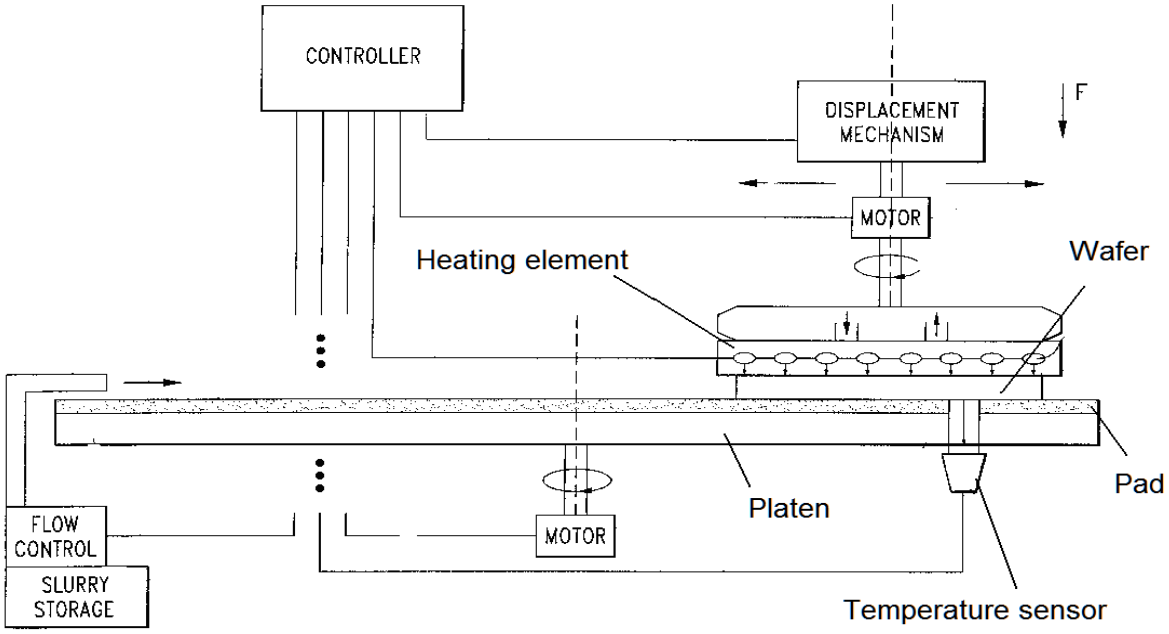

Fig. 3-3: Setup proposed by Ono et al. [32]

3.4.2: Uniform polishing of wafer

Heating and measuring temperature of the slurry: During polishing of the wafer, some slurry is trapped in the center where maximum temperature is generated. Since the slurry around the edges of the wafer is cooler, the material removal from edges is lesser which leads to non-uniformity. To eliminate this problem, the incoming slurry can be heated to a temperature equivalent at the center of the wafer.

Fig. 3-4 shows the method proposed by Lin [33], the temperature of the slurry just below the wafer is measured by a temperature sensor which is fixed in the pad. The slurry temperature at the inlet nozzle is also measured by a temperature sensor. A controller measures the difference between the

temperature values from the two temperature sensors and operates a heater to raise the temperature of the incoming slurry.

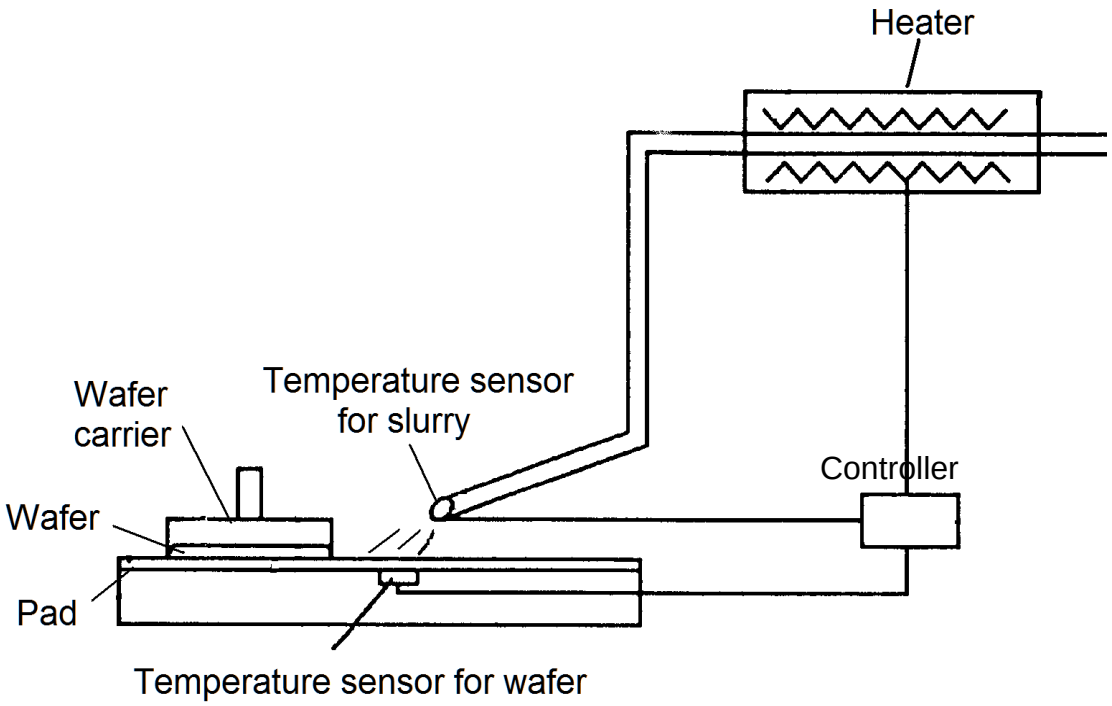

Fig. 3-4: Setup proposed by Lin [33]

During the start of the polishing process less heat is liberated and with the advancement of the process the total heat generated increases. This non-uniform heat leads to non-uniform wafer polishing and defects. Naujok *et al.* [34] proposed a method in which the slurry is heated initially when it is relatively cold and at a later stage of polishing when the slurry is hot, it is cooled to maintain nearly the same temperature throughout polishing process. Temperature sensor is used to measure the temperature of the slurry.

Heating and measuring temperature of the pad: In the case of a belt pad, the position of the pad relative to the wafer is fixed. The temperature of the pad can be varied along the width to ensure more heat is provided at the edges of the wafer during polishing.

In a method devised by Wu *et al*. [35] which is shown in Fig. 3-5, slurry of different temperatures are dispensed at different widths of the belt pad. This creates zones of different temperatures on the belt pad. Accordingly, the wafer being polished would have different temperatures across it's width which can be monitored via temperature sensors and controllers to uniformly polish wafer.

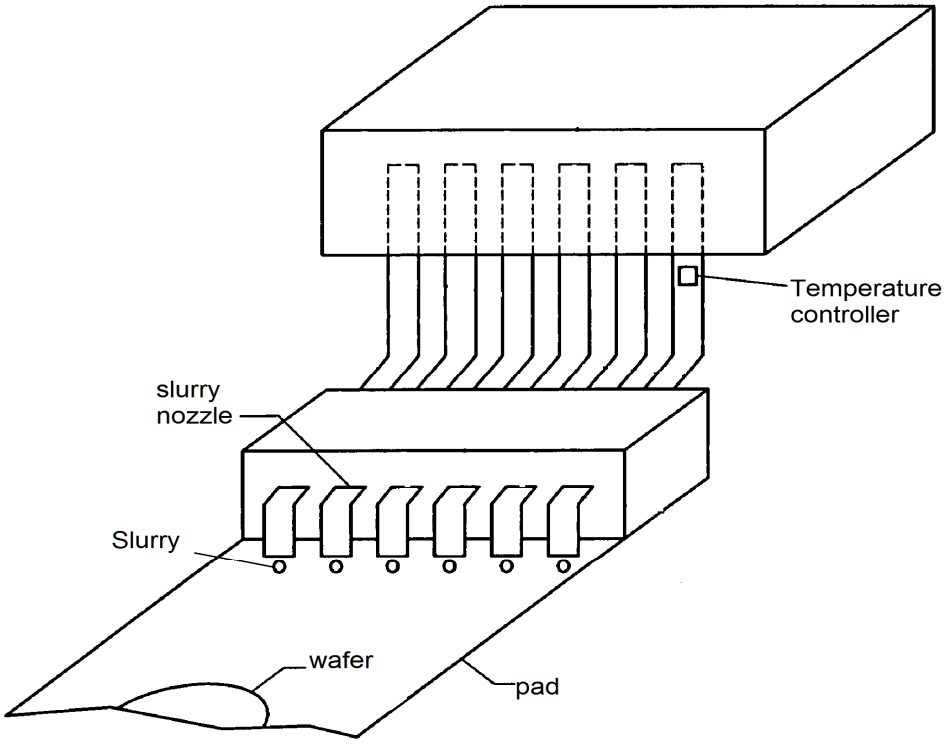

Fig. 3-5: Setup proposed by Woo et al. [35]

Pham *et al*. [36] proposed a method of zonal heating of belt pad as shown in Fig. 3-6. There is a heating arrangement in the platen which consists of outlets through which a hot fluid is released to heat the belt pad. There is a temperature differential in the fluid released through the outlets in the radial direction. This temperature difference ensures that the wafer which sits over the platen is heated more on the periphery than the center. Temperature sensors are used to measure the temperature of the slurry and the pad. The signals from the sensors are used by a controller to heat the fluid accordingly.

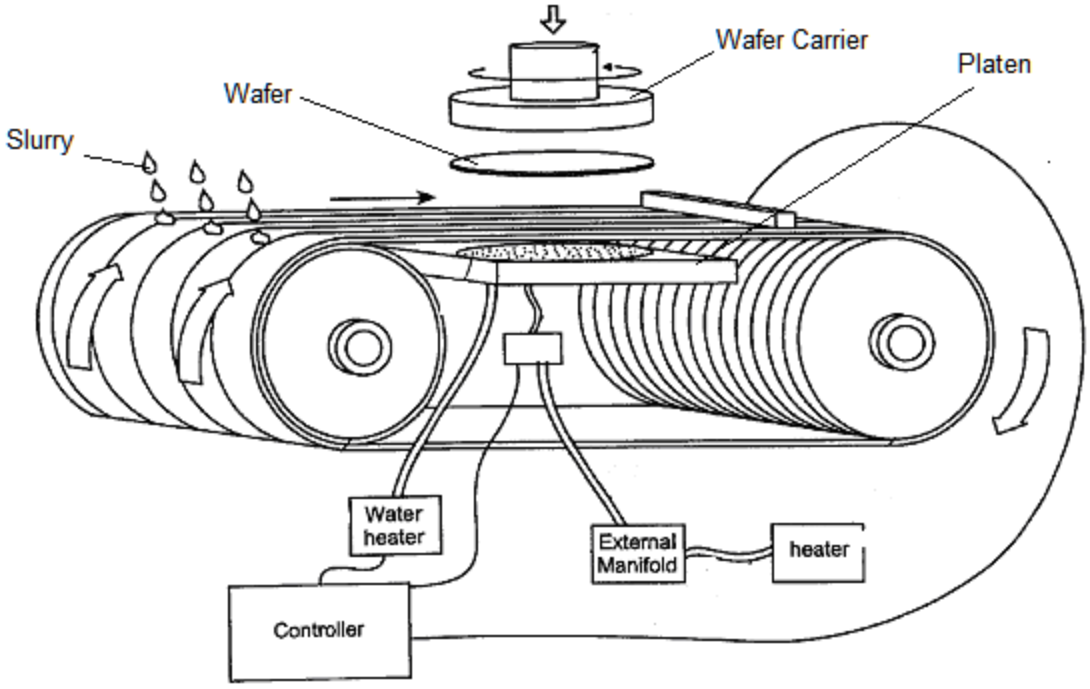

Fig. 3-6: Setup proposed by Pham et al. [36]

Zonal heating of the wafer: By a heating arrangement in the wafer carrier just behind the wafer, the wafer is heated in zones of different temperatures from higher at the periphery to lower at the center to ensure uniform polishing.

In a method proposed by Robinson *et al*. [37], which is shown in Fig. 3-7, a heater coil is supported at the guide ring of the wafer to heat the periphery of the wafer. A controller uses signal from a temperature sensor in the guide ring to operate the heater coil.

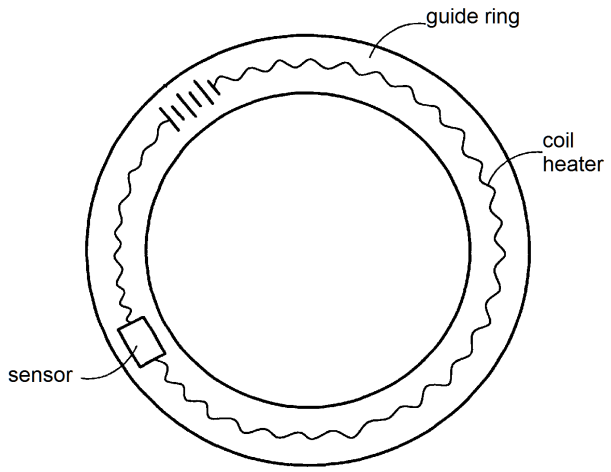

Fig. 3-7: Arrangement of heating coil in the guide ring proposed by Robinson et al. [37]

In a method devised by Bright *et al*. [38], which is shown in Fig. 3-8, the wafer carrier has a heating arrangement in the form of concentric zones of different temperatures. The heating temperature is kept in increasing order from the inner zone to the outer zone. Temperature sensors are arranged radially in the wafer carrier to measure temperature in those zones. The heating arrangement consists of either resistive heating or a fluid of different temperatures supplied in those zones. Signals from the temperature sensors are used by the controller to adjust the temperature of the zones.

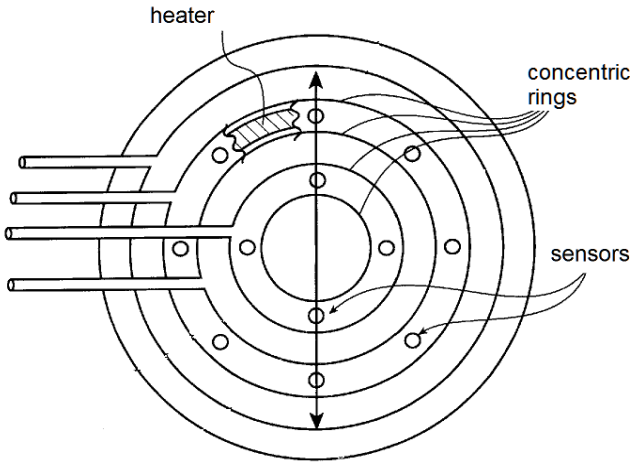

Fig. 3-8: Setup proposed by Bright et al. [38]

In a method proposed by Ide [39], which is shown in Fig. 3-9, the wafer carrier consists of multiple sensors and heating elements arranged radially in concentric circles. Temperature sensors measure the temperature in their locality which is heated by the heating elements. The heating process by small and numerous heating elements can minutely control the wafer polishing rate. Thus by selecting the amount of heat supplied by the heating elements a desired polishing profile of the wafer can be generated as shown in Fig. 3-10. A controller assesses the temperature at various locations measured by the sensors and controls the heating elements accordingly to get uniform polishing on the wafer.

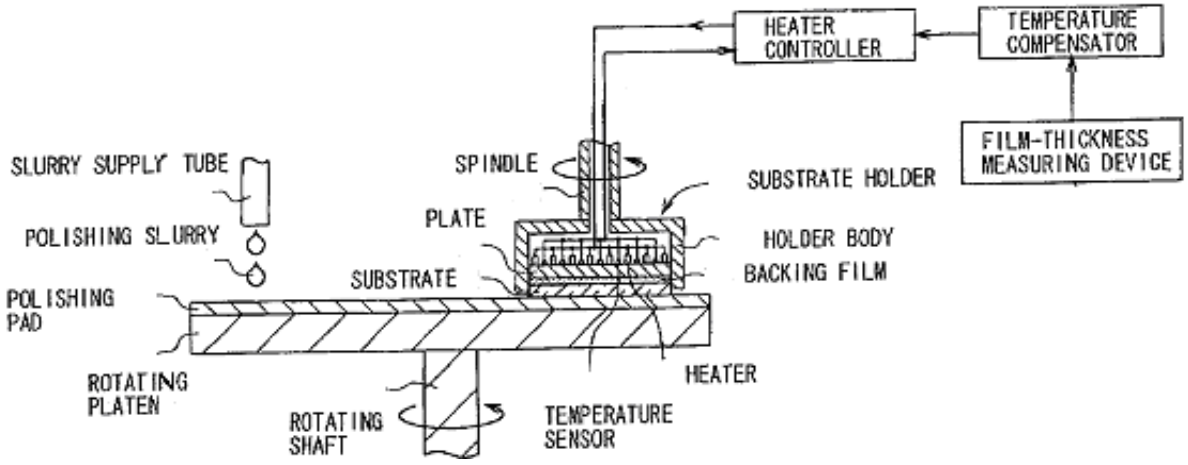

Fig. 3-9: Setup proposed by Ide [39]

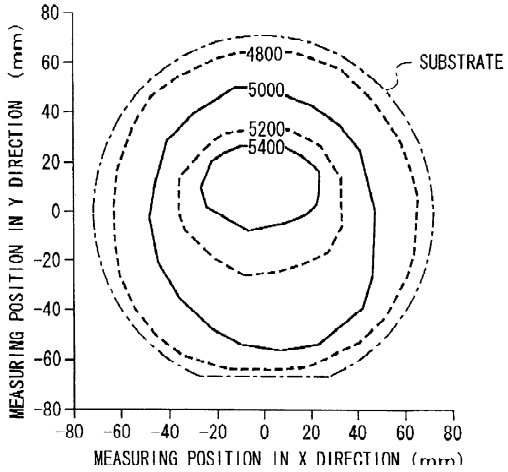

Fig. 3-10: Contour of wafer material removal [39]

3.4.3: To detect and relieve thermal stresses in wafer

Yahiel *et al.* [40] proposed a method of using temperature sensors for predicting thermal stresses. Temperature sensors are mounted in the wafer carrier just behind the wafer to obtain the temperature values at various locations of the wafer. More the number of sensors, more accurate would be the estimation of thermal stresses in the wafer. A computer is connected to these sensors to generate a thermal map which can be used to compute the thermal stresses in the wafer. Such a thermal map of a wafer is shown in Fig. 3-11.

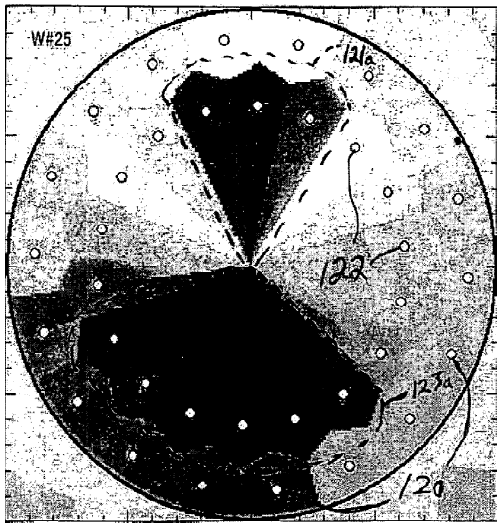

Fig. 3-11: Wafer showing thermal stress distribution [40]

3.4.4: To maintain temperature in a temperature control unit

In a setup proposed by Tzeng *et al.* [41], temperature sensor is used to maintain the temperature of the polishing belt pad. A fluid is circulated in pipes around the pad to heat the pad. The heating arrangement is connected to a temperature control unit which maintains the temperature of the fluid and thus of the pad. The temperature sensor is a part of the temperature control unit which measures and maintains the temperature of the fluid.

3.5: Layout of temperature sensors in the CMP apparatus

In wafer carrier: Temperature sensors can be used inside the wafer carrier just behind the wafer. The sensors can be arranged in a multitude of concentric circles as suggested by Bright *et al.* [38] and Ide [39] so that they can provide a thermal map of the wafer. A single ring thermocouple can be used to give the average temperature of the wafer.

On wafer carrier: As applied by Koo *et al*. [31], a temperature sensor mounted on the side of the carrier can indicate the temperature of the slurry which comes in contact with the wafer carrier.

In the pad: As applied by Sandhu [30] and Koo *et al.* [31], a temperature sensor placed in the polishing pad can indicate the temperature of the pad, while a sensor placed in the pad very near to the polishing surface of the pad can indicate the pad-wafer interface temperature.

Besides Platen: A temperature sensor can be placed besides the platen where the slurry is collected to indicate the temperature of the slurry byproducts formed (as applied by Sandhu [30]).

Inside the wafer: Fig. 3-12 shows the temperature sensors arrangement in the wafer proposed by Avanzino *et al.* [42]. Single or multiple temperature sensor(s) can be embedded in the wafer to indicate precise temperature of the wafer substrate. Radial arrangement is preferred which helps to reduce the within wafer non uniformity. The multitude of sensors in the wafer gives precise value of temperature which is used to monitor the polishing process closely.

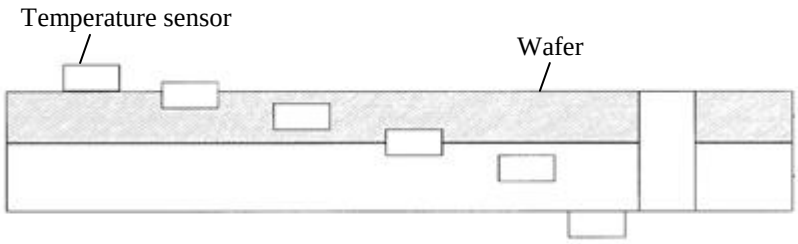

(a)

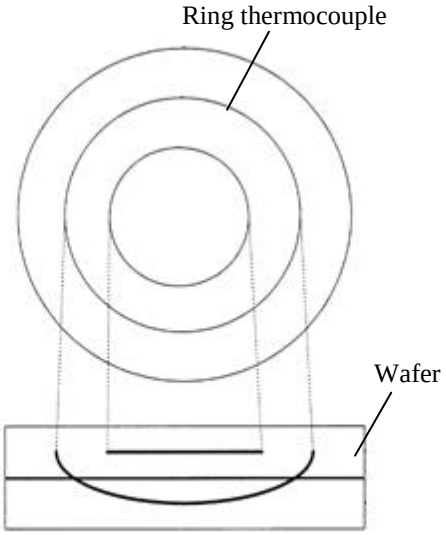

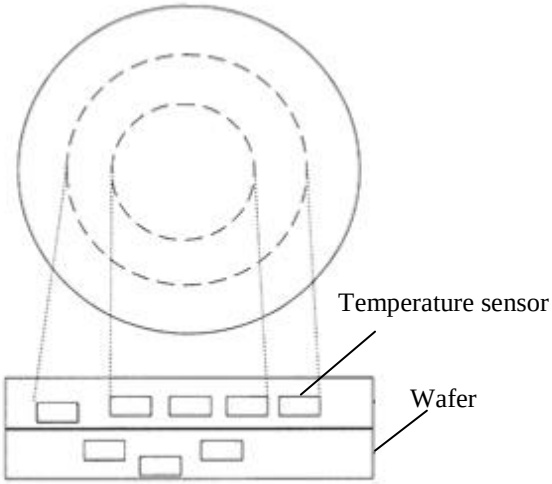

(b) (c)

Fig. 3-12: Temperature sensor layout proposed by Avanzino et al. [42] (a) Temperature sensors inside the wafer (b) Continuous ring thermocouple used in wafer (c) Multitude of temperature sensors concentrically arranged in wafer

Chapter 4: Experimental Setup and Procedure

The objective of this investigation was to polish copper wafers with good planarity and finish and to implement sensors in the polishing setup to monitor or predict the process output variables, such as MRR and Ra from the sensor data. Two experimental setups were used: Face up CMP setup (fabricated in the laboratory) and commercial Buehler Automet 250 polishing machine. Both the setups were integrated with temperature sensors. A set of polishing tests were conducted following DOE approach. The temperature signals collected from the experiments were used for statistical modeling of the CMP process. The details of the polishing setups, sensor instrumentation, and experimental procedure are given in the following sections.

4.1: The face up CMP setup without planetary motion

A polishing setup was built which implemented the face up CMP for polishing copper wafers. Unpatterned 4'' diameter copper wafers of 1.25 mm thickness were used for polishing. Suba IV Pad made of polyurethane material was used. Colloidal silica slurry (from Nalco company) which primarily consists of SiO_2 and NaOH was used for polishing. The setup (as shown in Fig. 4-1(a)) comprised of a Speedway mini milling machine with an R8 spindle in which the R8 collet was used to clutch a polyethylene pad holder where the pad was adhered. The pad holder and the pad were of 4 inch diameter in order to cover the entire wafer from top. A polyethylene tank of 8'' side was mounted on a polyethylene base plate which was fixed to the worktable of the milling machine. As shown in Fig. 4-1(b), a thick block of PVC plastic with a circular cavity on the top was press fitted in the tank to hold the wafer. It was made sure using a spirit level that the wafer was ok. The wafer was placed in the tank with a measured quantity of slurry (a mixture of colloidal silica and water in a fixed ratio). The pad was lowered to apply some load

onto the wafer. An Omega LCM 302 button load cell was used to measure the load applied on the wafer. As shown in Fig. 4-1(c), the load cell was placed below the tank with the sensitive button aligned axially with the pad and the wafer. After starting the milling machine, the RPM of the pad holder was measured by a Tachometer.

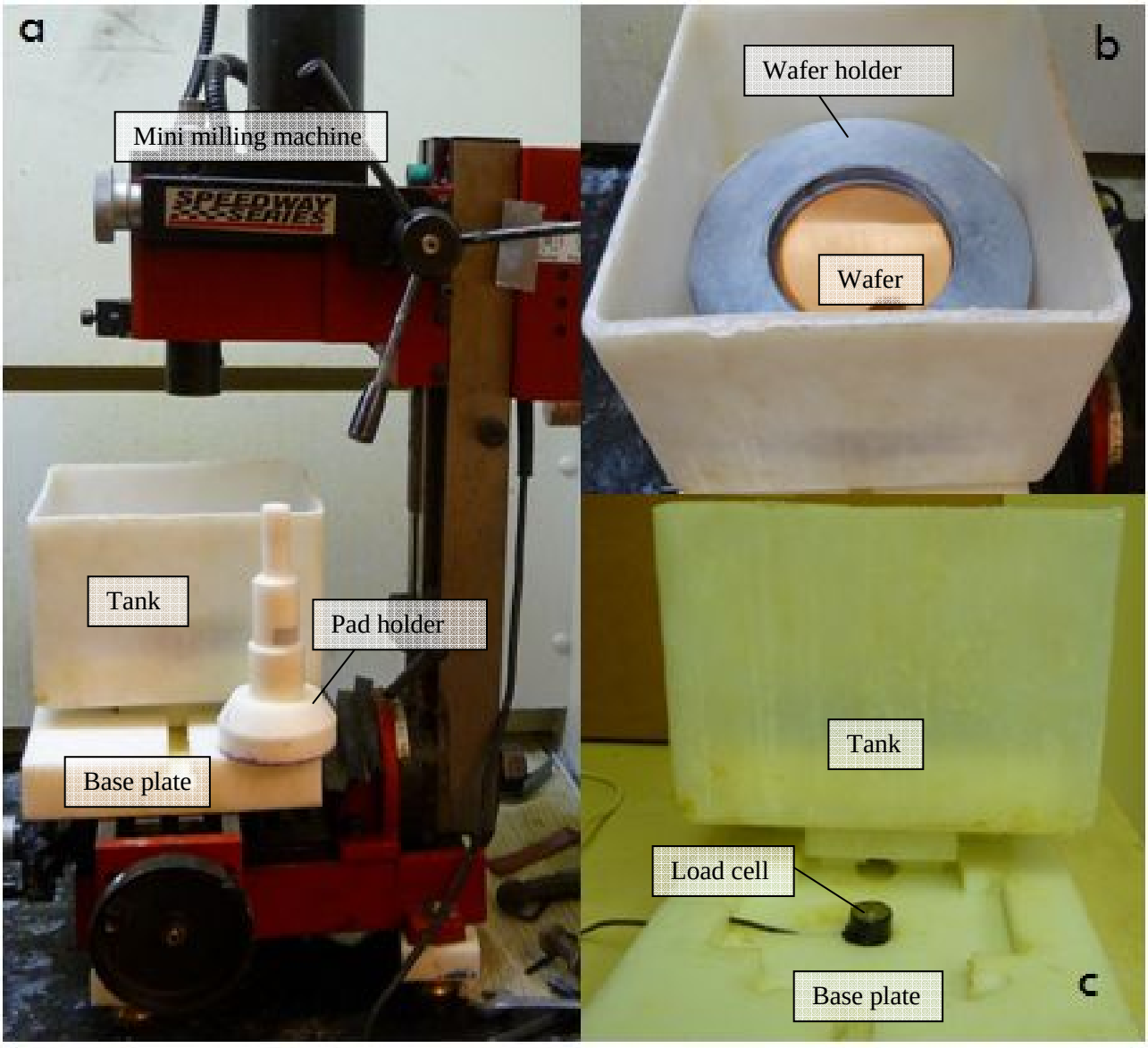

Fig. 4-1: (a) The face up CMP setup without planetary motion (b) Tank with wafer holder (c) Load cell arrangement below the tank

After initial trials of polishing at various combinations of load, RPM and slurry concentration it was found that polishing of the wafer was not acceptable. There were circular rings observed in the wafer with more polished surface near periphery and lesser near the center. The reason for lesser polish in the central region of the wafer was that the relative velocity between the wafer and the pad is nearly zero. There, the pad was completely superimposing the wafer with the stationary center of the rotating pad just over the center of the wafer. While there were rings observed on the other parts of the wafer. The pad was not subjected to a uniform load distribution at every circular ring section of the exposed area. This is because of the pliability of the pad, which leads to unequal exposure of the pad and the more exposed/pressed ring sections giving more polishing compared to lesser pressed pad sections. Consequently, concentric rings of more and less polished parts were observed on the wafer. This lead to the conclusion that planetary motion was required for polishing of copper wafers.

4.2: The face up CMP setup with planetary motion

A mechanism of planetary motion was applied in the face up CMP setup to obtain overall polishing on the copper wafers. Fig. 4-2 shows the difference in the polishing mechanism of the first and the second face up CMP polishing setup. Diameter of the pad was reduced by half from 4 inch to 2 inch. Central axis of the pad was moved so that there was a distance of 1 inch between the centers of the pad and the wafer. Also, the wafer was given a rotary motion. Planetary motion due to the off centered position of the pad with respect to the wafer ensured that there was no point between pad and wafer with zero relative velocity. The circular rings were avoided because of the rotary motion of the wafer. Thus, the new mechanism was able to give uniform polish on the copper wafers.

Another setup was built (as shown in Fig. 4-3) which followed the planetary motion mechanism. Diameter of the pad holder was reduced from 4 inch to 2 inch. The bottom part of the polishing setup comprising of the tank with the wafer rest was given rotational motion through a chain drive. On one side, the chain drive was connected to a pinion on the drive shaft of a Baldor 0.5 hp DC motor, and on the other

side to a bigger diameter sprocket which was attached below the tank. There was a thrust bearing attached at the bottom of the sprocket. The thrust bearing was press fitted into a Teflon rest plate which was attached on the worktable of the milling machine. There was a button load cell under the Teflon rest plate which was aligned with the center of the pad.

Two small boxes each having a Tmote platform were attached with the help of strap clamps to an end mill holder which was clutching the pad holder shaft. Sensors were connected with thin wires to the Tmotes. Temperature sensor was placed behind the pad to take its temperature. The sensor was not attached to the pad directly; instead there was a copper foil between the pad and the sensor to protect the sensor from the slurry. The pad holder was modified to incorporate a temperature sensor. As shown in Fig. 4-4, through holes slightly bigger than the sensor were made at the base of the pad holder. A cup made of copper foil which was of the same size as that of the pad holder was adhered at the bottom of the pad holder. The sensor was placed into one of the holes and was attached on the copper foil. Pad was adhered on the other side of the copper foil.

At the start of a polishing experiment, rotation of the wafer and the pad was started simultaneously. RPM of the wafer was selected by a controller of the motor. Polishing was done at different combinations of load, RPM, and slurry concentration. The polishing was found to be uniform on the entire wafer but the surface roughness values had a scope of improvement. Multistage polishing process was applied to improve the surface roughness values.

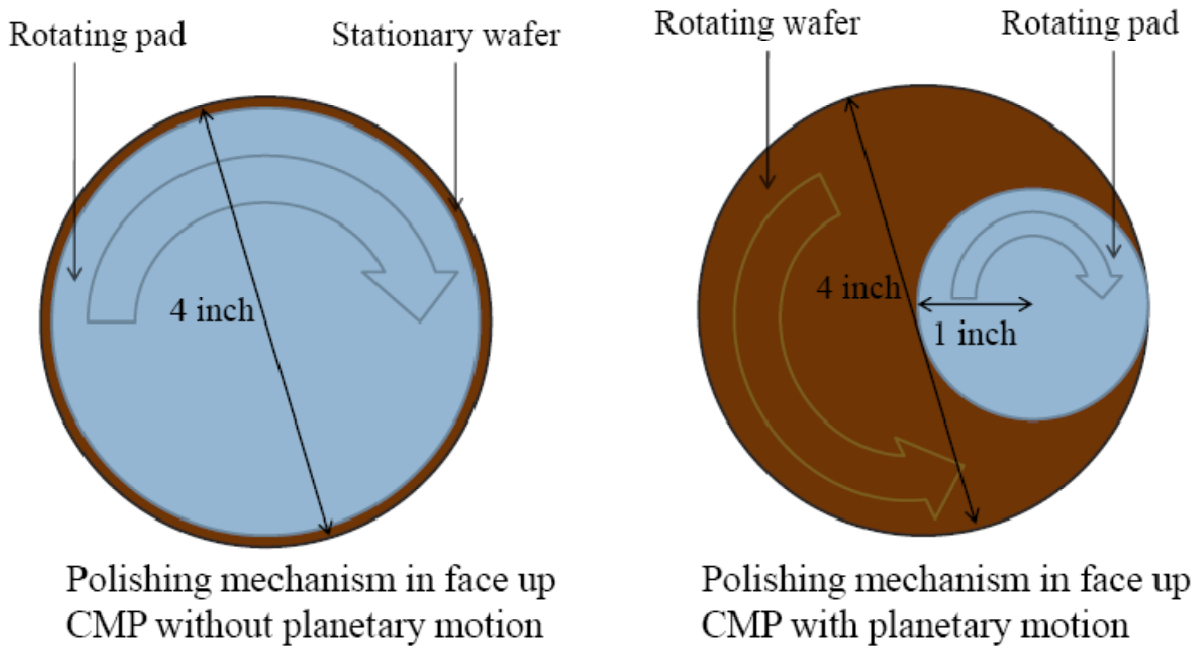

Fig. 4-2: Difference in the polishing mechanism of the setups without and with planetary motion

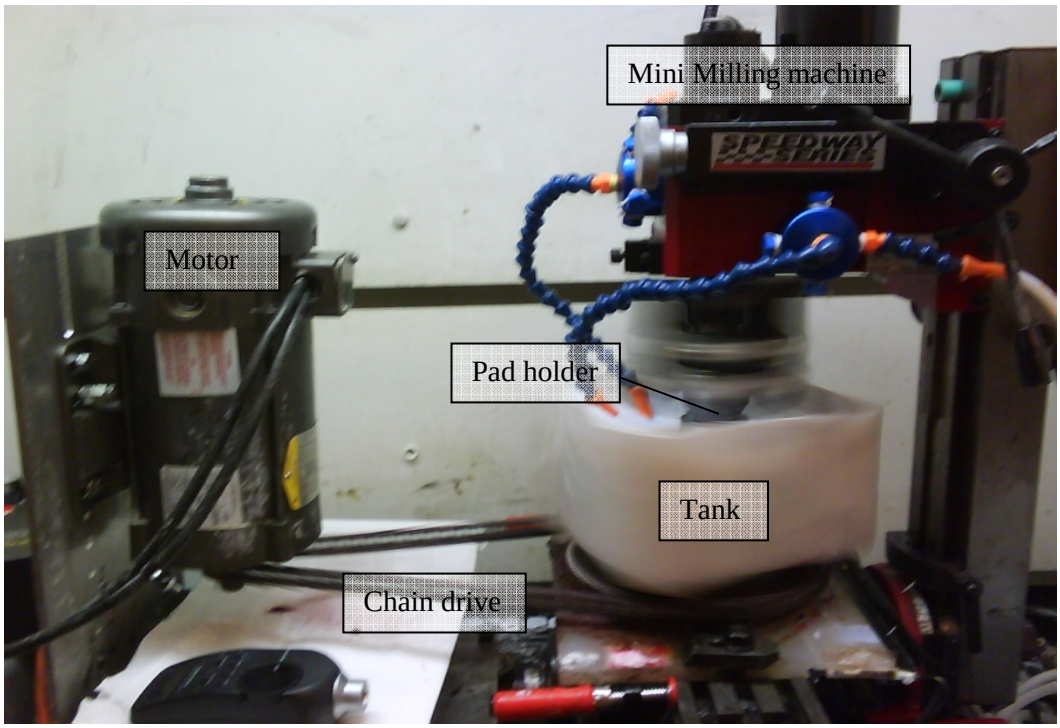

Fig. 4-3: Face up CMP setup with planetary motion

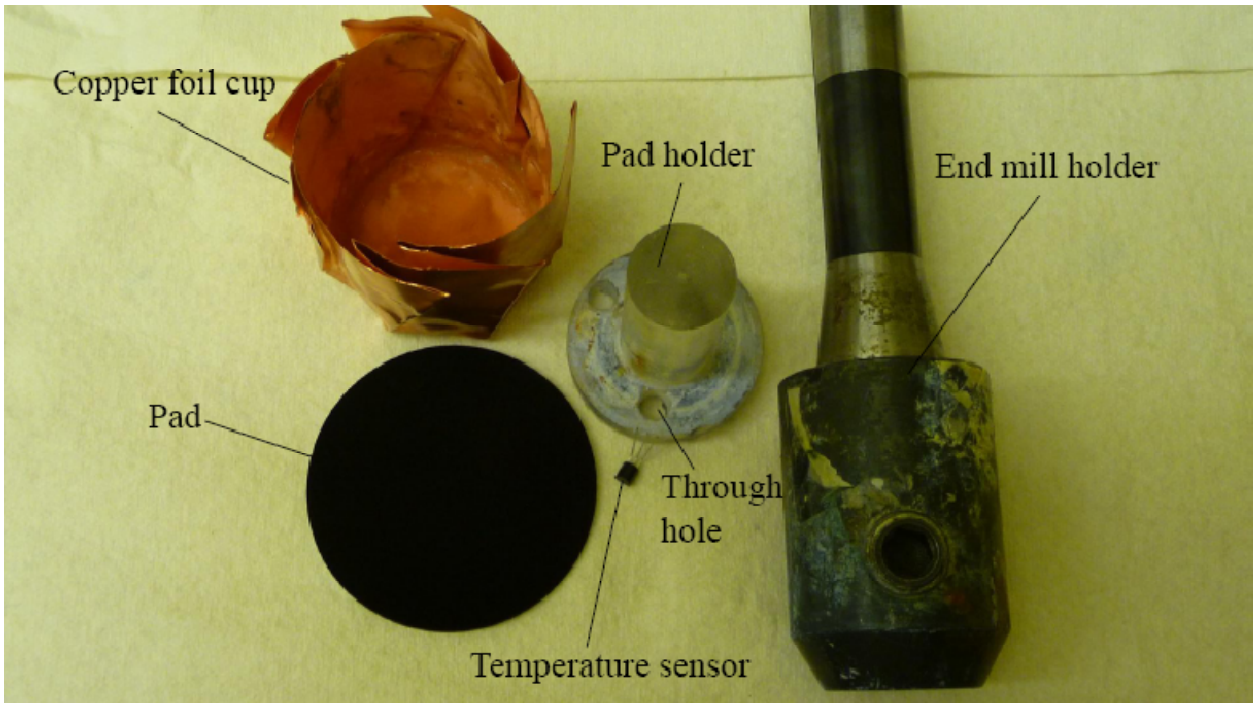

Fig. 4-4: Arrangement for attaching temperature sensor behind the pad

4.3: Multi stage polishing process

The polishing results obtained from continuous polishing of the wafer with a single pad were not satisfactory. Hence, the polishing process was changed from a continuous process to a process comprising of smaller duration stages. The pad, RPM and load conditions were changed in each stage. The change in polishing conditions of the stages was intended to give coarse polish initially and fine polish in the later stages. The multistage polishing process had 3-4 stages in it. The initial stages of polishing were accomplished with hard pad and at higher load with lesser relative velocity to remove more material. The later stages of polishing were done with softer pad at lower load and higher relative velocity to give a soft polishing or buffing action. Various combinations of hard pads, soft pads, load, velocity and polishing time for each stage were investigated. The conditions for the multi stage polishing experiment which gave best polishing results are given in Table 4-1 and the images of the wafer are shown in Fig. 4-5.

Table 4-1: Polishing conditions for multistage polishing experiments with best polishing results

Stage	Pad Type	Load (lb)	Wafer RPM	Pad RPM	Polishing Time (min)
1	Suba IV	35	40	500	30
2	FBP	25	50	700	30
3	Beuhler MicroCloth	15	75	700	15

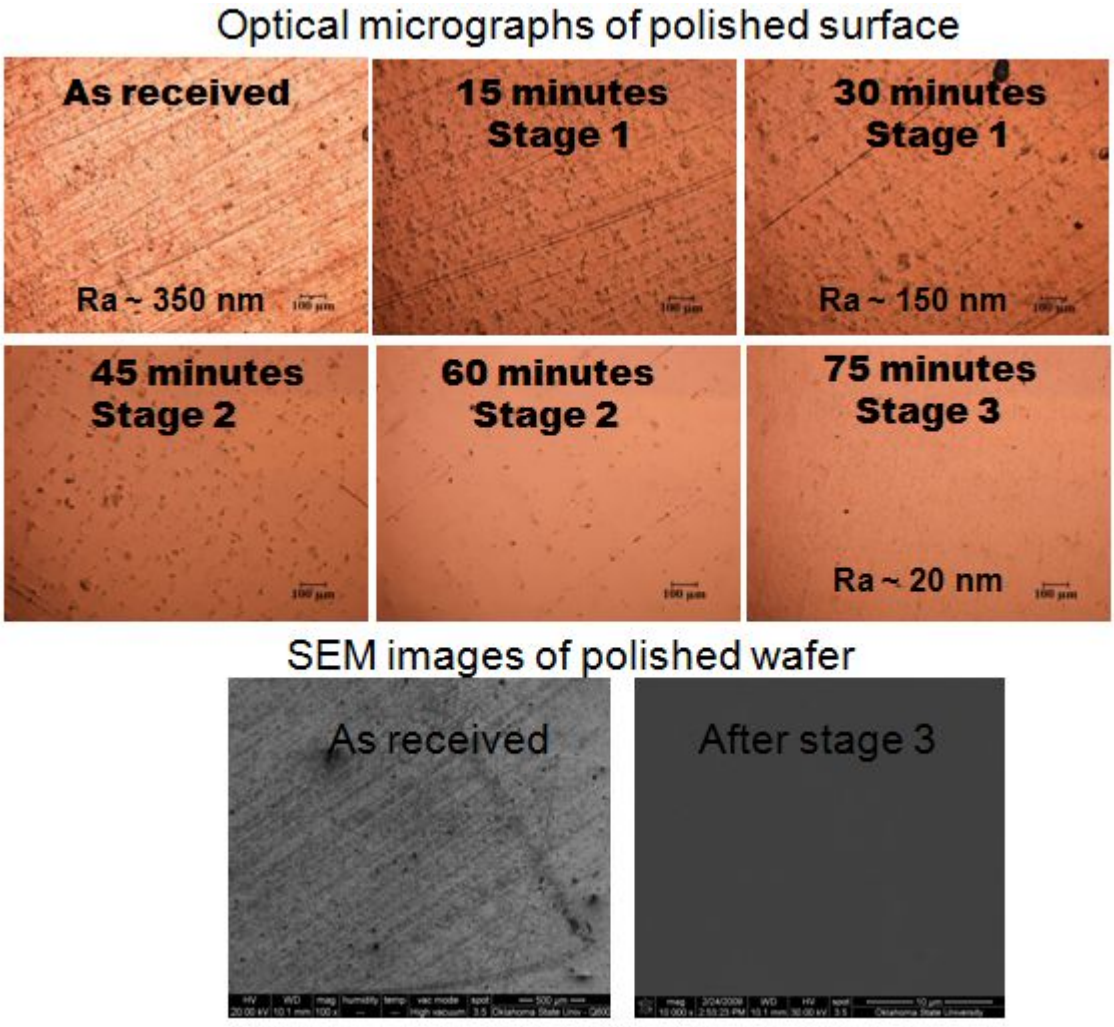

Fig. 4-5: Optical microscope and SEM images of wafer in a multistage polishing experiment

4.4: Buehler Automet 250 Polishing machine

Buehler Automet 250 polishing machine is shown in Fig.4-6a. A specimen holder is used to hold the samples to be polished. The specimen holder consisted of three holes of 1inch diameter and three holes of 1.6 inch diameter arranged symmetrically. The copper wafer samples used for polishing experiments had 1.6 inch outer diameter and cup like shape as shown in Fig. 4-6b. The sample was 1 inch high and thickness of the base was 0.1 inch. A temperature sensor was attached on the base of the sample to measure the pad-wafer interfacial temperature. The sensor was connected through wires to a Tmote platform placed in a box attached to the rotary part of the polishing machine. There were six fingers on the machine head which were pushed down pneumatically at the start of polishing to apply the selected amount of downforce on the samples in the specimen holder. The specimen holder was inserted into a lift lock chuck which was connected to the motor drive shaft. The specimen holder was not clutched in the chuck very firmly, rather the specimen holder was allowed to have a floating motion. Also, the copper wafer samples were minutely smaller than the holes in the specimen holder. The clearance between the samples and the holes in the specimen holder and the floating motion of the specimen holder gave the samples ability to comply with the variations in the pad profile during polishing process. Polishing pad was adhered on a bimetallic plate which was attached magnetically to a platen. Microcloth which is a soft felt pad and Masterprep which is an alumina based slurry (both from Buehler company) were used for polishing experiments. Slurry falling off the pad during the polishing tests was collected in a drain besides the platen. The slurry flowed through a drain hose into a small tank. A peristaltic pump was used to circulate the slurry. Thin rubber pipes connected to the pump circulated slurry from the small tank to the pad during the polishing tests. There was a control panel on the machine. The RPM of the specimen holder and the platen, the down force applied by each finger could be controlled from the control panel.

Fig. 4-6: (a) Buehler Automet 250 polishing machine (b) Copper wafer sample with a temperature sensor

4.5: Wireless sensor network, Tmote, temperature sensor and data acquisition procedure

A wireless sensor network comprises of two basic nodes. One or more sensor nodes, and a single display node that is connected to the computer as a base station to collect and format data from other nodes. The sensor nodes communicate with the base node via radio network. The computer provides the graphical user interface, display, and control.

Tmote is a mote platform for extremely low power, high data-rate sensor network applications. It has an integrated radio, antenna, microcontroller, and programming capabilities. TinyOS was used as the development environment for Tmote, which is an event-driven operating system intended for sensor

networks. The TinyOS applications are written in nesC language, a version of C language that was designed for programming embedded systems. A Java application Serial Forwarder is used for communication between computer and Tmote. Java tools Oscilloscope and Trawler can be used to display the readings on the computer. Cygwin which is similar to Unix environment and command-line interface for Microsoft Windows is used to activate Serial Forwarder, Oscilloscope, and program Tmote to function as transmitter or receiver, as well as for selecting ADC ports, sampling rate and the number of sensor channels.

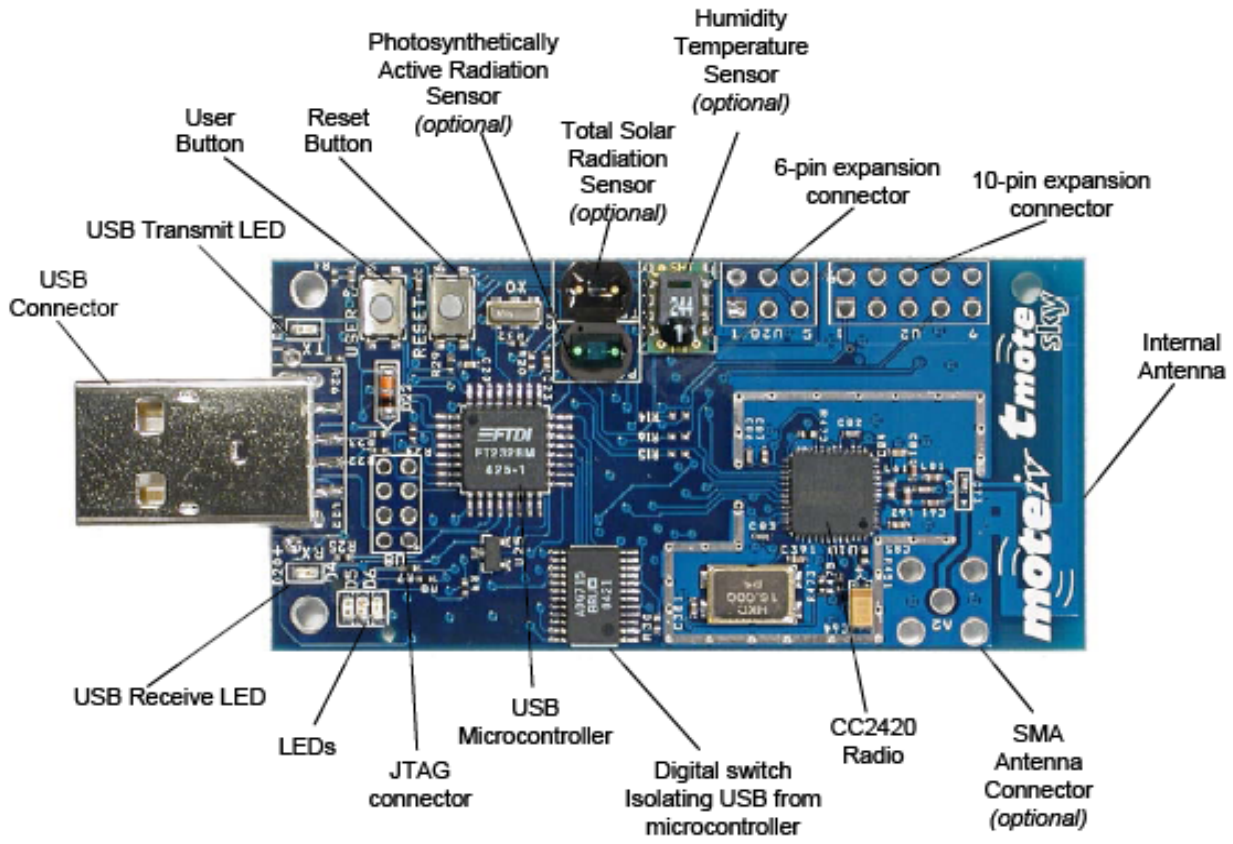

Fig. 4-7: Moteiv Tmote sky mote platform

A temperature sensor AD 22103 from Analog devices was used for sensing temperature. As shown in Fig. 4-8, the flat part is the temperature sensitive component of the sensor. The three leads correspond to ground, supply voltage, and output voltage, respectively. These were connected to the

Tmote through lead wires. The sensor has temperature sensitivity of 28mV/°C, the supply voltage range of 2.7 V to 3.3 V, and temperature measurement span of 0°C to 100°C.

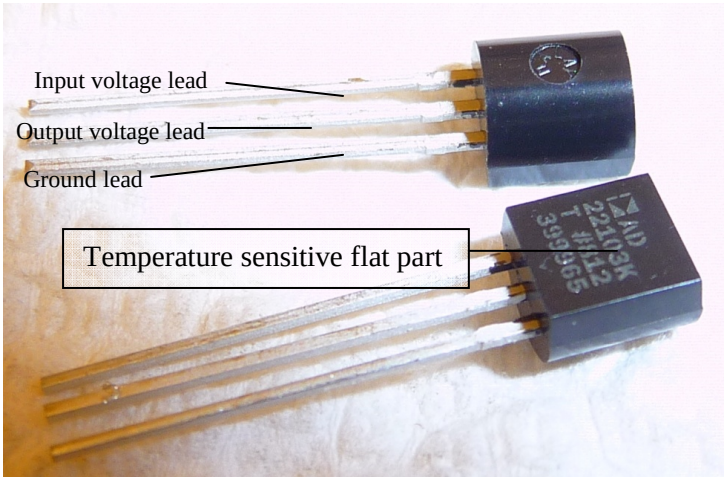

Fig. 4-8: Analog Devices AD 22103 temperature sensor

Two temperature sensors were connected to a Tmote platform which was programmed as a transmitter. The Tmote platform was programmed to display two channels of the sensor data corresponding to the two temperature sensors. The sampling rate was set as 4 Hz for each sensor. Another Tmote platform programmed as a receiver was connected to a computer. On initiating the Trawler application the signal from the two temperature sensors were displayed as two time series of different colors representing two channels. The temperature signal was displayed in mV. The signal was converted to temperature units (°C) by using a relation obtained from the datasheet of the temperature sensor. At the start of a polishing experiment, previous signal was deleted to clear the screen by selecting clear data screen option in Trawler. At the end of the experiment, save option was used to save the data until that point of time. The data was stored in the form of text file which was used for further analysis.

4.6: Experimental procedure

Copper polishing tests were conducted on Buehler Automet 250 polishing machine with the objective of correlating material removal with the temperature rise and polishing conditions. The

experiments were based on L-8 Taguchi design as shown in Table 4-2. Each polishing run had some fixed values of relative velocity, load and, slurry concentration.

Table 4-2: Taguchi L-8 design of experiments

Run	**Relative velocity (m/sec)**	**Down Force (lbs)**	**Slurry Concentration (alumina: water)**
R1	5.7	10	1:3
R2	5.7	10	1:5
R3	5.7	5	1:3
R4	5.7	5	1:5
R5	3.7	10	1:3
R6	3.7	10	1:5
R7	3.7	5	1:3
R8	3.7	5	1:5

Table 4-3: Each run had 4 experiments and were carried away as shown

Scratched wafer , new pad, new slurry	30 sec →	polish, polished wafer rescratched
Scratched wafer , new pad, new slurry	60 sec →	polish, polished wafer rescratched
Scratched wafer , new pad, new slurry	90 sec →	polish, polished wafer rescratched
Scratched wafer , new pad, new slurry	120 sec →	polish

Each polishing run consisted of four polishing experiments. As shown in Table 4-3, the polishing experiments were conducted under the same polishing conditions for different amounts of time. Two copper wafer samples, each with a temperature sensor were used for the polishing experiments. The second copper wafer sample was used for the repetition of polishing experiment conducted using the first sample. Both of the samples were polished together, thus the repetition of the experiments were accomplished along with the original experiments at the same conditions. Copper wafer samples were initially polished/scratched with a 600 grit SiC paper on their polishing surface before polishing experiment. The surface roughness of the copper samples was measured by MicroXAM shown in Fig. 4-9, which is a laser interference microscope from ADE Phase Shift Technologies.

Fig. 4-9: MicroXAM from ADE Phase Shift technologies

Values of the surface roughness were measured at 4 random points on the polishing surface of the samples. New pad and fresh slurry (alumina and distilled water mixed in a specific ratio) were used for

each polishing experiment. The copper wafer samples were polished/scratched to obtain the average roughness of the polishing surface between 350 and 400 nm. This was to ensure the same initial polishing condition regarding pad, slurry and, polishing surface of wafer sample at the start of every polishing experiment. For weighing the sample, a digital weighing machine from Sartorius shown in Fig. 4-10 with a precision of 0.1mg was used.

Fig. 4-10: Sartorious digital weighing machine

At the start of a typical experiment, a new pad was adhered on the bimetallic plate and the bimetallic plate was attached on the platen. Nearly 120 ml of the slurry was placed in the small tank behind the drain hose. Two copper wafer samples were mounted in the specimen holder. The sensors were attached on the base of the samples. The values of load and RPM were selected from the control panel. The slurry circulation from the tank to the pad was initiated. Thereafter, the machine was started. The data acquisition was started at this point. The polishing process stopped after a predetermined time

which was selected on the control panel. The data acquisition was stopped and the sensors were removed from the samples. The samples were then rinsed with distilled water and placed in an ultrasonic cleaner which is shown in Fig. 4-11.

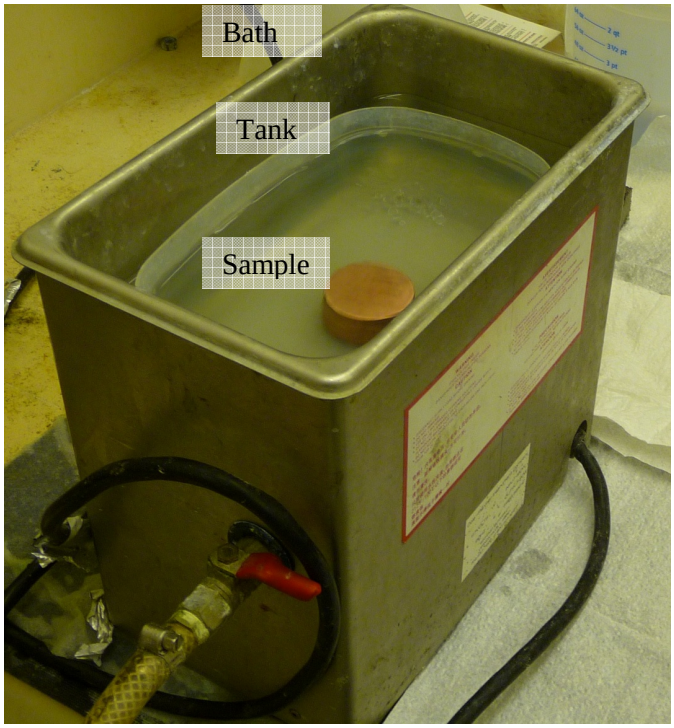

Fig: 4-11: Ultrasonic cleaner

The ultrasonic cleaner consisted of a bath which was filled with water. A plastic tank partially filled with distilled water was immersed in the bath. The samples were placed in the plastic tank. Ultrasonic vibrations generated in the cleaner assisted in removing the slurry particles adhered on the samples. The samples were dried with air and cleaned with acetone. Weight of the samples was measured by the weighing machine. The MRR was calculated using the relation:

MRR = (weight of sample before polishing – weight of sample after polishing) / time of polishing

Fig. 4-12(a) shows an optical microscope image of the polishing surface of the copper wafer sample at the beginning of 2 min of polishing experiment following R1 run. Fig. 4-12(b) shows the 3d

profile of the polishing surface. Ra of this surface was 340 nm. Fig. 4-13(a) shows optical microscope image of the polishing surface of the copper wafer sample after 2 min polishing experiment following R1 run. Fig. 4-13(b) shows the 3d profile of the polishing surface. Ra of this surface was 3.5 nm.

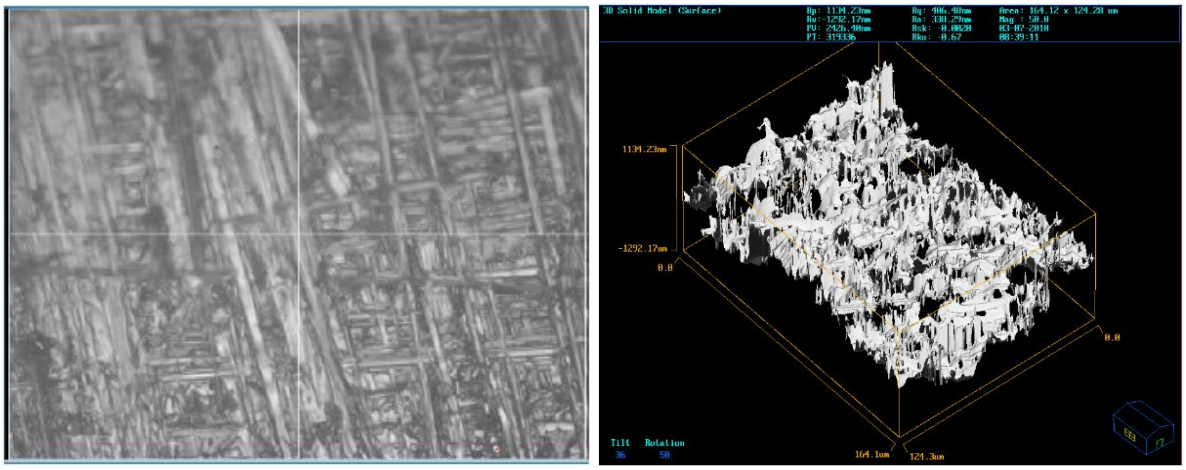

(a) (b)

Fig. 4-12: (a) optical microscope image and (b) 3d profile for starting condition with Ra of 340 nm

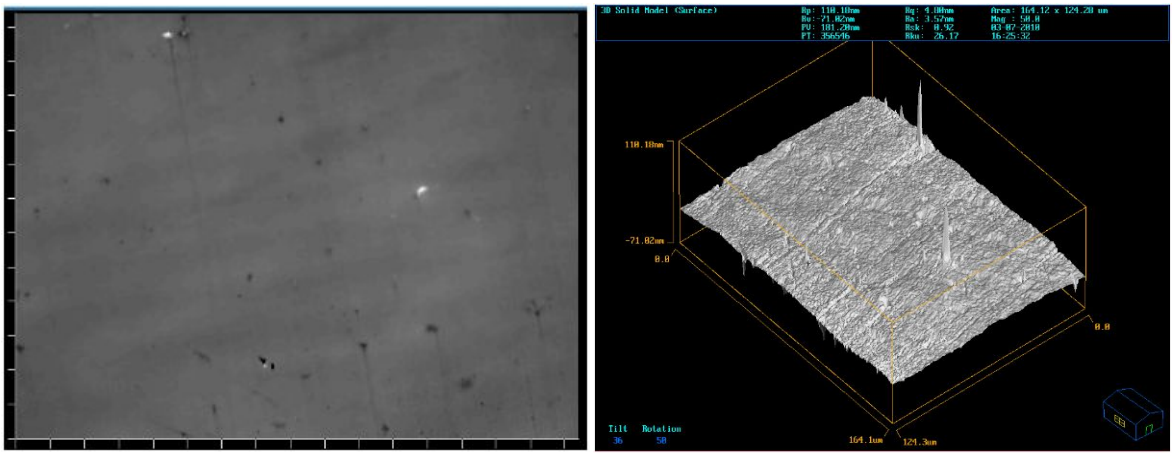

(a) (b)

Fig. 4-13: (a) optical microscope image and (b) 3d profile after 2min of polishing with Ra of 3.5 nm

Chapter 5: Qualitative analysis of temperature sensor signal

Copper wafer polishing experiments were performed on the face up CMP setup. A temperature sensor was attached behind the pad to measure the pad-wafer interface temperature. Temperature profiles (temperature signal time series) were obtained for various polishing conditions. Temperature profiles, variation in the temperature profiles with load, RPM, and slurry conditions, temperature profiles for multistage polishing and relation of temperature with PV and MRR are presented in the following sections.

5.1: Temperature profiles

A typical temperature profile observed in the copper wafer polishing experiments is shown in Fig. 5-1. The profile resembles with the temperature profiles observed by Sampurno *et al.* [43] shown in Fig. 5-2. It can be observed from the temperature profile in Fig. 5-1 that the rate of increase of temperature decreases with polishing time. After some time of polishing either the temperature value or the rate of increase of temperature becomes constant. According to White *et al.* [44], the heat generated during polishing process is transferred into the pad where it resides before being transferred to the slurry. The pad accumulates more thermal energy than it loses during the initial phase of polishing. As the temperature of the pad increases, the temperature difference between the slurry and the pad increases which increases the rate of heat flow by the slurry. The pad temperature reaches a steady state when the flow rate of energy input in the pad due to polishing action is equal to the flow rate of energy dissipated by the slurry.

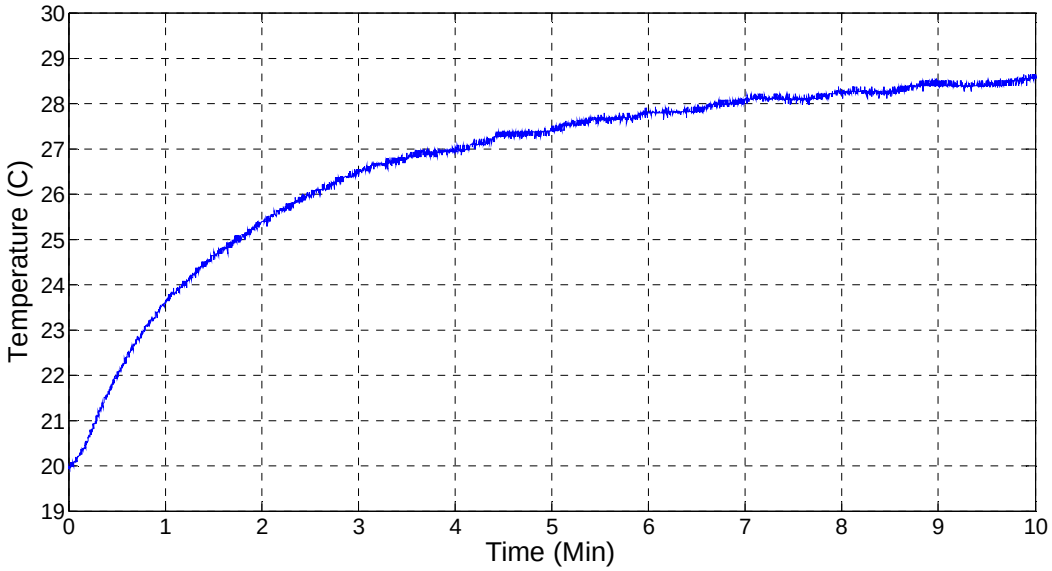

Fig. 5-1: A typical temperature profile observed during the polishing experiment

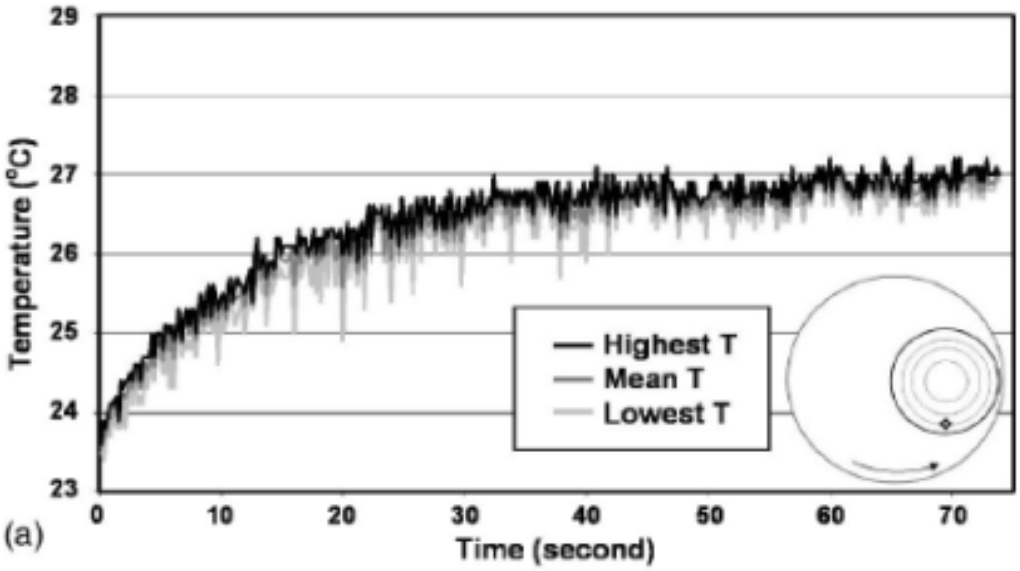

Fig. 5-2: Temperature profiles observed by Sampurno et al. [43]

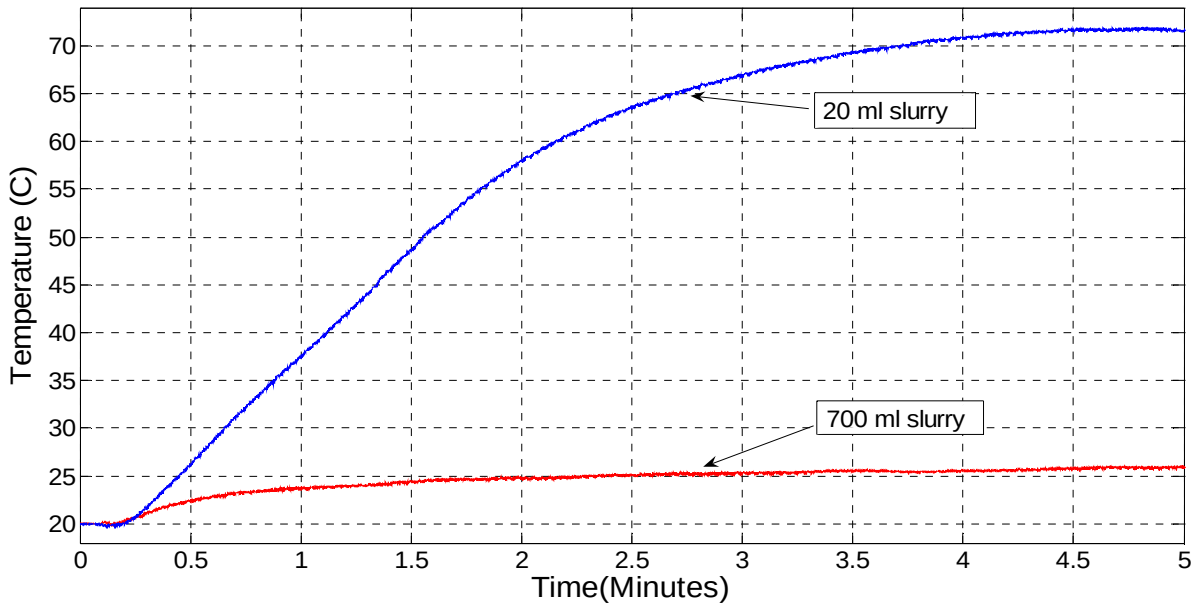

Fig. 5-3: Temperature profiles for polishing experiments with different amounts of slurry

The amount of slurry over the wafer influences the net temperature rise and the time in which the temperature profile stabilizes in a polishing experiment. Fig. 5-3 shows the temperature profiles for polishing experiments with the same polishing conditions apart from the slurry present in the tank. For the experiment in which lesser slurry (20 ml) was used shows a higher temperature rise and more time is taken for temperature stabilization. For the experiment in which more slurry (700ml) is used, temperature stabilizes to nearly a constant value in lesser time and the net rise in temperature is also lesser. Higher amount of slurry dissipates more heat and achieves a thermal equilibrium early.

Increase in the load applied on the wafer by the pad and the relative velocity or RPM of the pad and the wafer show increase in the value of temperature rise during polishing. Fig. 5-4 shows two temperature profiles for polishing experiments under the same polishing conditions except the pad RPM. For higher pad RPM of 200, the temperature of the pad raised from 20°C to around 25.5°C in 6 minutes of polishing compared to 23°C for 30 RPM of pad. Fig. 5-5 shows two temperature profiles for a polishing experiment under same polishing conditions except the load applied on the wafer by the pad.

For higher load of 45lbs the temperature of the pad raised to 37°C in 6 minutes of polishing compared to 26.5°C for 10lbs of load.

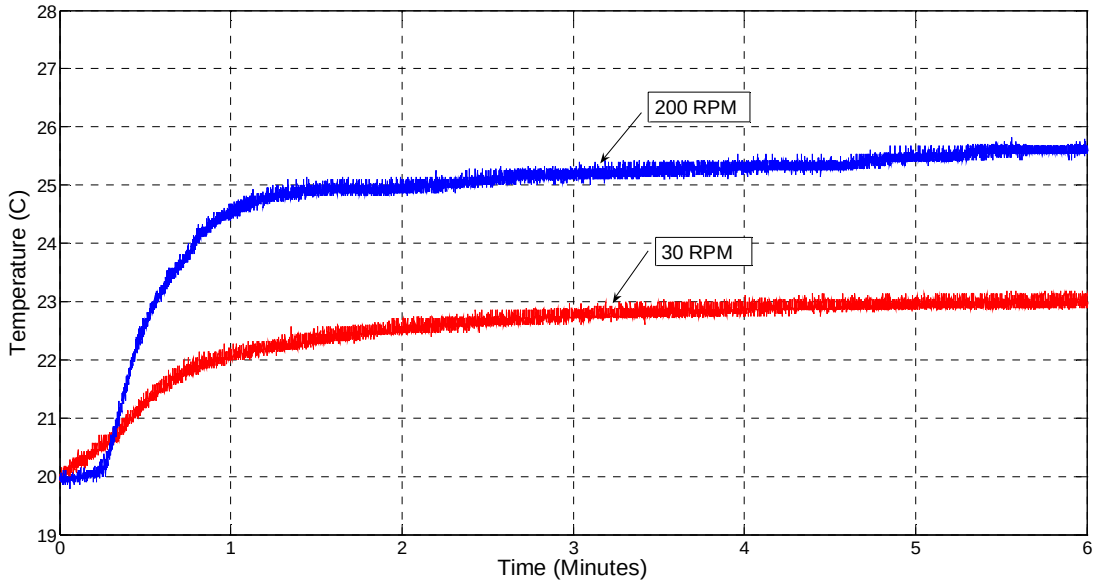

Fig. 5-4: Variation of temperature with time for two pad RPM

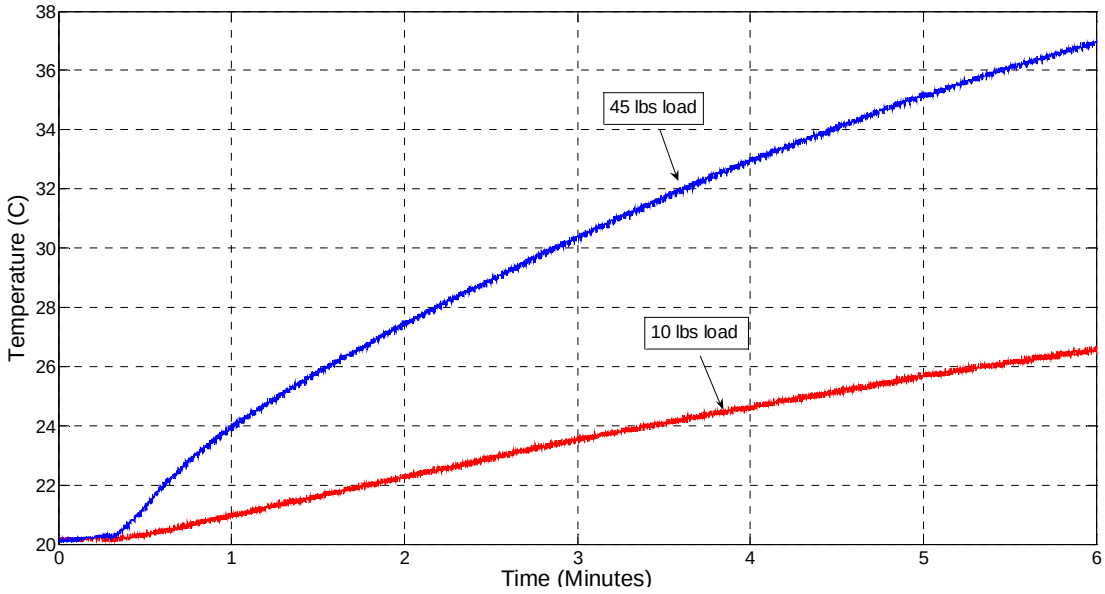

Fig. 5-5: Higher temperature rise observed for higher load

5.2: Relation of temperature rise with product of pressure and velocity (PV)

Fig. 5-6 shows the temperature profiles for a set of experiments following a 3x3 Design of Experiments (DOE) in which three values of pad RPM and three values of load were taken as variable experimental conditions. The experimental conditions for the profiles are given in Table 5-1. It can be observed in Fig. 5-6, the temperature profiles for the polishing conditions with lower PV (product of load and RPM here) values have lower temperature rise values and vice-versa. The temperature raised to around 30°C for polishing condition I (highest load and RPM) compared to 22.5°C for polishing condition A (lowest load and RPM). The temperature rise values in the profiles are in accordance with the product of pad RPM and load. The product of pad RPM and load represent the mechanical power input which is converted into frictional heat. Higher value of PV implies more frictional heat and thus more temperature rise.

Table 5-1: Polishing conditions for the 3x3 DOE

Profile	RPM	Load (lb)
(A)	200	15
(B)	200	22.5
(C)	200	30
(D)	300	15
(E)	300	22.5
(F)	300	30
(G)	400	15
(H)	400	22.5
(I)	400	30

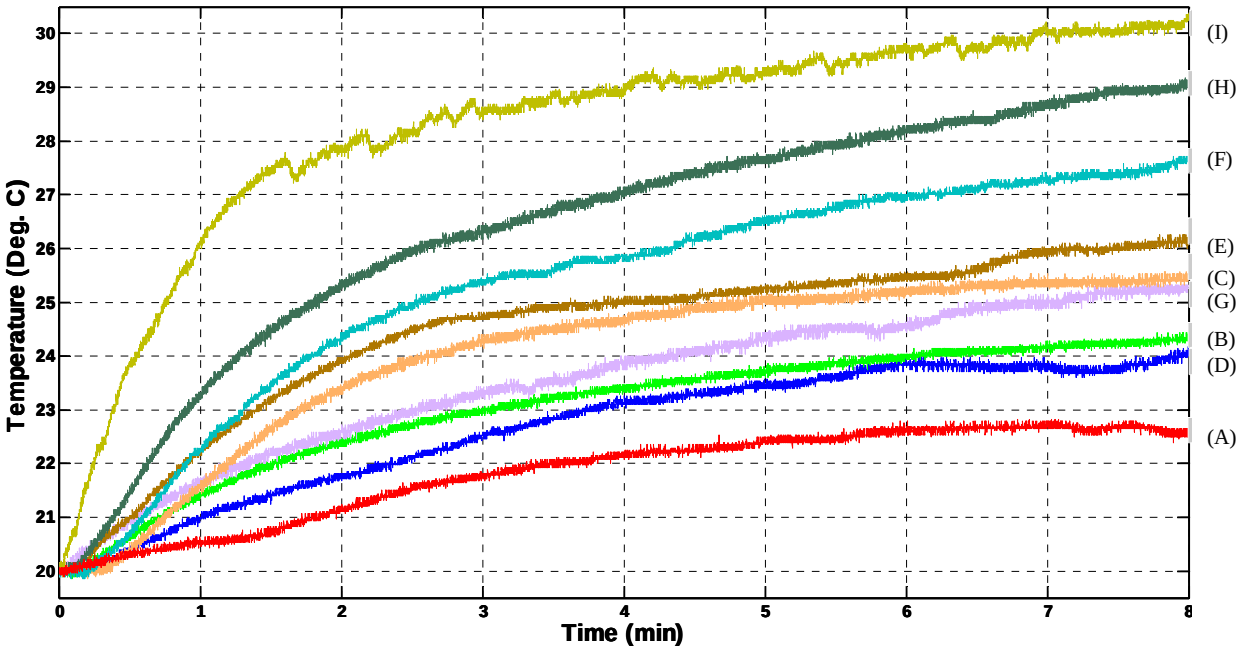

Fig. 5-6: Temperature profiles for the polishing experiments following the 3x3 DOE.

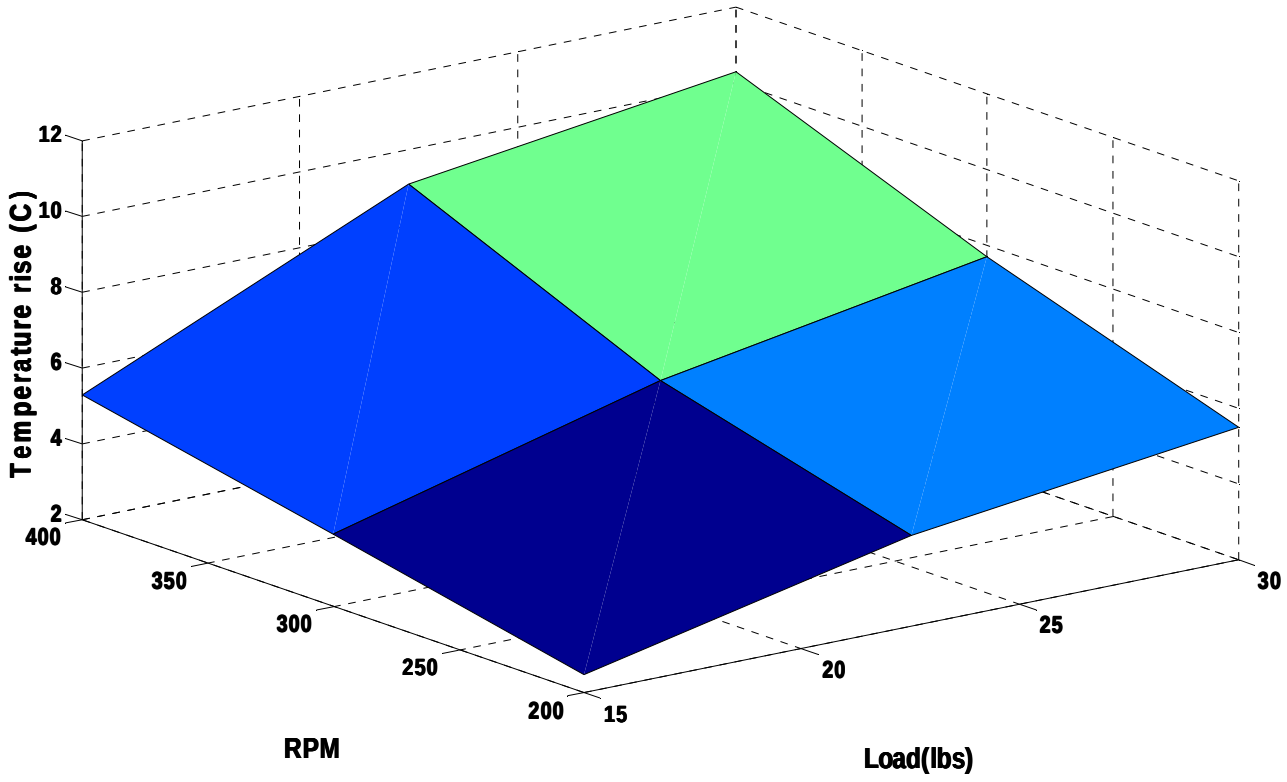

Fig. 5-7: 3D plot of the temperature rise, RPM, and load.

Fig. 5-7 is a 3D plot of temperature rise, load and RPM for the same experimental conditions given in Table 5-1.The plot has resemblance with Fig. 2-7 which shows the 3D plot of temperature, pressure and platen speed for the experiments conducted by Li *et al.* [21]. Both of the figures show that temperature values increase with the increase in load/pressure and velocity/RPM. Highest temperature rise is corresponding to the condition where both load and RPM are the highest and lowest temperature rise is for the condition having least values of both load and RPM.

Fig. 5-8 shows the plot of temperature rise vs. the product of load and pad RPM for the experimental conditions given in Table 5-1. It can be observed that the temperature rise values are linear with the product of load and pad RPM. The plot resembles with Fig. 2-6 which is discussed in the Literature review chapter.

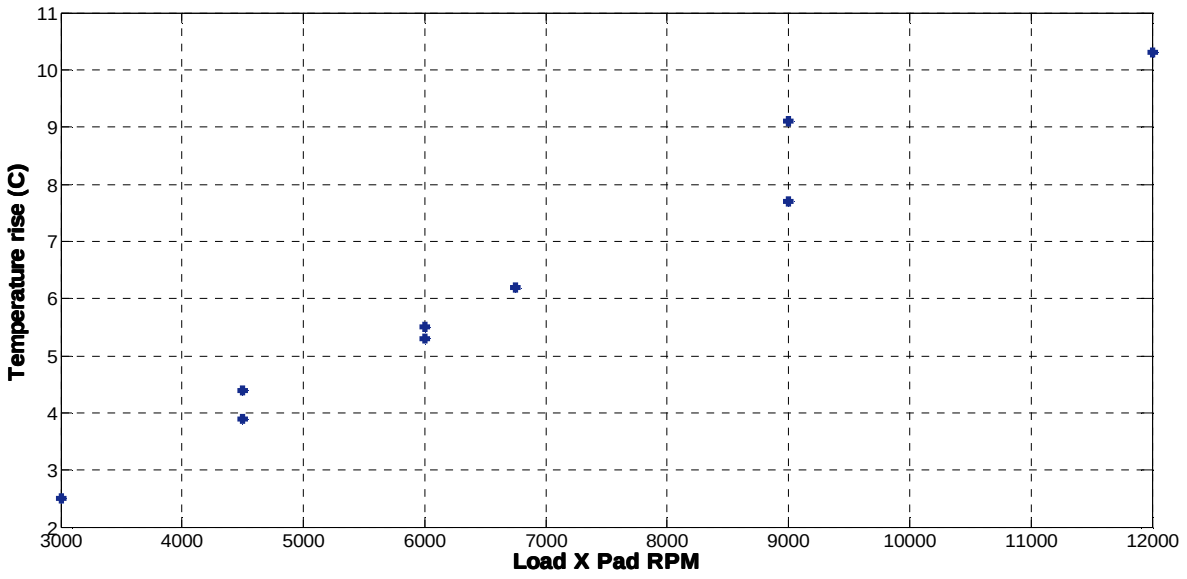

Fig. 5-8: Variations of temperature rise with the product of load and RPM

5.3: Multi stage polishing temperature profiles

Figs. 5-9 (a), (b), and (c) show the temperature profiles and average MRR values for a three stage polishing experiments. The polishing condition was changed from coarse removal of material (by selecting harder pad, higher load, and lesser relative velocity) to finer material removal (by selecting softer pad, lesser load, and higher velocity). The mildness of the polishing action in the subsequent stages is evident from the decrease in the value of temperature rise and MRR for the stages. The average MRR decreases from 0.53 mg/min to 0.5 mg/min and further to 0.48 mg/min in the three stages. The temperature rise during 12 min of polishing decreased from 32.5°C to 30.5°C and further to 29°C in the three stages.

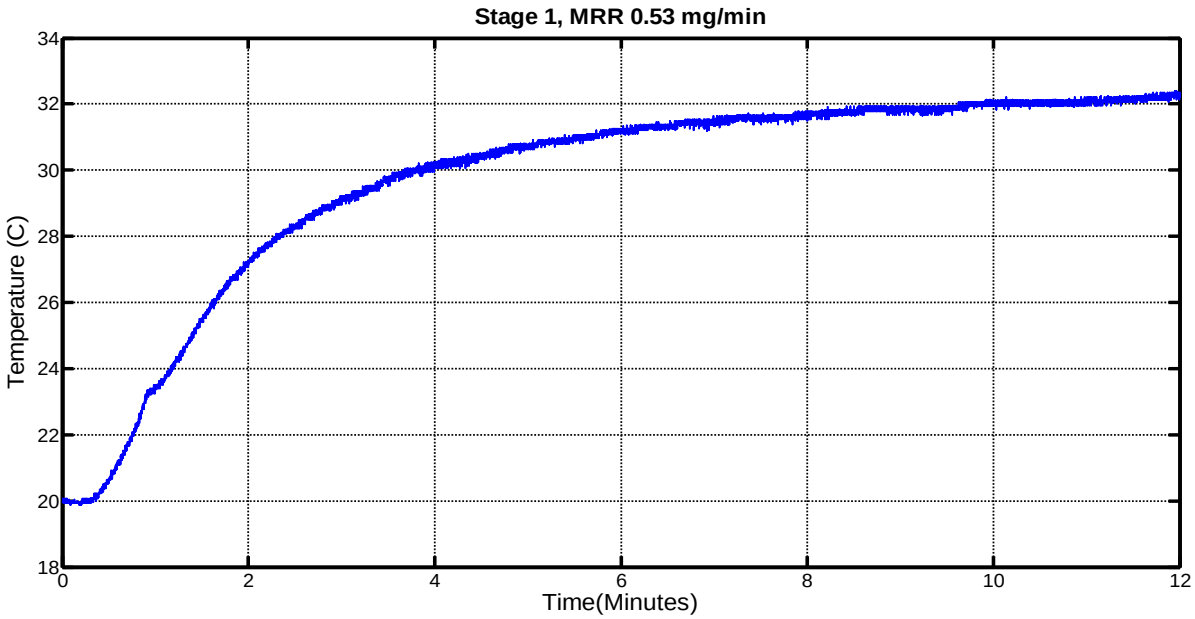

(a)

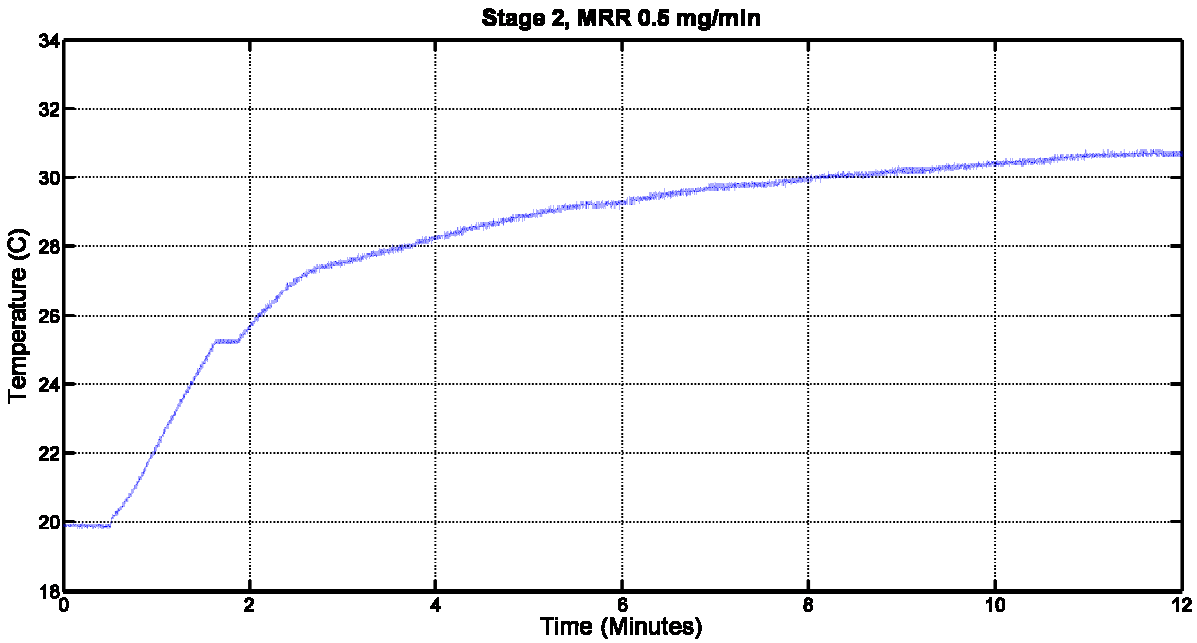

(b)

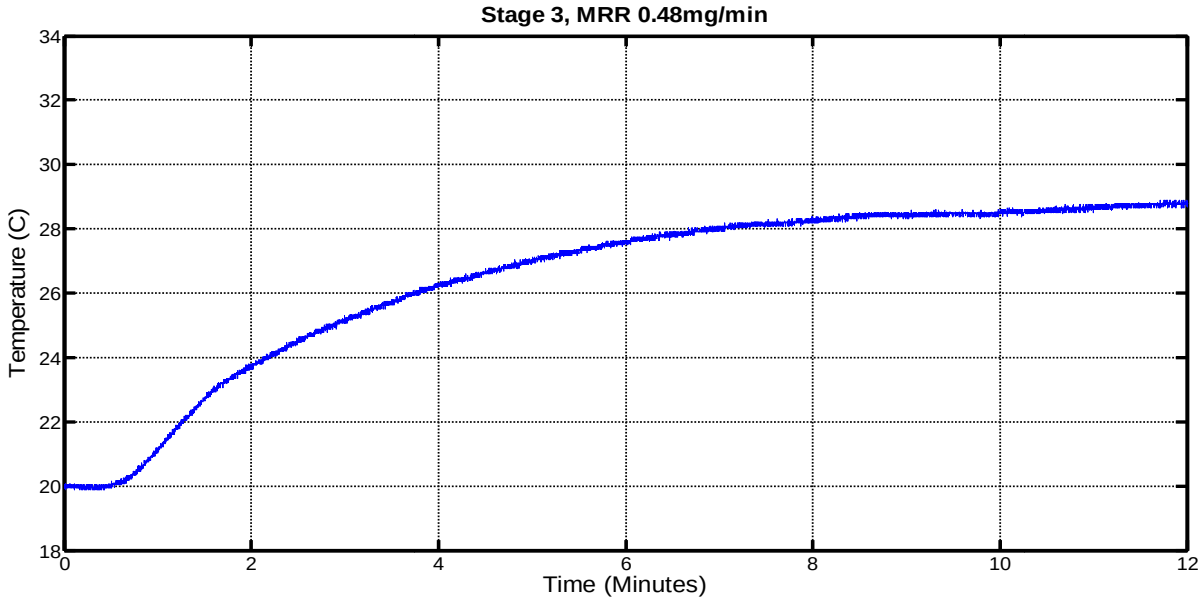

(c)

Fig. 5-9: Temperature profiles and MRR values corresponding to (a) stage 1 (b) stage 2 (c) stage 3 in a multistage polishing experiment

5.4: Decrease in MRR and temperature rise along with polishing time

Fig. 5-10 shows the temperature profile and material removal values in 2 minute durations for a polishing experiment. It can be observed that both material removed and temperature rise have higher values in the first two minutes of polishing (3.2 mg and 4.5°C, respectively) compared to the next 2 minutes of polishing (1.3 mg and 1.5°C, respectively) and so on. This indicates a relationship between the material removal and temperature rise in the polishing process. This relationship is investigated in depth in the next chapter.

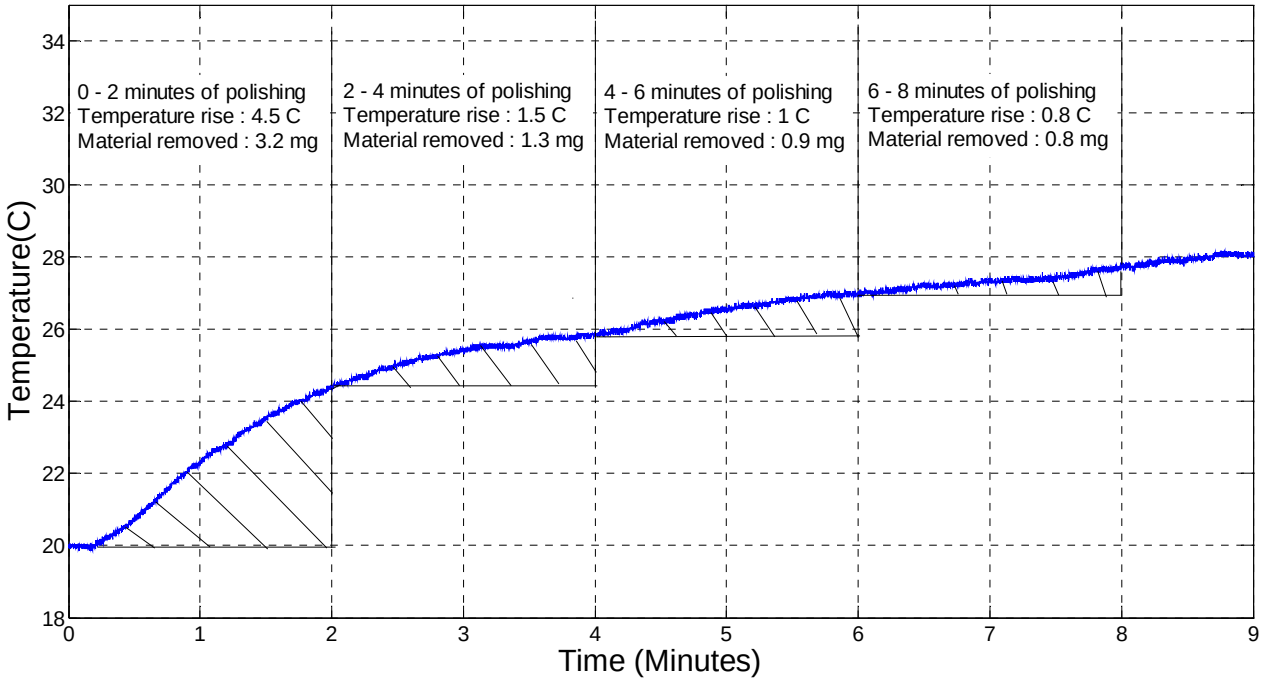

Fig. 5-10: Material removal and temperature rise decreasing with time in a polishing experiment

Chapter 6: Process modeling using response surface analysis

Four types of regression models are analyzed which are based on the experimental conditions and the temperature sensor data.

Model 1: Response variable is MRR and the predictor variables are the process parameters only which comprise of load, relative velocity, and slurry concentration. This model shows the predictability of MRR from the process parameters only.

Model 2: Response variable is MRR and the predictor variables are the process parameters and temperature rise rate. This model shows the importance of temperature rise rate to enhance the predictability of MRR.

Model 3: Response variable is the ratio of MRR and temperature rise and predictor variables are the process parameters, pad wear factor, and their two way interactions. This model shows the contribution of pad wear factor and two way interaction terms to increase the predictability of MRR.

Model 4: Response variable is the ratio of temperature rise and MRR and predictor variables are the process parameters and pad wear factor. Apart from predicting the MRR for new and worn pad with more accuracy, the model has physical interpretation to explain factors influencing the temperature rise and MRR.

Polishing experiments using copper wafer samples were conducted on a Buehler Automet 250 polishing machine following an L8 Taguchi design. The design of experiments constituted 8 runs. Each run had fixed values of the variables, namely, load, relative velocity, and slurry concentration. Every run constituted 4 polishing experiments in which the samples were polished under the same conditions for

different amounts of time. Each experiment was repeated. Temperature rise and material removal values were obtained for all the experiments. The conditions and procedure for the set of experiments are given in section 4.7. It was found from the experimental results that the temperature rise observed in the wafer during polishing had correlation with the material removed. For each run, the temperature rise in the wafer and the material removal values were found to be linear with respect to each other. Fig. 6-1 shows a scatter plot of temperature rise and material removed values for the polishing experiments.

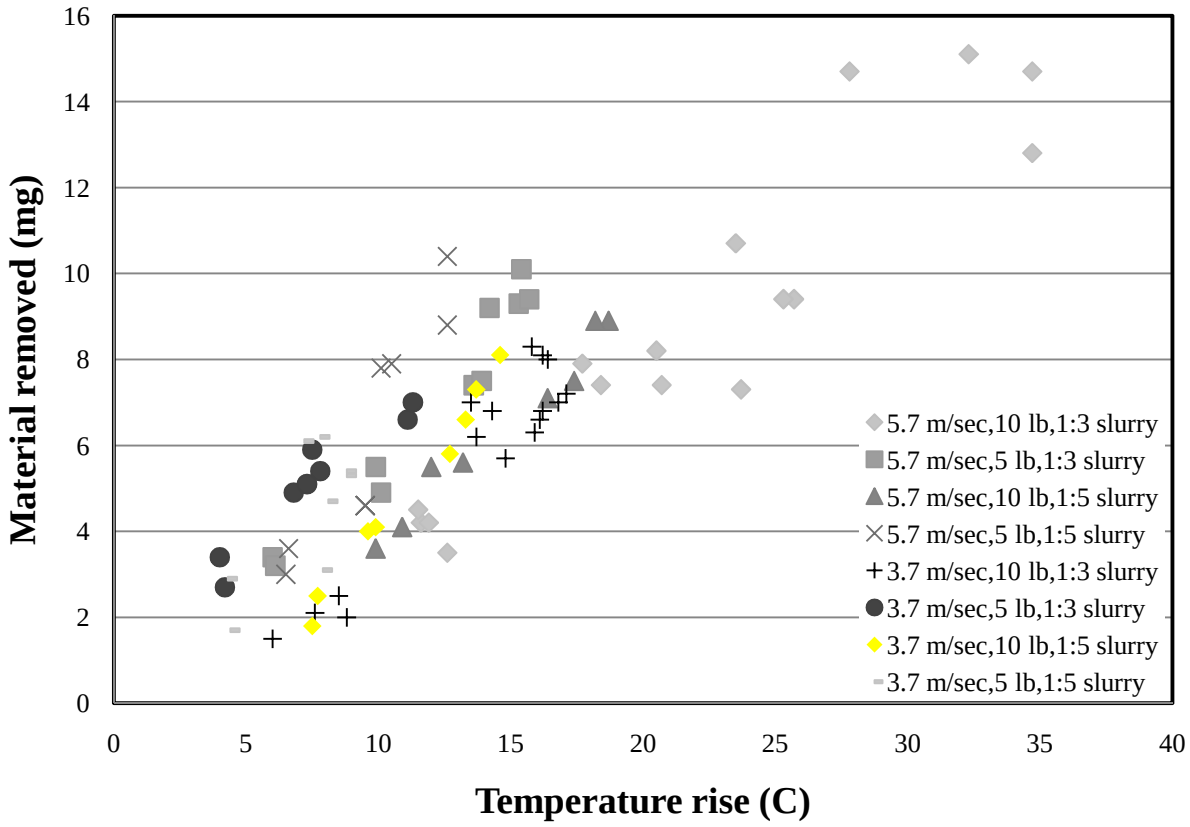

Fig. 6-1: Plot of material removed and corresponding temperature rise under various polishing conditions

Response surface analysis models which correlate MRR with temperature rise and process parameters are discussed in detail in the following sections.

6.1: Model 1: Regression model for the prediction of MRR from the process parameters only

MRR is fitted against the process parameters which are slurry concentration, load, and relative velocity. The model shows the predictability of MRR solely from the process parameters. Table 6-1 shows the predictor variables in the model and their p values.

Table 6-1: Regression model of MRR as the response variable and process parameters as the predictor variables (R^2 = 51.7%, R^2 adjusted = 49.8%)

Predictors	P value
Slurry concentration (C)	0.0008
Load (L)	0.0041
Relative velocity (V)	0

$$MRR = 1.71*C + 0.14*L + 0.91*V - 1.49$$

The low value of R^2 in the model suggests that MRR has a poor predictability only using process parameters as the predictor variables.

6.2: Model 2: Regression model for prediction of MRR from process parameters and temperature rise rate

MRR is fitted against temperature rise rate and process parameters, namely, load, relative velocity, and slurry concentration. 80% of the total experimental observation points were used to make this regression model and the rest 20% points were used for the verification of the model. Table 6-2 shows the results of the response surface analysis along with p values for the predictor variables.

Table 6-2: Regression model of MRR with temperature rise rate and process parameters (R^2 = 73.5%, $R^2_{adjusted}$ = 72.1%)

Predictors	P value
Slurry concentration (C)	0.0599
Load (L)	0.0146
Relative velocity (V)	0.0001
Temperature rise rate (Tr)	0

$$MRR = 0.21*Tr + 0.73*C - 0.12*L + 0.43*V + 1.10 + \varepsilon$$

This model has higher R^2 and thus higher accuracy for prediction of MRR as compared to model 1. This model shows the importance of temperature rise rate values to enhance the predictability of MRR in polishing process. Here ε is the white noise sequence.

6.3: Model 3: Regression model for prediction of MRR/Temperature rise from process parameters, pad wear factor and their two way interactions

MRR/ΔT is fitted against load, relative velocity, slurry concentration, pad wear factor, and their two way interactions. 80% of the total experimental observation points (66 data points) were used to make this regression model and the rest 20% points (16 data points) were used for the verification of the model. Table 6-3 shows the results of the response surface analysis along with p values for the predictor variables.

Table 6-3: Regression model of ratio of MRR and temperature rise with process parameters, pad wear factor, and their two way interactions
(R^2 = 82.1%, $R^2_{adjusted}$ = 79.3%)

Predictors	P value
Slurry Concentration (C)	0.040
Load (L)	0.029
Velocity (V)	0.017
Pad wear factor (Pw)	0.000
Pw*Pw	0.000
C*L	0.037
C*V	0.251
C*Pw	0.013
L*V	0.416
L*Pw	0.003
V*Pw	0.035

$$MRR/\Delta T = 0.04*C + 0.04*V - 0.04*L - 0.36* Pw + 0.37Pw*Pw - 0.03C*L - 0.02 C*V - 0.1 C*Pw - 0.01 L*V + 0.12 L*Pw - 0.08 V*Pw + 1.61+ \varepsilon$$

This model shows higher R^2 and thus higher predictability of MRR as compared to previous two models. This model shows the importance of pad wear factor and the two way interaction terms between pad wear factor and process parameters to enhance the predictability of MRR in polishing process. However, there are too many interaction terms in the model. There is a need for more physically motivated model which could enhance predictability of MRR.

6.4: Model 4: Regression model for prediction of Temperature rise/MRR from process parameters and pad wear factor

Ratio of temperature rise and material removal rate (ΔT/MRR) was fitted against process parameters, namely, load, relative velocity, and slurry concentration and pad wear factor. Table 6-4 shows the results of the regression fit and the p values of the predictor variables.

Table 6-4: Regression model of ratio of temperature rise and MRR with slurry concentration, load, relative velocity and pad wear factor (R^2 = 87.7%, $R^2_{adjusted}$ = 86.9%)

Predictors	P value
Concentration (C)	0.0003
Load (L)	0.0001
Velocity (V)	0
Pad wear factor (Pw)	0

$$\Delta T/MRR = 3.86*Pw - 0.23*V + 0.08*L - 0.81* C + 1.96 + \varepsilon$$

This can be also written as:

$$MRR = \Delta T\,(3.86*Pw - 0.23*V + 0.08*L - 0.81* C + 1.96 + \varepsilon)^{-1}$$

6.4.1: Physical significance of the model

Apart from being a regression fit with good R^2 value and thus good predictability, the model also has physical significance and provides experimental verification to a physical term related to MRR and temperature which is deduced from previous research work. This is explained below:

$$\kappa_w \frac{\partial T_w}{\partial z} = \gamma_w \mu_k(t) pV - h_{ws}(T_w - T_s)$$

This equation given by Li *et al*. [21] explains the heat entering the wafer during polishing. Here κ_w is the conductivity of the wafer, μ_k is the coefficient of friction, γ_w is the heat partitioning fraction, p is the load, V is the relative velocity, T_w is temperature of the wafer, h_{ws} is the heat transfer coefficient between slurry and wafer and T_s is the temperature of slurry.

Under steady state condition this equation simplifies to:

$\Delta T_w = \gamma_w \mu_k / \kappa_w (PV)$

Also, Preston's equation is MRR = KPV where K is Preston's constant.

Using these two equations we obtain $\Delta T/MRR = \gamma_w \mu_k / K \kappa_w = \varphi$

The factor φ is a function of heat partitioning fraction, coefficient of friction, and Preston's constant which themselves depend on various factors. Heat partitioning fraction primarily depends upon the velocity, coefficient of friction is related to pad surface condition and normal load, and Preston's constant is a combination of various factors including pad surface properties and abrasive properties. Other factors, such as slurry flow rate, material of the wafer and the pad, thermal and dimensional properties of the wafer and pad were not changed during experimentation and were not accounted. The model gives an expression for φ as a function of velocity, load, pad condition and abrasive concentration which is obtained experimentally. This further explains that $\Delta T/MRR$ is not a linear term. Rather the value of $\Delta T/MRR$ depends upon some variables. The roles of these variables are given in the following section.

Velocity: As shown in the equation for the model in Table 6-4, velocity is inversely related to the temperature rise. This may be explained by the concept of heat partitioning in the polishing process. Heat partitioning is described in the literature review chapter. Heat partitioning factor refers to the fraction of heat flowing into the wafer from the total heat generated during polishing. The mathematical term of heat partitioning factor comprises of sliding velocity along with pad and wafer properties. Thus, if the material properties are fixed, heat partitioning is solely dependent on the sliding velocity. Heat

partitioning fraction is inversely related to the square root of the sliding velocity. Increase in velocity would decrease the heat transferred to the wafer and thus the temperature rise in it. Also, higher sliding velocity would result in more convective cooling of the wafer and thus lowers the temperature rise compared to expected values [21].

Load: As shown in the equation for the model in Table 6-4, the ΔT/MRR value increase with increase in load. The reason for this is the increase in the pad contact area with the increase in the load. When the normal load at the pad wafer interface increases, more pad asperities are pressed to come in contact with wafer. As shown in the Literature Review Section 2.5, the increase in the load on the pad increases the contact area and the pad bends around the abrasive particles to press the wafer. This region of the pad rubs against the wafer and generates heat which is not due to material removal. There is a decrease in the force on the abrasive particles due to increase in the area of contact which decreases the MRR compared to the expected values [22]. This overall implies an increase in the ΔT/MRR term.

Concentration: There is an inverse relation between ΔT/MRR and slurry concentration (C) shown in the equation for the model in Table 6-4. As explained by Luo and Dornfeld [23], MRR is directly related to the number of active abrasive particles or the slurry concentration.

$MRR = \rho N V$ Where ρ is the density of copper, N is the number of active abrasive particles and V is the volume removed by each abrasive particle.

This implies that increase in the slurry concentration would increase the MRR and thus decrease ΔT/MRR term.

Pad wear factor: This is a factor incorporated in the model which signifies the observed pad wear condition for each polishing experiment. The value of the pad wear factor is based on fuzzy logic. Fuzzy logic is a type of multi valued logic which deals with reasoning which is approximate rather than precise. It has truth values lying between 0 and 1, just like binary logic but the values are more than two. The

values of pad wear factor were taken as 0, 0.2, 0.4, 0.6, 0.8, and 1 representing the pad condition as new, fresh, good condition, intermediate, nearly bad and bad, respectively. Table 6-5 tabulates the pad conditions along with values of corresponding pad wear factor values. Fig. 6-2 shows the pad images corresponding to the pad condition and pad wear factor values.

Increase in the pad wear factor corresponds to the increase in the pad wear. This would result in a decrease in the MRR as explained in section 2.8. This in turn would increase the $\Delta T/MRR$ term. It can be noted from Fig. 6-1 that the data points corresponding to polishing run of 5.7 m/sec, 10lb, and slurry concentration of 1:3 at higher temperature values are more scattered. This can be attributed to high wear in the pad which was observed after the polishing. The pad was more worn than expected and thus the value of the pad wear factor was taken higher accordingly.

Table 6-5: Pad conditions and corresponding pad wear factor values

Pad condition	**Pad wear factor (Pw)**
New	0
Fresh	0.2
Good condition	0.4
Intermediate	0.6
Nearly bad	0.8
Bad	1

New pad, Pw = 0, Fibers equally arranged

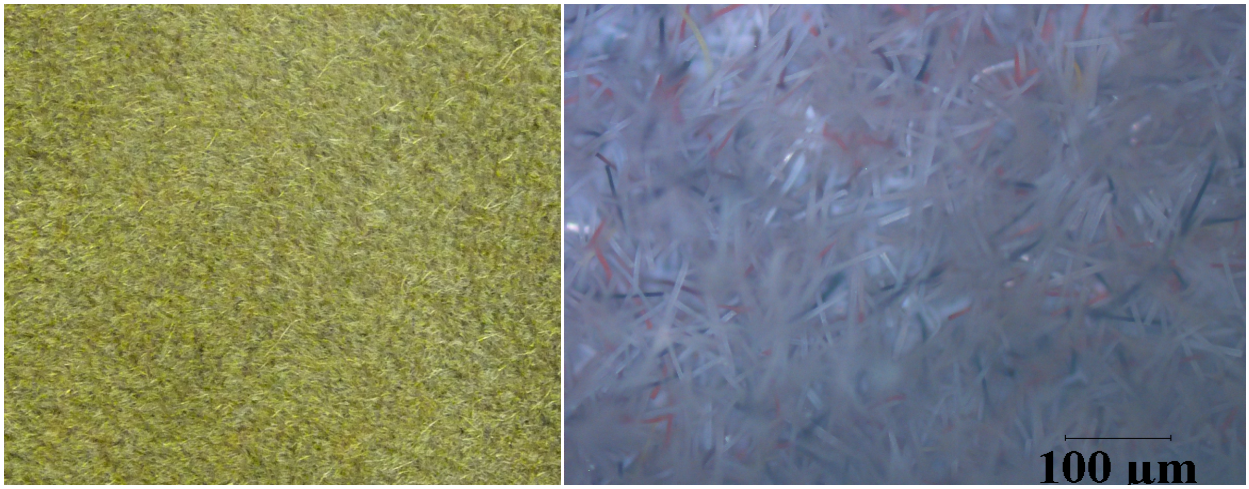

Fresh pad, Pw = 0.2, Fibers equally arranged, nap can be observed

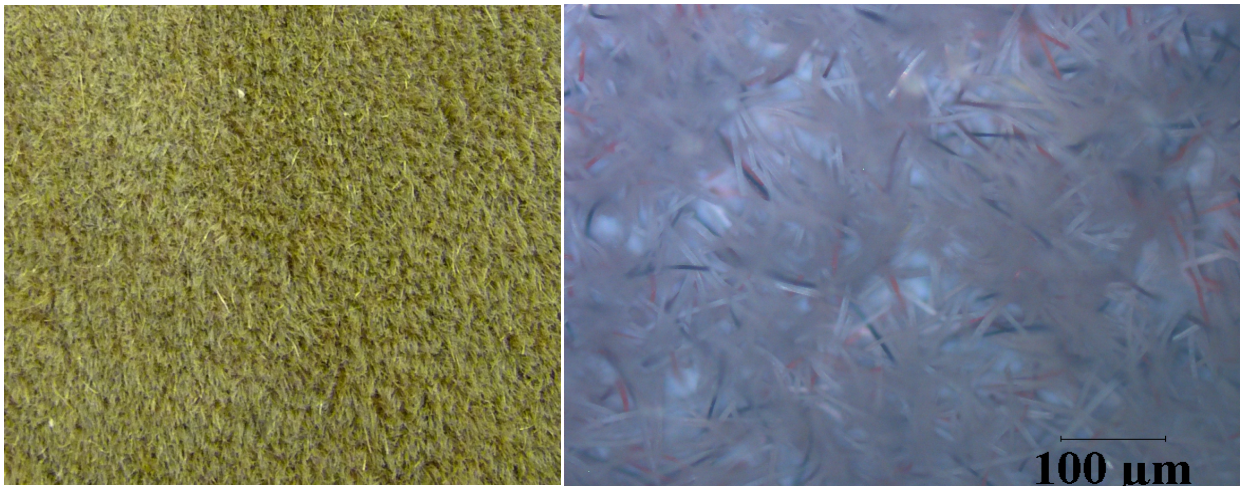

Good condition pad, Pw = 0.4, Fibers squashed, nap can be observed

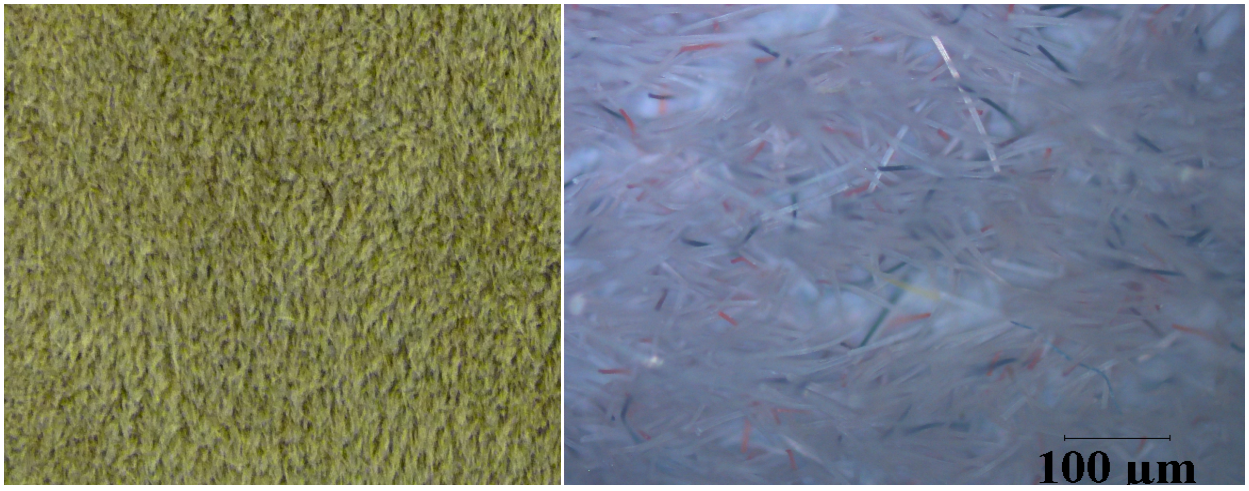

Intermediate pad, Pw = 0.6, Fibers getting directional, nap decreased

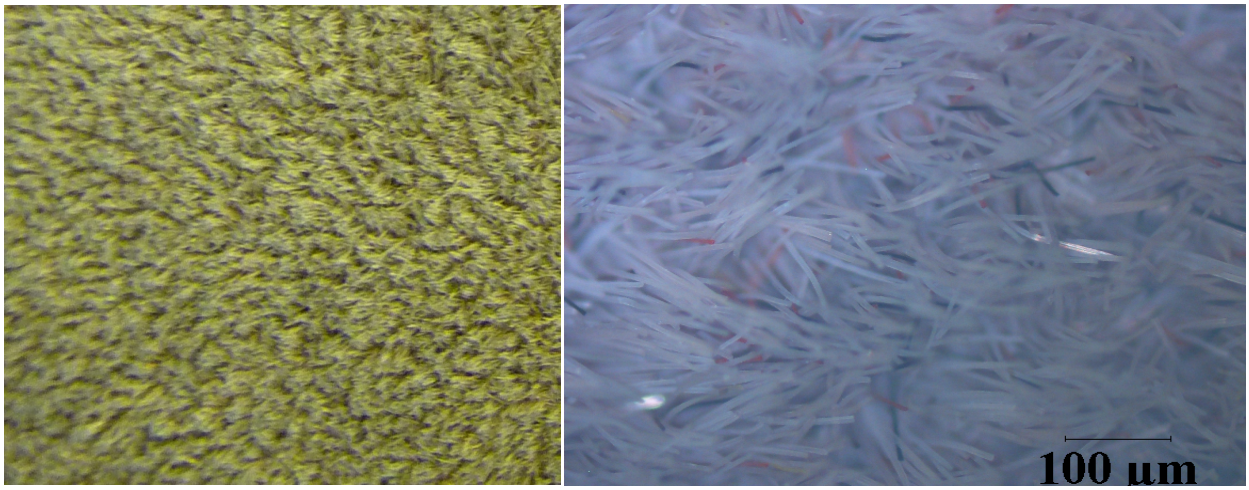

Nearly bad pad, Pw = 0.8, Fibers highly directional, nap almost gone

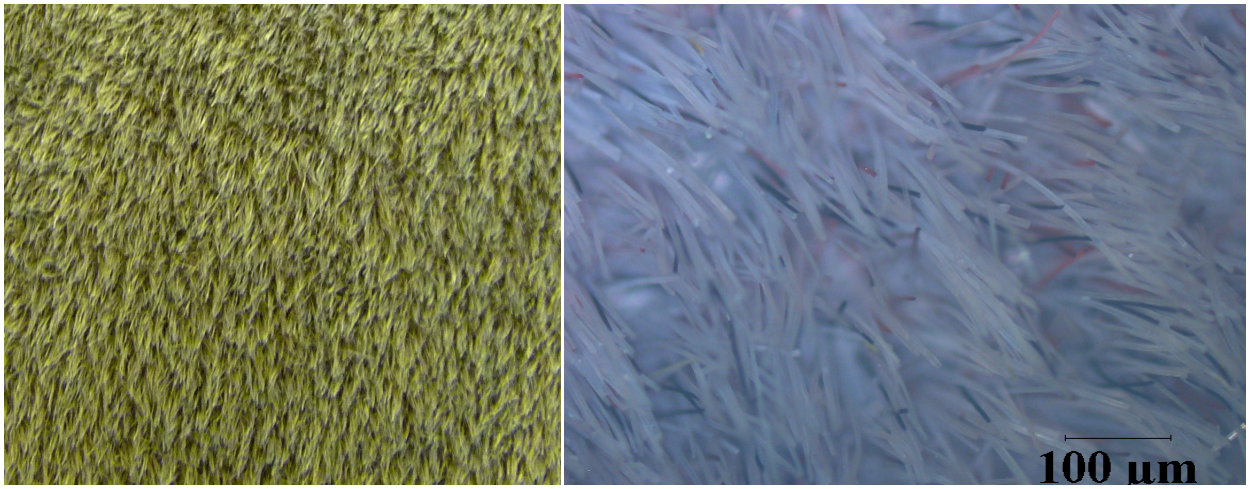

Bad pad, Pw = 1, Fibers severely pulled directionally, nap gone

Fig. 6-2: Pad images corresponding to the pad wear factor and pad conditions

6.4.2: Using the model

The model can be used to predict the average MRR during the polishing with a new pad and also when the initial condition of the pad is worn.

For a new pad: The model can be used to predict the MRR for any polishing experiment which was included in the set of experiments conducted. From the total 82 experimental observation points, 66 points were used to build the model and 16 points were used for verification. Fig. 6-3 shows the observed and predicted values of the MRR for verification experimental points.

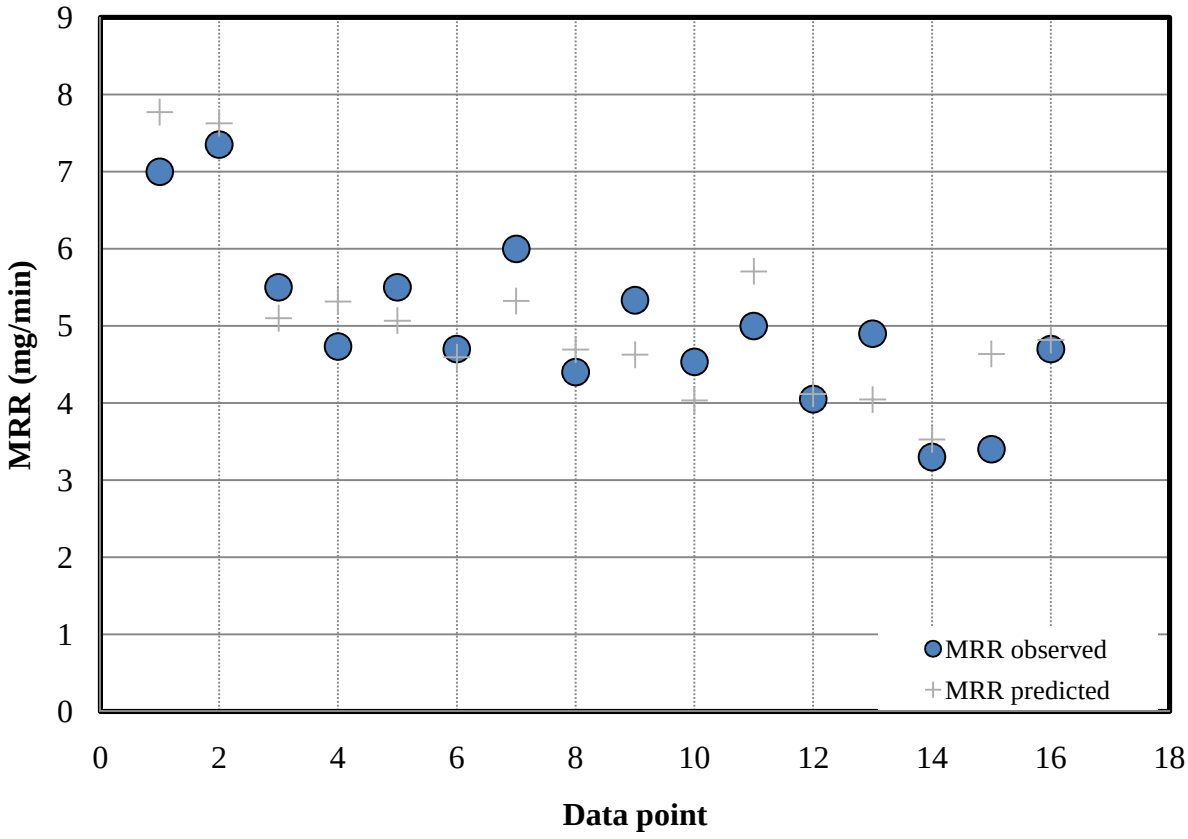

Fig. 6-3: Plot of MRR observed and MRR predicted by model for the verification points

For old/worn pad: The model can be used to calculate the MRR when the initial condition of pad is worn. As discussed in the Literature Review chapter, MRR decreases with the pad wear. Thus, the average MRR for a same polishing experiment would be lower when a worn pad is used instead of new pad for polishing. The starting pad condition is assigned a pad wear factor on the basis of observation. After polishing with the pad, the pad is assigned a pad wear factor corresponding to the pad condition. The average of the two pad wear factors is then used in the same equation (model 4) to calculate the MRR.

Chapter 7: Conclusions and Future Work

Process monitoring and control is important for obtaining desirable process output. The output or performance parameters (MRR here) are dependent on the input parameters (machine settings, properties of consumables, etc). A relationship between the performance parameter as a function of input parameters can facilitate in predicting and thereby controlling the performance parameters. To find such a relationship, copper polishing experiments, based on L8 Taguchi design, were conducted on a Buehler Automet 250 polishing machine. MRR was the output parameter while load, relative velocity, and slurry concentration were taken as the input parameters. A regression model was developed for the prediction of MRR from the input parameters. The relationship had a low predictability (R^2 = 51.7%, R^2_{adjusted} = 49.8%) indicating that the input parameters were not sufficient to predict the MRR.

A temperature sensor was attached behind the copper wafer sample to monitor the pad-wafer interface temperature during the set of experiments. Temperature rise in the wafer is related to the heat generated during polishing which is directly related to the material removal. The temperature sensor measured one of the process output parameter (temperature rise in the wafer) which was closely related to the desired performance parameter (MRR) and thus helped to predict the MRR by incorporating temperature in the relationship of MRR and input parameters. A regression model was made for prediction of MRR from the input parameters and temperature rise rate values. Increase in the accuracy of regression fit (R^2 = 73.5%, R^2_{adjusted} = 72.1%) shows the contribution of temperature rise rate values in enhancing the predictability of MRR as compared to the input parameters only.

A regression model was made having ratio of MRR and temperature rise, namely, MRR/ΔT as the response variable and load, relative velocity, slurry concentration, pad wear factor, and their two way

interactions as the predictor variables. Increase in the accuracy of regression fit (R^2 = 82.1%, $R^2_{adjusted}$ = 79.3%) shows the contribution of pad wear factor and the interaction terms in enhancing the predictability of MRR.

A regression model was made taking the ratio of temperature rise in wafer and MRR, namely, ΔT/MRR as the response variable and load, relative velocity, slurry concentration and pad wear factor as predictor variables. The model can predict MRR with high predictability (R^2 = 87.7%, $R^2_{adjusted}$ = 86.9%) for new as well as for worn pad used at the start of polishing. The term of ΔT/MRR was deduced as a function of velocity, load, pad condition and abrasive concentration from well established mathematical relations. This model represents the deduced function/relationship between ΔT/MRR and velocity, load, pad wear factor, and abrasive concentration for the applied set of experimental conditions. The model explains the effect of load, relative velocity, slurry concentration and pad wear on the slope of relation between ΔT and MRR. Increase in the load increases the area of contact between pad and wafer. This decreases the force on the abrasives and a lower than expected MRR is observed, hence, increasing ΔT/MRR term. Increase in the relative velocity increases the convective cooling of wafer. This decreases the ΔT value, thereby, decreasing the ΔT/MRR term. Increase in concentration of abrasive slurry increases MRR, hence, decreases the ΔT/MRR term. As MRR decreases with pad wear, increase in the pad wear factor decreases MRR, hence, increasing the ΔT/MRR term.

Similar to the models proposed here, models incorporating more input parameters, such as the slurry flow rate, abrasive size, pad and, abrasive types along with a bigger set of experimentation can provide a relationship of MRR with a wider scope.

The model proposed here can be extended for more sophisticated planarizing machines where the radial variation of temperature in the pad and wafer can be measured through multiple temperature sensors and thus can account the variation of MRR in the wafer radially.

Surface roughness of the wafer can be modeled on a more sophisticated planarizing machine. WIWNU and WTWNU can also be accounted.

References

[1] J.M. Steigerwald, S.P. Mururka, and R.J. Guttman, *Chemical Mechanical Planarization of Microelectronic Materials*, New York: Wiley, 1996.

[2] H. Landis, P. Burke, W. Cote, W. Hill, C. Hoffman, C. Kaanta, C. Koburger, W. Lange, M. Leach, and S. Luce, "Integration of chemical- mechanical polishing into CMOS integrated circuit manufacturing", Thin Solid Films,1992. Vol. 220 (1-2), pp. 1-7.

[3] G. B. Basim and B. Moudgil, "Slurry design for chemical mechanical polishing", KONA Powder and Particle journal, 2003. Vol. 21, pp. 178-183.

[4] T. Kasai and B. Bhushan, "Physics and tribology of chemical mechanical planarization", Journal of Physics: Condensed Matter, 2008. Vol. 20, pp. 225011, 13pp.

[5] T. Gupta, *Copper interconnect technology*, New York: Springer, 2009.

[6] R.K. Singh and R. Bajaj, "Advances in chemical–mechanical planarization", MRS Bulletin, 2002. Vol. 27 (10), pp. 743-751.

[7] H. Lu, Y. Obeng, and K.A. Richardson, "Applicability of dynamic mechanical analysis for CMP polyurethane pad studies", Mater Character, 2002. Vol. 49 (2), pp. 177-186.

[8] M. R. Oliver, *Chemical Mechanical Planarization of Semiconductor Materials*, New York: Springer, 2004.

[9] Y. Li, *Microelectronic applications of chemical mechanical planarization*, New Jersey: Wiley, 2008.

[10] H. Liang, F. Kaufman, R. Sevilla, and S. Anjur, "Wear phenomenon in chemical mechanical polishing", Wear, 1997. Vol. 211, pp. 271-279.

[11] C.B. Kim, S.W. Park, J.W. Kim, W.S. Lee and Y.J. Seo," Polishing performance of double XY- groove pattern pad for W-CMP application", 207th ECS meeting, 2006. Abstract #323.

[12] M. Fayolle, E. Sicurani, and Y. Morand,"W CMP process integration: consumables evaluation-electrical results and end point detection", Microelectronic engineering, 1997. Vol. 37(38), pp. 347-352.

[13] H. Kim, D.W. Park, C.K. Hong, W.S. Han and J.T. Moon, "The effect of pad properties on planarity in a CMP process" Material Research Society Symposium Proceedings, 2003. Vol.767, pp. F2.4.1-F2.4.7.

[14] J. Hernandez, P. Wrschka, Y. Hsu, T.S. Kuan, G.S. Oehrlein, H.J. Sun, D.A. Hansen, J. King and M.A. Fury, "Chemical mechanical polishing of Al and SiO_2 thin films: the role of consumables", Journal of Electrochemical Society, 1999. Vol.146, pp. 4647-4653.

[15] A. Misra, "Stabilized slurry compositions", U.S. Patent 6530967, 2003.

[16] A. Vijayakumar, T. Du, K.B. Sundaram, and V. Desai, “Polishing mechanism of tantalum films by SiO_2 particles”, Microelectronic Engineering, 2003. Vol.70 (1), pp. 93-101.

[17] A.K. Sikder, F. Giglio, J. Wood, A. Kumar, and J.M. Anthony, “Optimization of tribological properties of silicon di oxide during chemical mechanical planarization process”, Journal of Electronics Material, 2001. Vol. 30, pp. 1522-1526.

[18] T.H. Tsai and S.C. Yen, “Localized corrosion effects and modifications of acidic and alkaline slurries on copper chemical mechanical polishing”, Applied Surface Science, 2003. Vol. 210 (3–4), pp.190-205.

[19] D. Kwon, H. Kim, and H. Jeong, “Heat and its effects to chemical mechanical polishing”, Journal of Materials Processing Technology, 2006. Vol.178, pp. 82–87.

[20] H.J. Kim, H.Y. Kim, H.D. Jeong, E.S. Lee, and Y.J. Shin, “Friction and thermal phenomena in chemical mechanical polishing”, Journal of Materials Processing Technology, 2002. Vol. 130–131, pp. 334–338.

[21] Z. Li, L. Borucki, I. Koshiyama, and A. Philipossian, “Effect of Slurry Flow Rate on Tribological, Thermal, and Removal Rate Attributes of Copper CMP”, Journal of the Electrochemical Society, 2004. Vol.151 (7), pp. G482-G487.

[22] C.J. Evans, E. Paul, D. Dornfeld, D.A. Lucca, G. Byrne, and M. Tricard, “Material removal mechanisms in lapping and polishing”, Precision manufacturing group,UCB, 2003. Vol. STC G 52 (2), pp. 611–634.

[23] J. Luo and D.A. Dornfeld, “Material removal mechanism in chemical-mechanical polishing: theory and modeling”, IEEE Transactions on Semiconductor Manufacturing, 2001. Vol.14 (2), pp. 112–133.

[24] B. Zhao and F.G. Shi, “Chemical mechanical polishing in IC processes: New fundamental insights”, Proceeding of fourth International Chemical-Mechanical Planarization for ULSI Multilevel Interconnection Conference, Santa Clara, CA, Feb. 11–12, 1999, pp. 13–22.

[25] C. Wang, P. Sherman, A. Chandra and D. Dornfeld, “Pad Surface Roughness and Slurry Particle Size Distribution Effects on Material Removal Rate in Chemical Mechanical Planarization”, Annals of the CIRP, 2005. Vol. 54 (1), pp. 309–312.

[26] G. Fu and A. Chandra, “A Model for Wafer Scale Variation of Material Removal Rate in Chemical Mechanical Polishing Based on Viscoelastic Pad Deformation”, Journal of Electronic Materials, 2002. Vol. 31(10), pp. 1-8.

[27] K. H. Park, H.J. Kim, O.M. Chang, and H.D. Jeong,” Effects of pad properties on material removal in chemical mechanical polishing”, Journal of Materials Processing Technology, 2007. Vol.187–188, pp. 73–76.

[28] C. Zhou, L. Shan, J.R. Hight, S. Danyluk, S.H. Ng and A.J. Paszkowski, “Influence of colloidal abrasive size on material removal rate and surface finish in SiO_2 Chemical Mechanical Polishing”, Tibology transactions, 2002. Vol. 45(2), pp. 232-238.

[29] M. Moinpour, A. Tregub, A. Oehler, and K. Cadien, “Advances in characterization of CMP consumables”, MRS Bulletin, 2002. Vol.27(10), pp.766-771.

[30] G.S. Sandhu, “Method and apparatus for endpointing mechanical and chemical-mechanical polishing of substrates”, U.S. Patent 6007408, 1999.

[31] J. Koo, J. Lee, S. Lee, D. Hong, S. Hah, and H. Son, “Chemical mechanical polishing apparatus”, U.S. Patent 6976902, 2005.

[32] K. Ono, S. Oguri, K. Sasabe, M. Kurita, Y. Kojima, T. Egawa, and K. Shigeta, “Polishing apparatus”, U.S. Patent 6634924, 2003.

[33] C.L. Lin, “Method and apparatus for slurry temperature control in a polishing process”, U.S. Patent 6315635, 2001.

[34] M. Naujok and E. Kaltalioglu, “Polishing methods and apparatus”, U.S. Patent 7201634, 2007.

[35] P. Wu, X. Pham, T. Nguyen, and R. Zhou,” Methods and systems for controlling belt surface temperature and slurry temperature in linear chemical mechanical planarization”, U.S. Patent 6953750, 2005.

[36] X. Pham, T. Nguyen, R. Zhou, D. Wei, L. Jiang, K. Ramanujam, J.P. Simon, T. Luong, S. Srivatsan, and A.J. Jin, “Method and apparatus for heating polishing pad”, U.S. Patent 6896586, 2005.

[37] K.M. Robinson and P. Pan, “Methods, apparatuses, and substrate assembly structures for fabricating microelectronic components using mechanical and chemical-mechanical planarization processes”, U.S. Patent 6552408, 2003.

[38] N. Bright and D.J. Hemker, “Apparatus and methods for controlling wafer temperature in chemical mechanical polishing”, U.S. Patent 6736720, 2004.

[39] S. Ide, “Method and apparatus for chemical-mechanical polishing”, U.S. Patent 6638141, 2003.

[40] G. Yehiel, K. Rodney, O. Aleksander, H. David, and J.B. Nicolas, “Method and apparatus for wafer mechanical stress monitoring and wafer thermal stress monitoring”, Patent application no: U.S. 2005/0066739.

[41] H.M. Tzeng, G.C. Lee, G. Simon, H. Lee, D. Weldon, G. Kwong, W. Lapson, G. Appel, and P. Mok, “Temperature regulation in a CMP process”, U.S. Patent 6000997, 1999.

[42] S.C. Avanzino, B. Singh, B. Rangarajan, and R. Subramanian, “Wafer based temperature sensors for characterizing chemical mechanical polishing processes”, U.S. Patent 6562185, 2003.

[43] Y.A. Sampurno, L. Borucki, W. Zhuang, D. Boning, and A. Philipossian, “A Method for Direct Measurement of Substrate Temperature during Copper CMP”, Journal of the Electrochemical society, 2005. Vol. 152(7), pp. G537-G541.

[44] D. White, J. Melvin, and D. Boning, “Characterization and Modeling of Dynamic Thermal Behavior in CMP”, Journal of the Electrochemical society, 2003. Vol. 150(4), pp. G271-G278.

Appendix

The figures show the temperature profiles and the tables enumerate the temperature rise and material removed values corresponding to the polishing experiments discussed in section 4.6.

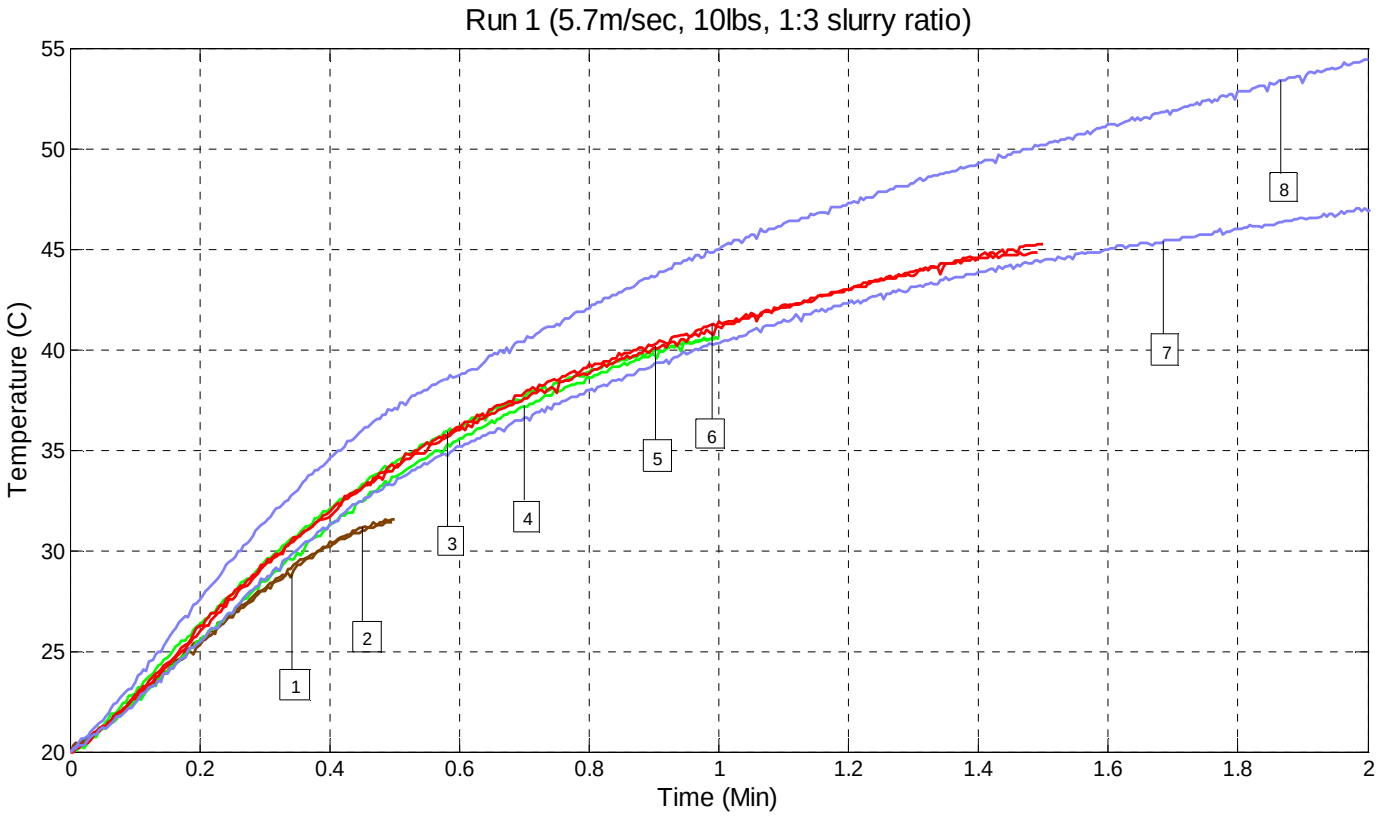

Profile	Polishing time (min)	Temperature rise (C)	Material removed (mg)
1	0.5	11.6	4.5
2	0.5	11.5	4.2
3	1	20.7	8.2
4	1	20.5	7.4
5	1.5	25.7	9.4
6	1.5	25.3	9.4
7	2	27.8	14.7
8	2	34.7	14.7

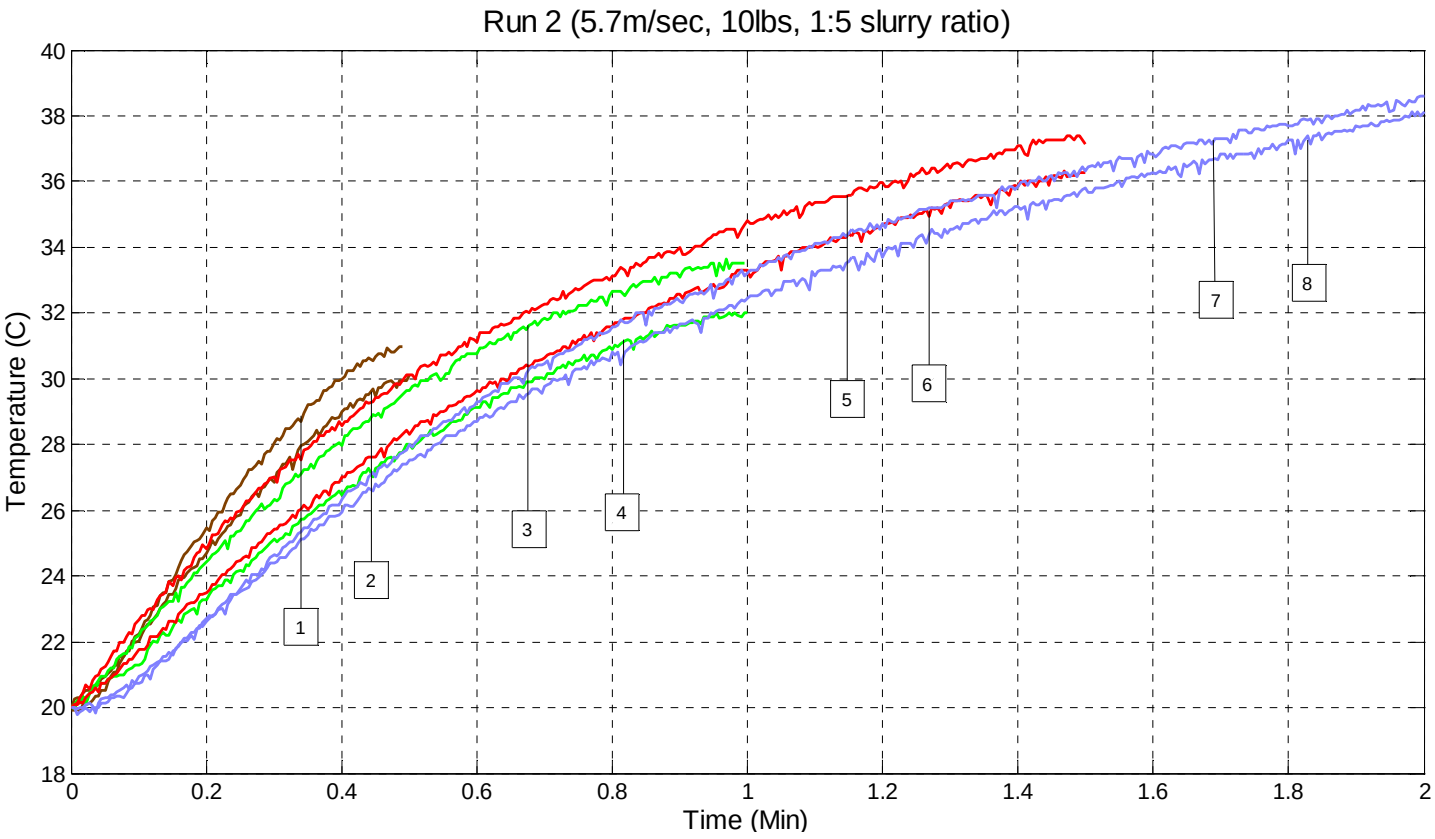

Profile	Polishing time (min)	Temperature rise (C)	Material removed (mg)
1	0.5	10.9	4.1
2	0.5	9.9	3.6
3	1	13.2	5.6
4	1	12	5.5
5	1.5	17.4	7.5
6	1.5	16.4	7.1
7	2	18.7	8.9
8	2	18.2	8.9

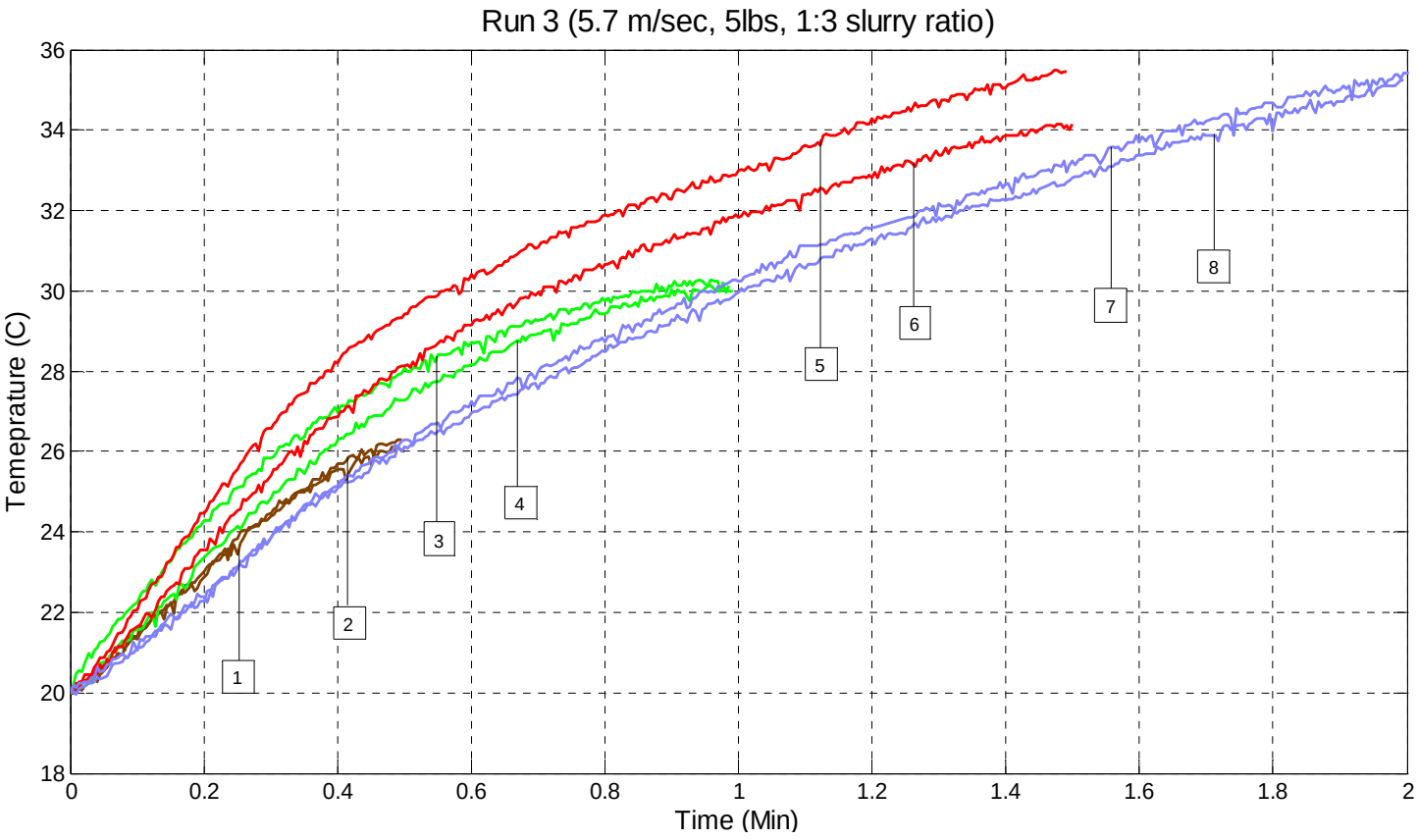

Profile	Polishing time (min)	Temperature rise (C)	Material removed (mg)
1	0.5	6	3.4
2	0.5	6.1	3.2
3	1	10.1	4.9
4	1	9.9	5.5
5	1.5	15.3	9.3
6	1.5	14.2	9.2
7	2	15.7	9.4
8	2	15.4	10.1

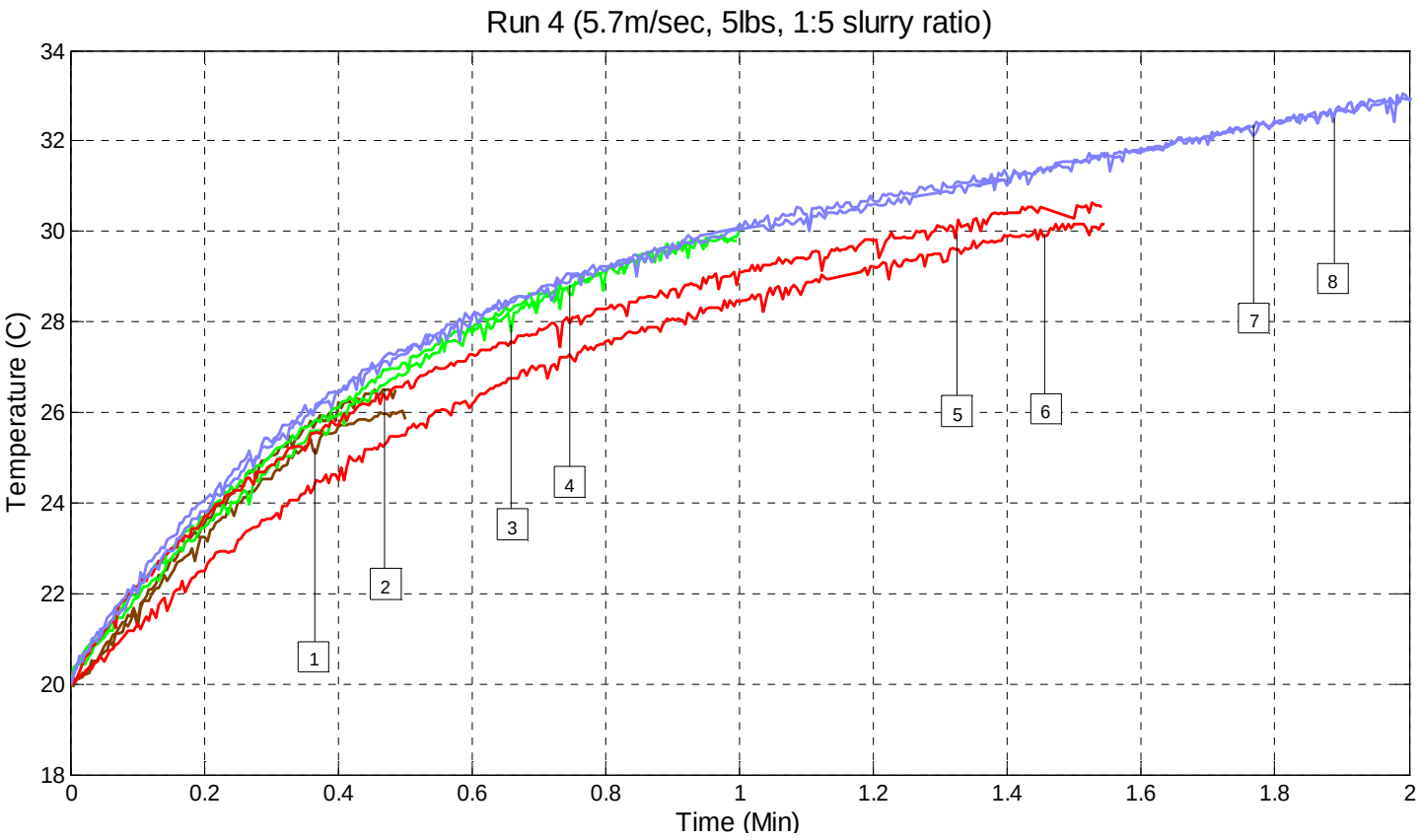

Profile	Polishing time (min)	Temperature rise (C)	Material removed (mg)
1	0.5	6.5	3
2	0.5	6.6	3.6
3	1	9.5	4.6
4	1	9.5	4.6
5	1.5	10.5	7.9
6	1.5	10.1	7.8
7	2	12.6	8.8
8	2	12.6	10.4

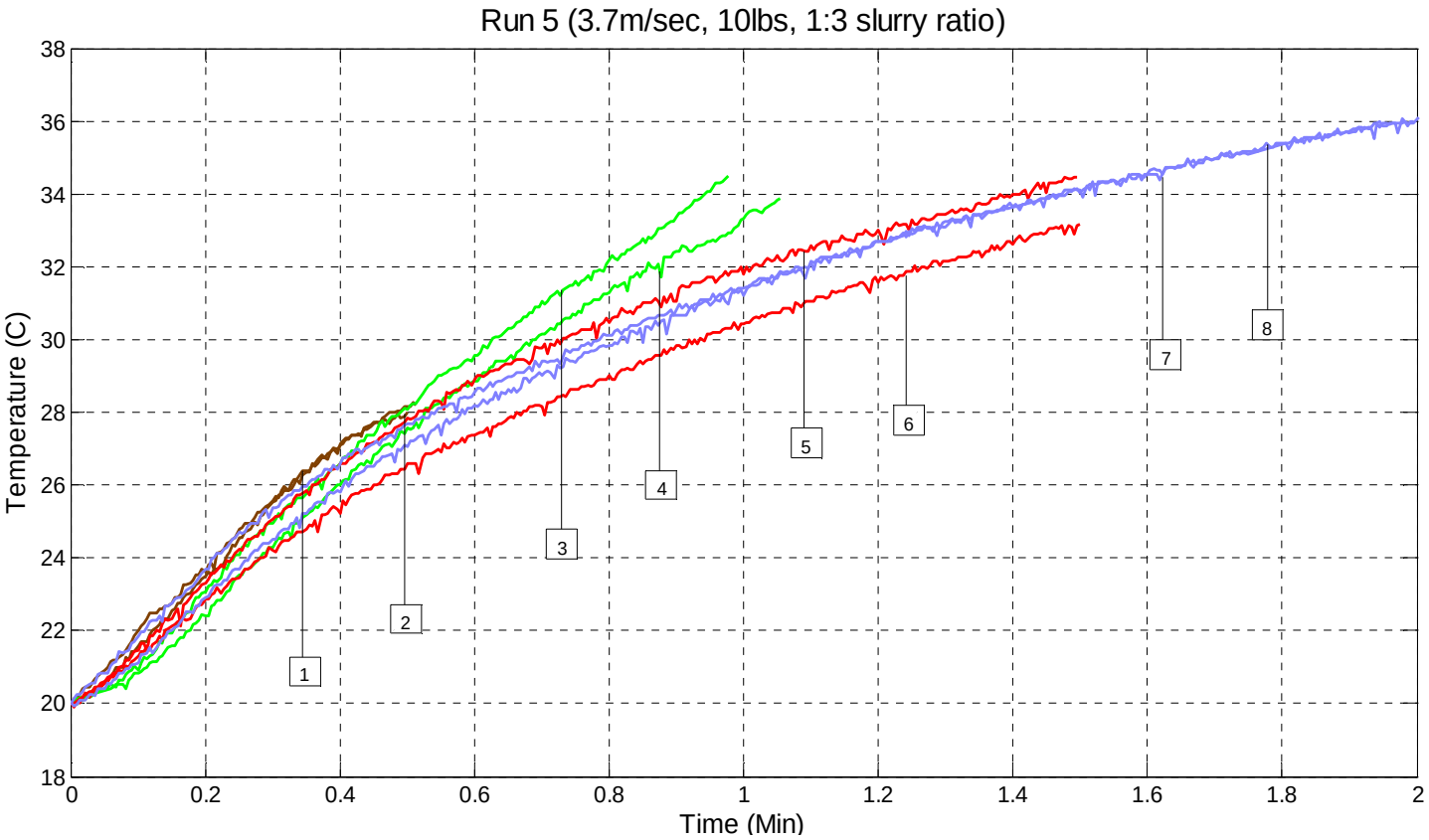

Profile	Polishing time (min)	Temperature rise (C)	Material removed (mg)
1	0.5	8.8	2
2	0.5	8.5	2.5
3	1	14.8	5.7
4	1	13.7	6.2
5	1.5	14.3	6.8
6	1.5	13.5	7
7	2	16.1	6.6
8	2	16.2	6.8

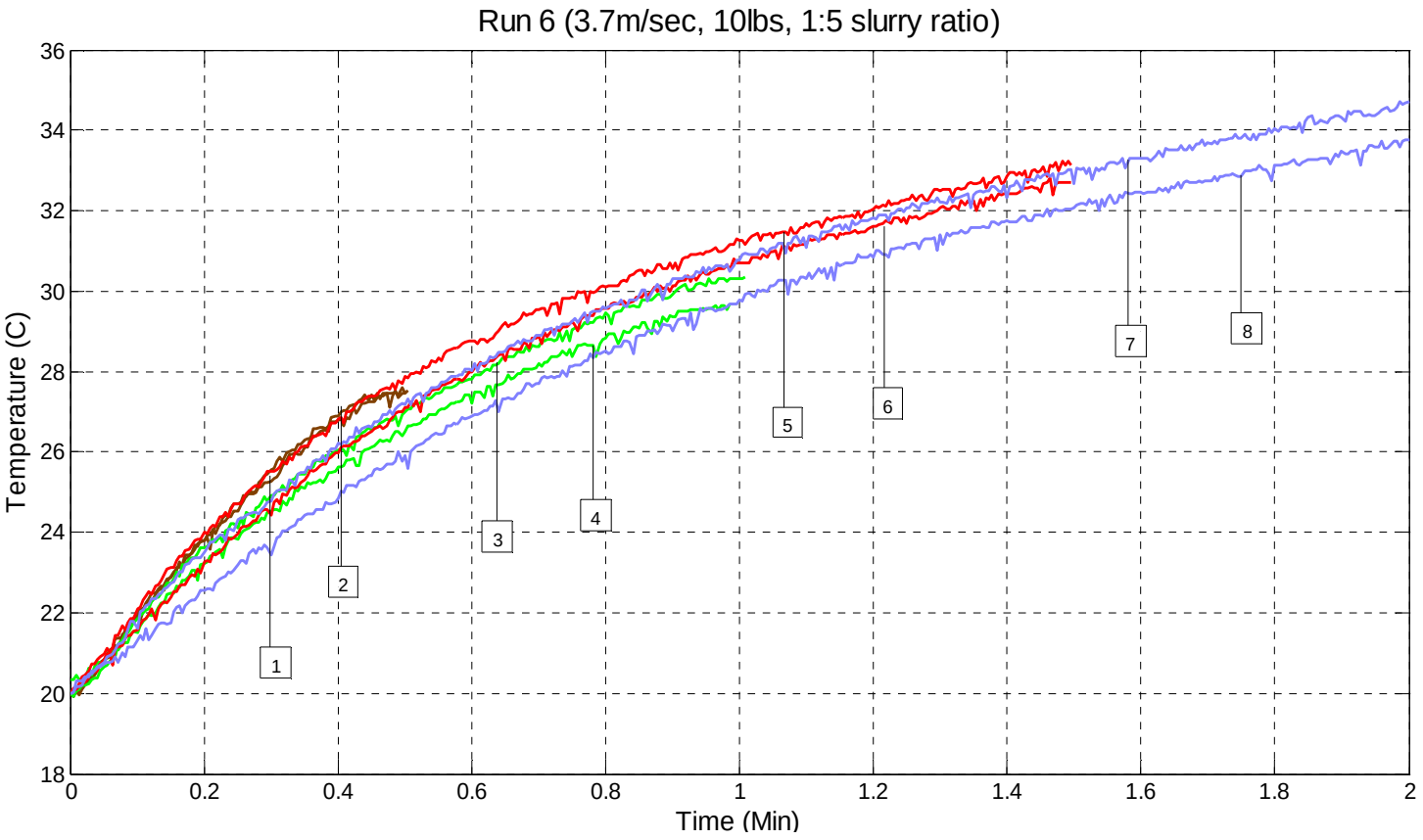

Profile	Polishing time (min)	Temperature rise (C)	Material removed (mg)
1	0.5	7.5	1.8
2	0.5	7.7	2.5
3	1	9.9	4.1
4	1	9.6	4
5	1.5	13.3	6.6
6	1.5	12.7	5.8
7	2	14.6	8.1
8	2	13.7	7.3

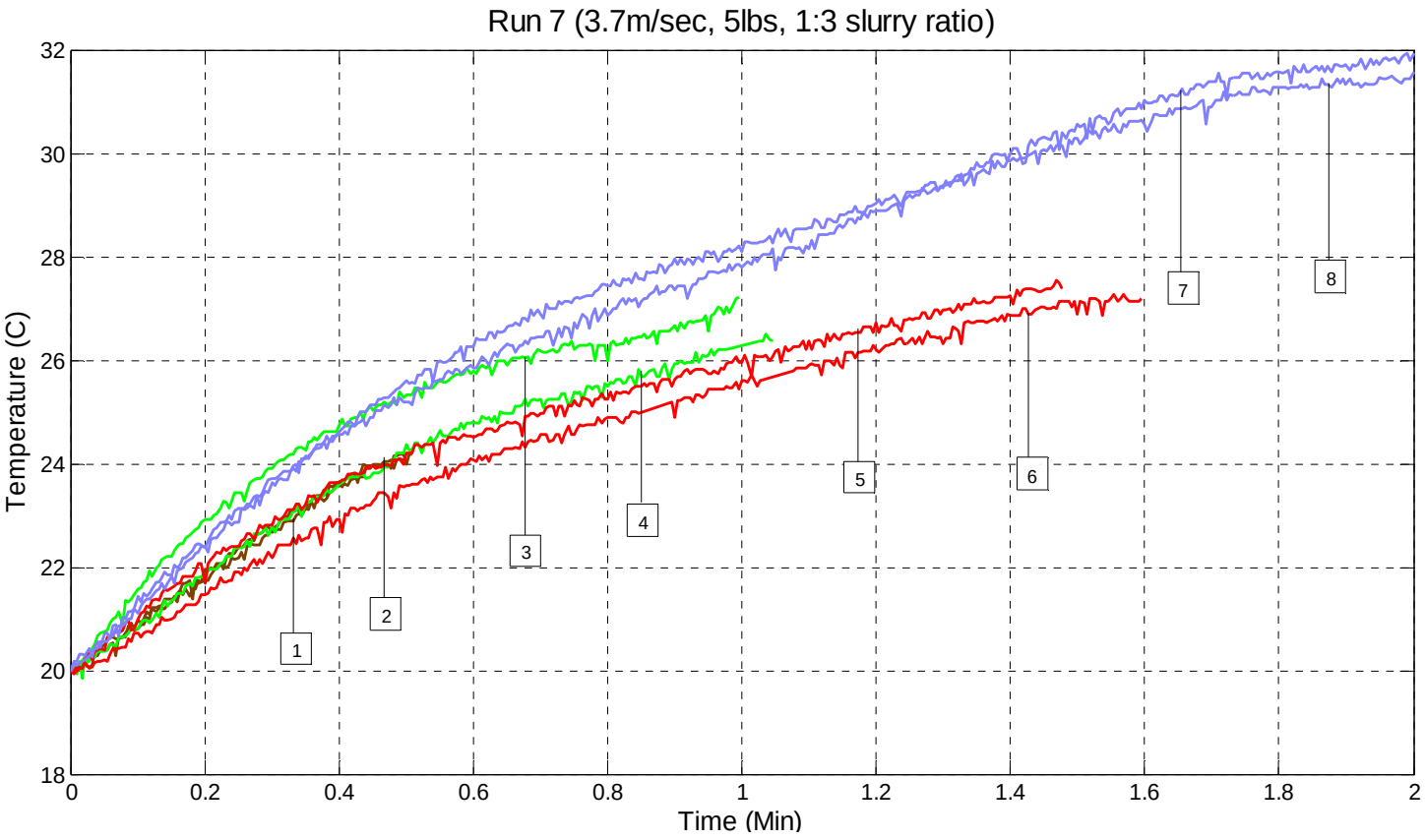

Profile	Polishing time (min)	Temperature rise (C)	Material removed (mg)
1	0.5	4	3.4
2	0.5	4.2	2.7
3	1	7.8	5.4
4	1	6.8	4.9
5	1.5	7.5	5.9
6	1.5	7.3	5.1
7	2	11.3	7
8	2	11.1	6.6

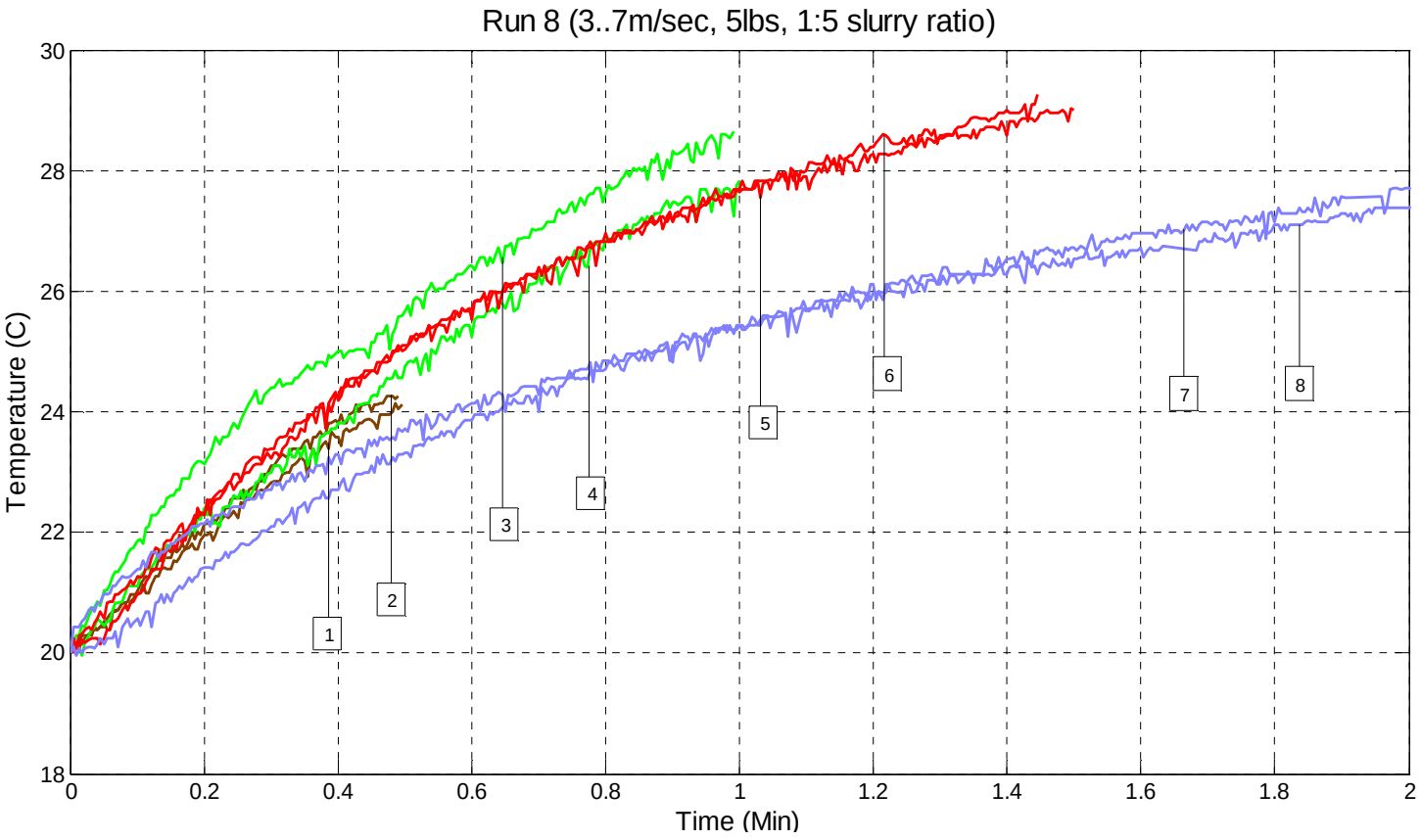

Profile	Polishing time (min)	Temperature rise (C)	Material removed (mg)
1	0.5	4.3	2.9
2	0.5	4.4	1.7
3	1	8.1	4.7
4	1	7.9	3.1
5	1.5	8.8	5.4
6	1.5	8.8	5.3
7	2	7.8	6.2
8	2	7.2	6.1

VITA

Ekansh Gupta

Candidate for the Degree of

Master of Science

Thesis: REAL-TIME ESTIMATION OF MATERIAL REMOVAL RATE (MRR) IN COPPER CHEMICAL MECHANICAL PLANARIZATION (CMP) USING WIRELESS TEMPERATURE SENSOR

Major Field: Mechanical Engineering

Education:

Completed the requirements for the Master of Science in Mechanical Engineering at Oklahoma State University, Stillwater, Oklahoma in December, 2010.

Completed the requirements for the Bachelor of Engineering in Mechanical Engineering at Institute of Engineering and Technology, DAVV, Indore, India in May, 2007.

Experience:

Graduate Research Assistant, Chemical Mechanical Planarization Lab, Advanced Technology Research Center (ATRC), Oklahoma State University (Jan. 2008 – May 2010).

Graduate Teaching Assistant, Materials Science Course, Department of Mechanical and Aerospace Engineering, Oklahoma State University (Jan. 2009 – May 2009)

Graduate Research Assistant, Materials Processing and Testing Lab, Utah State University (Sept. 2007 – Dec. 2007)

Name: Ekansh Gupta Date of Degree: December, 2010

Institution: Oklahoma State University Location: Stillwater, Oklahoma

Title of Study: REAL-TIME ESTIMATION OF MATERIAL REMOVAL RATE (MRR) IN COPPER CHEMICAL MECHANICAL PLANARIZATION (CMP) USING WIRELESS TEMPERATURE SENSOR

Pages in Study: 104 Candidate for the Degree of Master of Science

Major Field: Mechanical Engineering

Scope and Method of Study: In this study, temperature sensor signals collected from a wireless temperature sensor were used to estimate MRR in Copper CMP (Cu-CMP). A set of Cu-CMP experiments were conducted on a Buehler Automet 250 polishing machine following L8 Taguchi design of experiments. Material removal and temperature rise (ΔT) in copper polishing samples was measured during experiments. Regression models based on process parameters (load, relative velocity, and slurry concentration), pad wear factor and temperature rise were developed and compared.

Findings and Conclusions: Temperature rise values observed during Cu-CMP experiments measured by temperature sensor with a sampling rate of 4Hz were used for estimation of MRR. The predictability of MRR through a regression model comprising of the process parameters only, was low (R^2 = 51.7%). The predictability of MRR increased (R^2 = 73.5%) after including temperature rise rate as a predictor variable in the regression model. A regression model having ratio of MRR and ΔT as the response variable and process parameters, pad wear factor, and their two way interactions as the predictor variables showed further increase in the predictability of MRR (R^2 = 82.1%). A regression model having ratio of ΔT and MRR as the response variable and process conditions and pad wear factor as the predictor variables improved the accuracy of estimation of MRR (R^2 = 87.7%). The improvement in the predictability of MRR is likely because the model accounts for the effect of load, relative velocity, slurry concentration, and pad wear on the slope of relation between ΔT and MRR.

ADVISER'S APPROVAL: Dr. Ranga Komanduri